PHOSPHORUS RECOVERY FROM INCINERATED SEWAGE SLUDGE ASH (ISSA) AND TRANSFERRING INTO PHOSPHATE FERTILIZER

LE FANG

PhD

The Hong Kong Polytechnic University

2021

The Hong Kong Polytechnic University

Department of Civil and Environmental Engineering

Phosphorus Recovery from Incinerated Sewage Sludge Ash (ISSA) and Transferring into Phosphate Fertilizer

Le FANG

A thesis submitted in partial fulfilment of the requirements for the degree of Doctor of Philosophy

January 2020

CERTIFICATE OF ORIGINALITY

I hereby declare that this thesis is my own work and that, to the best of my knowledge and belief, it reproduces no material previously published or written, nor material that has been accepted for the award of any other degree or diploma, except where due acknowledgement has been made in the text

_____(Signed)

Le FANG (Name of student)

ABSTRACT

The interest in recovery of phosphorus (P) from secondary P-sink is stimulated by global P scarcity and the current one-way flux of P-resources. Among the dominant P-sinks, incinerated sewage sludge (ISSA) is a promising secondary source for P recovery.

In Hong Kong, approximately 1200 tonnes of dewatered sewage sludge is produced and sent to the T·Park sludge treatment facility for incineration each day. The ISSA is eventually disposed by landfilling. However, it has been found that the P content in this ISSA is comparable to those in P ores (5-40 % P_2O_5) and has a high recovery potential.

In previous research studies of P recovery from ISSA using acid leaching. Both P and metal(loid)s were non-selectively extracted together making the recovered P unusable.

In this PhD study, Hong Kong ISSA was firstly characterized, followed by exploration of P leaching with three kinds of leaching agents: mineral acids, organic acids and chelating agents. Based on this, an extensive experimental campaign was carried out to develop a novel two-step leaching method. This method involved the use of a pre-extraction procedure using 0.02 mol/L of EDTA at a liquid to solid ratio (L/kg) of 20:1 for 120 min, followed by extraction with 0.2 mol/L sulphuric and at a liquid to solid ratio of 20:1 for 120 min. This resulted in the production of

a high purity P-extract. The pH of P-extract was raised to 4 by adding $Ca(OH)_2$ and the precipitate formed contained significant calcium phosphates.

A second method developed in this study used a modified biochar to sorb P from the acid-extract. This biochar was produced through pyrolysis of sugarcane biomass and modified by $MgCl_2$ at a temperature of 700 ^oC for 1 hour under an N_2 atmosphere. Sorption experiments found this biochar had a high P recovery efficiency, due to its positively charged surface with a consistent layered porous structure and a high surface area. P sorption of the optimal biochar was 131 mg P/g biochar. Post-sorption, this biochar was P-laden and was a high plant-available P fertilizer.

Along with struvite produced from ISSA, which was produced by our research team, three kinds of recycled phosphate fertilizers (RPF) were used to test their agronomic effectiveness by soilless cultivation and soil cultivation, separately. The results showed that these three kinds of RPF had comparable agronomic effectiveness to that of commercial fertilizers and posed no harm to plants in terms of heavy metal contamination. The biochar-P increased the germination rate significantly and enhanced the root system development. The study results showed that the P in the ISSA can be successfully extracted for use as a P fertilizer.

Key words: incinerated sewage sludge ash, wet-extraction, phosphorus

recovery, modified biochar, recovery phosphate fertilizer.

PUBLICATIONS ARISING FROM THE THESIS

Academic Journal Papers:

1. **Le Fang**, Jiang Shan Li, Ming Zhi Guo, C.R. Cheeseman, Daniel Tsang, Shane Donatello, Chi Sun Poon, 2017. Phosphorus recovery and leaching of trace elements from incinerated sewage sludge ash (ISSA), Chemosphere, 193, 278-287.

2. **Le Fang**, Jiang Shan Li, Shane Donatello, C.R. Cheeseman, Qi Ming Wang, Chi Sun Poon, Daniel Tsang, 2018. Recovery of phosphorus from incinerated sewage sludge ash by combined two-step extraction and selective precipitation, The Chemical Engineering Journal, 348, 74-83.

3. **Le Fang**, Jiang Shan Li, Shane Donatello, C.R. Cheeseman, Qi Ming Wang, Chi Sun Poon, Daniel Tsang, 2020. Using modified biochar to adsorb phosphorus from acid-extracts of incinerated sewage sludge ash (ISSA) for fertilizer application, Journal of Cleaner Production, 244, 118853.

4. **Le Fang**, Qi Ming Wang, Jiang-shan Li, Chi Sun Poon, 2020. Agronomic effectiveness of three kinds of recovered phosphate fertilizers (RPF) from incinerated sewage sludge ash, Environmental Science and Pollution Research (Under review).

5. **Le Fang**, Qi Ming Wang, Jiang-shan Li, Chi Sun Poon, 2020. Feasibility

of wet-extraction of phosphorus from ISSA and turn into phosphorus fertilizer: A critical review, Critical Reviews in Environmental Science and Technology, Critical Reviews in Environmental Science and Technology, 1080, 1740545.

6. Jiang Shan Li, Qiang Xue, **Le Fang**, Chi Sun Poon, 2017. Characteristics and metal leachability of incinerated sewage sludge ash and air pollution control residues from Hong Kong evaluated by different methods, Waste Management, 64, 161-170.

7. Qi Ming Wang, Jiang Shan Li, Pei Tang, **Le Fang**, 2018. Sustainable reclamation of phosphorus from incinerated sewage sludge ash as value-added struvite by chemical extraction, purification and crystallization, Journal of Cleaner Production, 181, 717-725.

8. Jiang Shan. Li, Daniel Tsang, Qi Ming Wang, **Le Fang**, Qiang Xue, Chi Sun Poon, 2017. Fate of metals before and after chemical extraction of incinerated sewage sludge ash, Chemosphere, 186, 350-359.

9. Jiang Shan Li, Zhen Chen, Qi Ming Wang, **Le Fang**, Qiang Xue, C.R. Cheeseman, Lei Liu, Chi Sun Poon, 2018. Change in re-use value of incinerated sewage sludge ash due to chemical extraction of phosphorus, Waste Management, 74, 404-412.

ACKNOWLEDGEMENTS

I am much indebted to my chief supervisor, Prof. Poon Chi Sun, for his guidance in my research which enlightened my own research skill. Also, thanks go to Dr. Li Jiangshan for his carefully guidance and help in the whole research.

I would like to acknowledge the financial supports of the Hong Kong Research Grants Council (PolyU 152132/14E) which made this research possible.

In the laboratory, I would like to thank Mr Lam, W.S. and Ms Che, Celine for their patience and help in the use and maintenance of instruments. I sincerely thank Prof. C.R. Cheeseman, Drs Shane Donatello, Ming Zhi Guo and Daniel C.W. Tsang for their unconditional guidance.

Research needs continual self-activating and ruminating on the critical thinking. In the period of my PhD study, I was not only enriched with knowledge but also gained friendship. I am grateful to all the groupmates who helped and guided me both in research and life. Especially thanks to Qiming Wang for his help in my research.

Finally, special thanks to my husband, Chunran Wu, who gives me lots of love, courage and company. I thank my mother, who gave me life and brought me up. I know she is happy to see all these in heaven and her love would be with me always.

Table of Contents

List of Figures

List of Tables

List of Abbreviations

A/O	Anaerobic/aerobic
AP	Apatite phosphate
BET	Brunauer-Emmet-Teller
BP	P-loaded biochar
CaP	Calcium phosphate compounds
CoP	Compound fertilizer
HK	Hong Kong
ICP-OES	Inductively coupled plasma optical emission spectroscopy
IP	Inorganic phosphorus
ISSA	Incinerated sewage sludge ash
L/S	Liquid to solid ratio
MP	Monopotassium phosphate
NMR	Nuclear magnetic resonance
OP	Organic phosphorus
P	Phosphorus
RPF	Recovered phosphate fertilizer
SEM-EDX	Scanning electron microscopy with energy dispersive X-ray spectroscopy
WWTP	Wastewater treatment plant
XRD	X-ray diffraction

XRF	X-ray fluorescence
ζ	Zeta potential

Chemical names

CA	Citric acid	$C_6H_8O_7$
EDTA	Ethylenediamine tetraacetate	$C_{10}H_{16}N_2O_8$
EDTMP	Ethylene Diamine Tetra	$C_6H_{20}N_2O_{12}P_4$
OA	Oxalic acid	$C_2H_2O_4$

Chapter 1 Introduction

1.1 Overview

1.1.1 Phosphorus (P) scarcity in sources and loss in waste

Global population growth and intensive farming methods demand increasing crop yields, which in turn lead to the greater need to replenish plant nutrients (mainly P, N and K) via fertilizer dosing. The production of P-fertilizers is mainly based on processing of phosphate rock (P-rock). The stable supply of these rocks in a long term is an issue of great concern since the consumption rate of P-rock has been increasing at over 2% per year according to the United Nations [1, 2].

The uneven distribution of the currently known deposits of P-rock ensures that most countries rely on importing P-rock, intermediary derivatives or final P-based products. As shown in Figure 1-1 [3], approximately 80% of global P rock reserves are located in Morocco and Western Sahara, China and Algeria [4, 5]. These deposits are principally exist as sedimentary rock formations with some of igneous occurrence [6]. According to UN FAO. (2015), the major users of P resources are China, India and the United States. And the consumption amounts are related both to the size of population and agricultural productivity (including for export) [2, 7]. Particularly, the local demand significantly outstrips its supply in less

developed regions with huge populations, for example Latin America and Asia whose populations accounts for almost 76% of the world total [8]. The inadequate local P-rock deposits and huge demand for P fertilizers will eventually result in most of the countries in the world importing P-rock or P fertilizers from Morocco and Western Sahara in the future. In Europe, concern about the future supply of P-rock has resulted in it being listed as a critical raw material by the European Commission in May 2014.

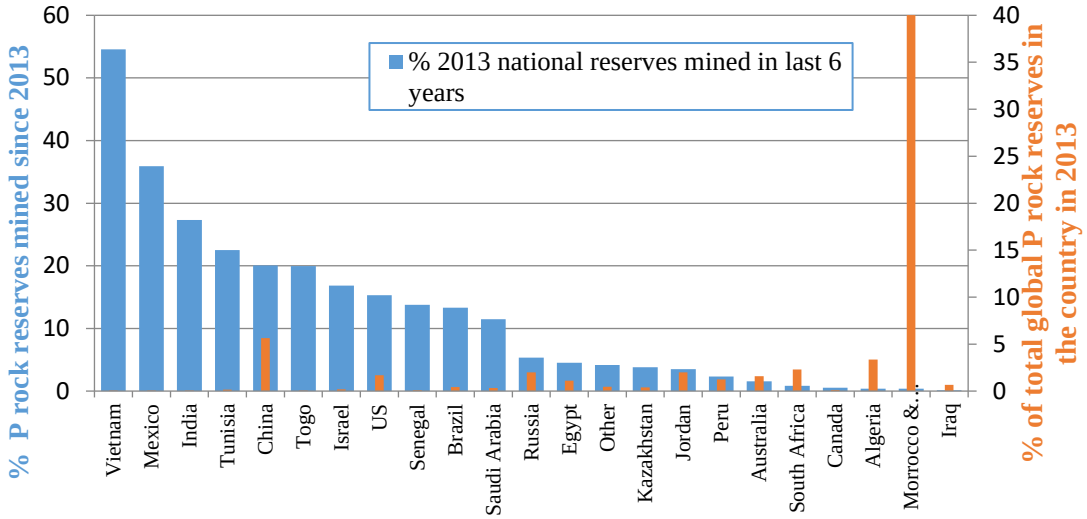

Figure 1-1 Regional P rock reserves mined since 2013 and the distribution of P rock reserves in each country in 2013 [2, 5]

Substantial losses of P resources for human activities occur at various stages of the P cycle. Losses of P due to runoff and erosion were estimated at 46% of mined P-rock [9]. In agricultural applications, over-fertilization and heavy rainfall at inopportune times can flush P away and cause acute

eutrophication events in natural watercourses. Major losses of potentially useful P from animal wastes and food wastes also occur due to a lack of waste collection and processing technology.

The P recovery potential of sewage is much higher than that of food wastes and animal wastes. All developed countries have the vast majority of their populations connected to main sewerage networks and approximately 95% of the P is emitted to the sewer and effectively concentrated in the sewage sludge which results from centralized sewage treatment processes. However, the direct application of sewage sludge on land is increasingly restricted by many countries due to concerns about pathogens, heavy metals and other emerging pollutants [10, 11]. In addition, the P in sewage sludge is mainly (90%) in the form of adenosine triphosphates in microbial cells and a minor part (10%) is precipitated as Fe-P or Al-P, which hampers P recovery [12, 13]. Incineration of the sewage sludge coverts all P into an inorganic form, which may improve the potential for P recovery into concentrated and/or purified forms [14]. Recovery of P from incinerated sewage sludge ash (ISSA) has been evaluated as superior to direct extraction from sewage sludge in terms of ecological and economical aspects [12]. Although the cost of the recovered P fertilizer (4~ 10 EUR/kg P) is higher than that of commercial fertilizer (1.6 EUR/kg P), the annual cost per population equivalent is less than 3% of the total costs of wastewater disposal [15]. This cost can be lower, if purity requirements of

recycled products are reduced and synergies with existing industrial processes are exploited [16].

The incineration of sewage sludge has the major advantage of significantly reducing the volume of sewage sludge by 90%, an odorous and putrescible material, to produce a sterile by-product (ISSA). Figure 1-2 shows the percentage of sewage sludge incineration in several regions [17-21]. The use of sewage sludge incineration can be driven directly by legislation restricting land application of sewage sludge and indirectly by factors such as a lack of locally available land for storage/disposal, congested road networks around sewage works and economic incentives for "green electricity generation" [22]. Meanwhile, plant macronutrients like K, P, Mg and Ca are enriched in the produced ISSA, enhancing its potential as an alternative P-source for fertilizer production [23, 24].

1.1.2 Feasibility of phosphorus recovery from ISSA

Approximately 1.7 million tonnes of ISSA are produced annually worldwide [22], with a typical content of 7 to 11 wt% as P [25, 26]. The direct disposal of ISSA in landfills is not only a waste of P resources but also would pose a risk to the environment as leachates from the leakage or percolating water of landfills contain a myriad of metal(loid)s which would pollute waterbodies [27, 28].

Common sorting methods, such as magnetic separation or flotation, are not

effective to recover P from ISSA, because most P in ISSA (about 4%-9%) is mainly present in combined phases and not as free phosphate [26]. P in ISSA is normally embedded in impure crystalline matrices with varying amounts of Ca, Mg, Al and Fe, such as partially substituted whitlockite [$Ca_9(MgFe)(PO_4)_6PO_3OH$], stanfieldite [$Ca_4Mg_5(PO_4)_6$] and berlinite [$AlPO_4$].

Techniques to recover P from ISSA can be broadly grouped into three categories, as shown in Table 1-1. The first is thermal treatment, which is realized by adding 5-15% of NaCl, KCl, $CaCl_2$ or $MgCl_2$ as additives to ISSA prior to volatilization of the metals as chlorides at sufficiently high temperature (e.g., 900 to >1000 ^oC) and residence time to produce an ash with much lower heavy metal content and a more bioavailable form of P [22, 29-32]. However, non-volatile heavy metals such as Ni and Cr remain in the ash and around 30% of P is lost in this high temperature process [22, 33]. In addition, it has been suggested that the thermo-extraction method is more suitable for Fe-poor ISSA (P/Fe>0.2) because the formation of ferric phosphate under the high pyrolysis temperature decreases the fertilizer value of final products [34]. The second is the electrodialytic method, after gradually dissolved in an anolyte, in which an electric field orientates the directional migration of metal cations from anolyte towards catholyte and they are separated from P by an ion-exchange membrane located between the cathode and anode [35, 36]. The operational cost of this process is

relatively high, the processing duration is long (up to 14 days) and the recurring blockage of the membrane is a problem yet to be resolved [36, 37]. The last method involves wet-extraction, which is extensively practiced, and which will be principally studied in this research [38-40]. This method normally uses inorganic acids to dissolve P from ISSA. Dissolution of other undesirable elements occurs simultaneously and so the extractant is subsequently treated to remove impurities and/or convert the P into plant-available forms suitable for fertilizer applications. The wet-extraction method has some crucial advantages over the other methods, such as lower energy consumption, it is simpler to set-up and has higher potential for large-scale application.

Table 1-1 Comparison of three P recovery methods from ISSA

methods	Process	P recovery efficiency (%)	Pros	Cons	Reference
Thermal treatment	Adding 5-15% of NaCl, KCl, $CaCl_2$ or $MgCl_2$ to ISSA and heating to around 1000 °C.	<70%	a) Bioavailability is significantly increased; b) High removal (around 90%) of Pb, Cd, Cu and Zn.	a) High energy input; b) Not suitable for Fe-rich ISSA; c) Unsatisfactory removal of non-volatile metals like Ni, Cr, etc.	[22, 29, 30, 32]
Electrodialysis	Suspending ISSA in electrolyte solutions in the electrodialytic reactor with a cation exchange membrane, which separates the catholyte and the anolyte while passes an electrical current through the system.	53~96	a) P and metal(loid) cations are simultaneously extracted and separated; b) Metals can be recovered as deposits on the cathode.	a) Operational set-up is complex and expensive; b) Long duration (up to 14 d). c) Treatment/disposal of insoluble residue	[35-37]
Wet-extraction	Acids or other leaching agents are applied to extract P from ISSA prior to purification of the extract.	70～95	a) Simple set-up; b) Low energy consumption; c) Potential for large-scale application.	a) Purification step needed; b) Treatment/disposal of acid insoluble residue.	[38, 40, 41]

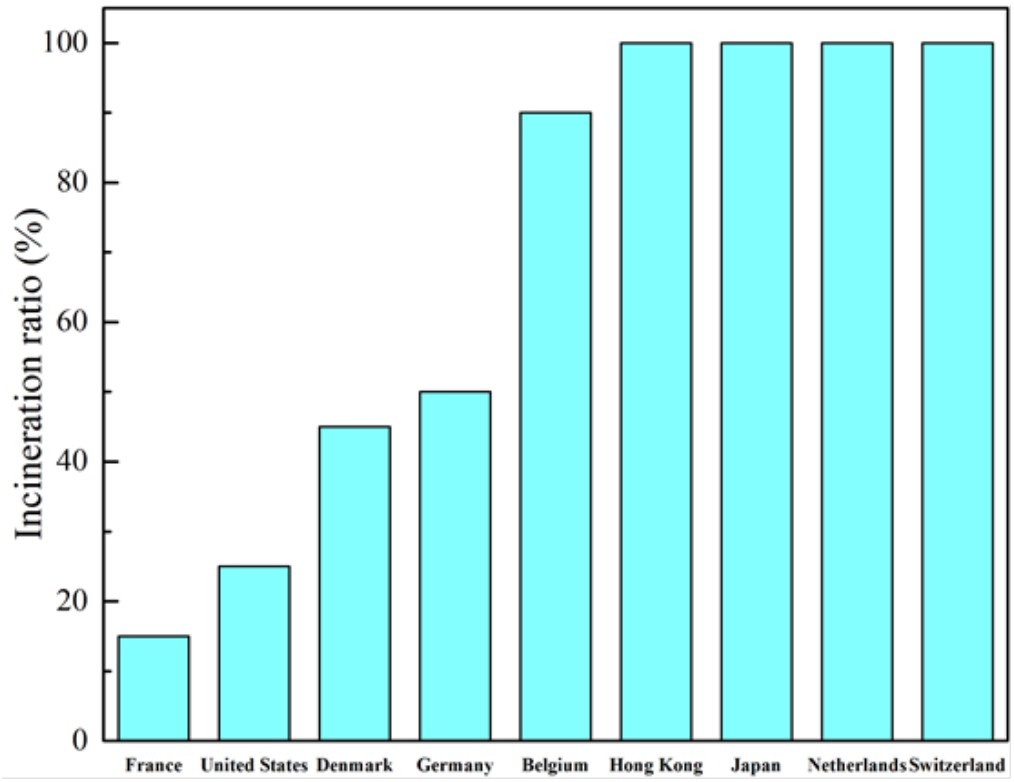

Figure 1-2 Incineration ratio (%) of sewage sludge in different regions [17-21, 42]

1.2 Research objectives

This study aims to explore a superior P extraction method, obtain a P-extract with high purity, produce plant-available phosphate fertilizers and study the agronomic effectiveness of the recovered P fertilizer.

The objective of this research:

I. To study the P extraction and co-dissolution of the metal(loid) from ISSA by different kinds of leaching agents;

II. To investigate a superior leaching method which produces a high-purity P-extract;

III. To produce solid P fertilizer with high P purity and plant-availability;

IV. To take up P from P extract by a plant-available sorbent and use it to produce with a P-enriched fertilizer;

IV. To evaluate the agronomic effectiveness of the recovered phosphate fertilizers.

1.3 Thesis outline

The main content of the research project is shown in Figure 1-3.

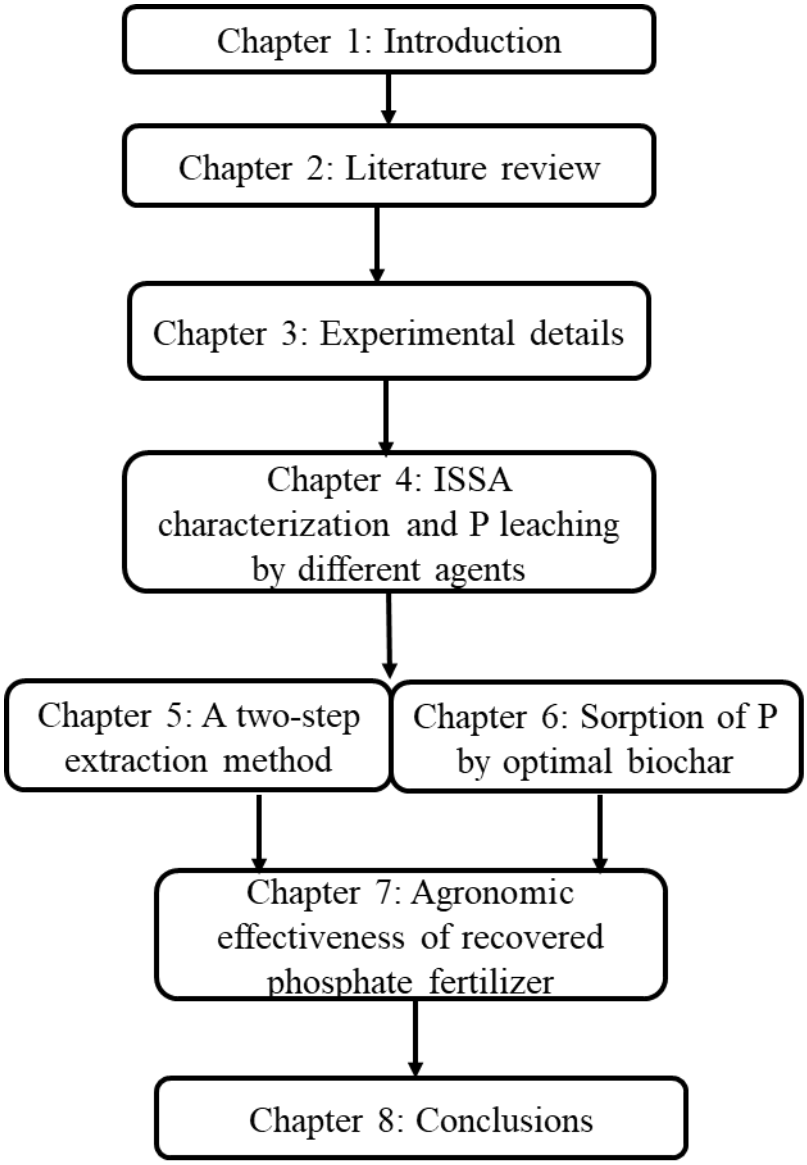

Figure 1-3 Flowchart of the thesis

As in Figure 1-3, this research was carried out as characterization of ISSA, development of P extraction method, and purification of P products for fertilizer application. Each chapter has its own introduction to the focused theme.

Chapter 1 presents the backgrounds and objectives of this research.

Chapter 2 critically reviews the relevant literature in terms of: feasibility

of P recovery from ISSA, wet-extraction of P from ISSA and recovered P fertilizers from ISSA.

Chapter 3 provides the materials, and experimental methods in this research.

Chapter 4 shows the characteristics of Hong Kong ISSA and applies six kinds of leaching agents to leach P from ISSA.

Chapter 5 proposes a novel two-step P extraction method which produces a high purity P-precipitate.

Chapter 6 explores a superior P sorption biochar which can selectively sorb P from P extract and produce with a P-enriched biochar for fertilizer application.

Chapter 7 studies the agronomic effectiveness of the produced recovered phosphate fertilizers.

Chapter 8 summarizes the conclusions of this research and presents limitation of this research and suggestions for further investigation.

Chapter 2 Literature Review

2.1 Introduction

Substantial losses of P resources for human activities occur at various stages of the P cycle. Figure 2-1 shows the P flow process from exploiting to waste-streams. As shown, in the P-ores exploiting stage, inappropriate technologies for instance exploiting bed too thin (100%), open pit (5-50%) and underground mining (15-35%) cause lots of P loss [43]. Approximately 82% of P-ores are exploited for fertilizer production [44]. Other consumption routes, including fertilizer application in agriculture, human-activities like the detergents production, food processing, industrial applications and P dosing in water treatment also consume P. Approximately 148 million tonnes of P-ores are exploited per year for fertilizer consumption globally [45-47]. After consumption, the disposed untreated waste-P pollutes waters posing a threat to animals, plants and human-being. Hence, P recovery can not only recover P from wastes but also avert the secondary pollution.

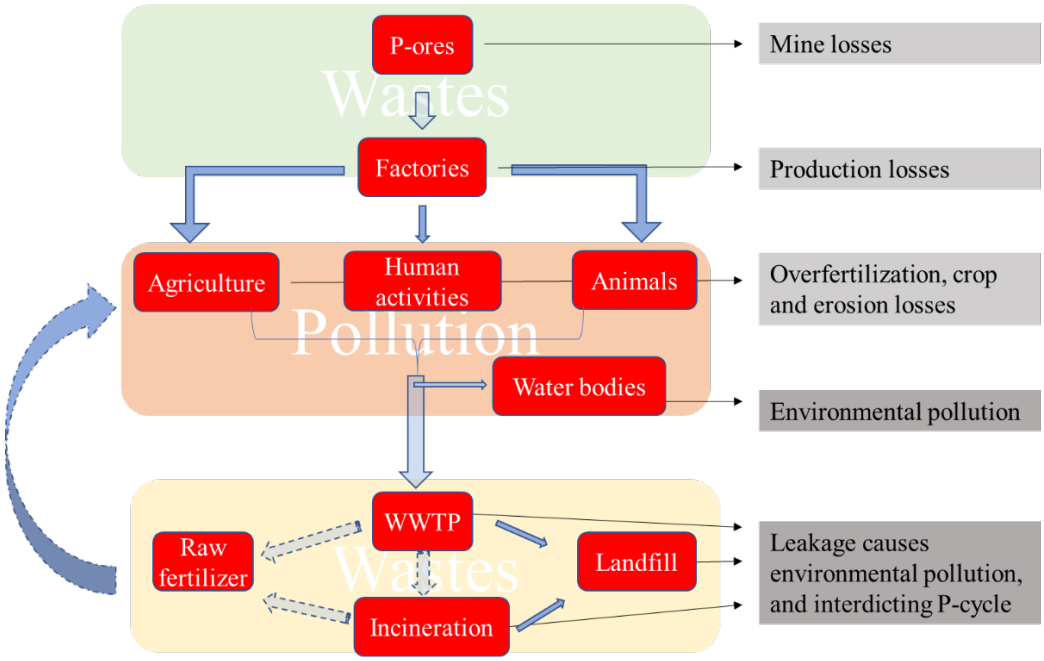

Figure 2-1 Global P-flows in production and consumption system

Of all P extraction methods, the wet-extraction method shows obvious advantage over the other methods, such as lower energy consumption, simpler set-up and higher potential for large-scale application, hence was specifically focused on. Although some previous literatures have reviewed the P extraction from ashes, this study critically reviewed P transformation in sewage sludge incineration, the characteristics of the resultant ISSA and processes that have been used to recover P from ISSA, with a particular focus on wet-extraction methods due to their greater feasibility.

2.2 Transformation of phosphorus in incineration process

2.2.1 Phosphorus in sewage sludge

The characteristics of P in sewage sludge are related to those of influent

wastewater, the sewage treatment process producing the sludge and subsequent sludge treatment operations [48, 49]. Currently, in China, approximately 63% of SS is landfilled, 14% is composted for agriculture use and 2% is incinerated. The remainder is disposed of by unknown means [49, 50].

For most WWTPs in China, the total P concentration in the influent sewage is in the range of 4~5 mg/L and the P concentration in the effluent is lower than 0.5 mg/L [49, 51], meaning that approximately 90% of P remains in sewage sludge (contain 80% of water). By using a sequential extraction procedure for P speciation, the species of P in sewage sludge can be sub-divided into inorganic-P (IP) and organic-P (OP) [52]. The IP can be further split into non-apatite inorganic-P (NAIP: P species related to oxides and hydroxides of Al, Fe and Mn), and the apatite-P (AP: P species related with Ca) [53, 54]. And the ortho-P, pyro-P and poly-P are three kinds of IP. The OP fraction includes monoester-P, diester-P and adenosine triphosphate, which are vital for the metabolism of microbial cells [55]. By using nuclear magnetic resonance, different molecular configurations of P can be identified in raw SS including orthophosphate, polyphosphate, pyrophosphate and organic phosphate (orthophosphate monoesters/diesters) [56, 57].

Table 2-1 compares the P distribution in several sources of sewage sludge [53, 55, 58-60]. As shown, most of sewage sludge is acidic and the total P

is highly variable (from 2.7 to 50.9 mg/g as P), which is dependent on the sewage sources, sewage treatment process, sludge collecting and processing procedures [61, 62].

The presence of different forms of P in sewage sludge can be explained by the structure of aerobic granular sludge, as shown in Figure 2-2. The extracellular polymeric substances form the backbone of the aerobic sludge granules, which assemble P minerals (predominantly in the center) and microbial cells (in outer layer) [62]. Since different P species have varying solubilities, information about P speciation in sewage sludge and resulting ashes is crucial for the choice and optimization of P recovery methods [56].

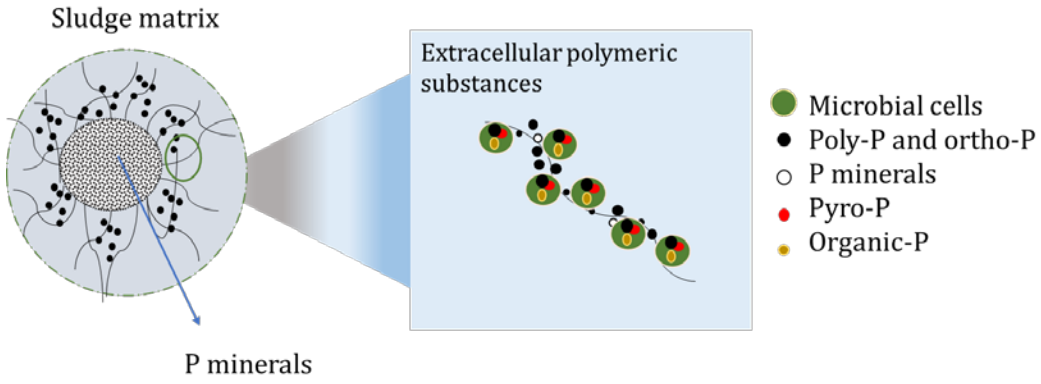

Figure 2-2 Schematic diagram of P distribution in aerobic granular sludge [62]

Table 2-1 P in different sources of sewage sludge

Sources of sewage sludge	Treatment process of wastewater in WWTP	SS treatment	Total P and different P species content (mg/g dry SS)			Reference
			TP	IP	OP	
A WWTP in New Zealand mainly receiving municipal wastewater with a small industrial contribution.	Primary sedimentation, a trickling filter then activated sludge aeration tanks with fine bubble diffusion.	Directly collected from the main waste activated sludge pipe, stored in air-tight plastic containers, transported to the laboratory.	17	11.56~12.41 NAIP (7.3), OP (3.7), AP (1.8)	4.59~5.44	[55]
A domestic WWTP in Paris.	-	The sewage sludge (P precipitated by ferric chloride) was anaerobically digested, dewatered and thickened.	50.84	41.67 (AP = 32.18, NAIP = 9.49)	9.17	[63]
A WWTP in Paris mainly receives domestic wastewater.	-	The sewage sludge was first anaerobically digested and then went through a compost process.	16.61	13.29 (AP = 12.46, NAIP = 0.83))	3.32	[63]
Several WWTPs in China which receive domestic and industrial wastewater.	A/O-sequencing batch (SBR), A/O, A2O-Flocculation and A/O-A/O.	Directly collected from different section during wastewater treatment process, dried, and ball-milled.	2.7~20.4	1.5-17.6 (OP = 1.4~17.6, NAIP = 1.2~14.6)	0.2~4.3	[53]
A WWTP (dewatered) in Shanghai, China.	A/O- anaerobic digestion		17.23	12.65	4.58	[58]
The secondary sedimentation tank of a WWTP in Harbin, China.	A2O	Collected from the secondary sedimentation tank, thickened and screened with a 1mm sieve.	31.54	27.71 (NAIP = 22.53, AP = 5.18)	3.83	[60]

2.2.2 Sewage sludge incineration and phosphorus transformation

The fluidized bed incineration process is the most widely used for incineration of sewage sludge. It is a mature technology with good energy recovery potential and a high degree of process control. A sewage sludge incinerator was installed in Hong Kong (T-Park) and the overall process is illustrated in Figure 2-3. The three main parts of the process are the pretreatment of sewage sludge, incineration in the fluidized bed and treatment of the flue gas. The dewatered sewage sludge which has a typical water content of around 70% firstly undergoes a deodorization process in the delivery bay and then is directly discharged from the truck to the bunker. The incineration process is carried out in a fluidized bed furnace operating at ~850 °C and the retention time of the sewage sludge is at least 2 seconds. The heat energy is transferred to a recovery boiler via pipes in the incinerator wall that generate steam for power generation. After incineration, the particulates and pollutants are removed by a highly efficient flue gas cleaning system which is composed of a) a multi-cyclone separator for large particle removal by spinning action; b) a dry reactor for neutralizing and capturing pollutants including acidic gases, heavy metals and dioxins via chemical and physical processes; c) a bag filter for removing fine particles through filtration. The ISSA used in was mainly sampled from the multi-cyclone separators.

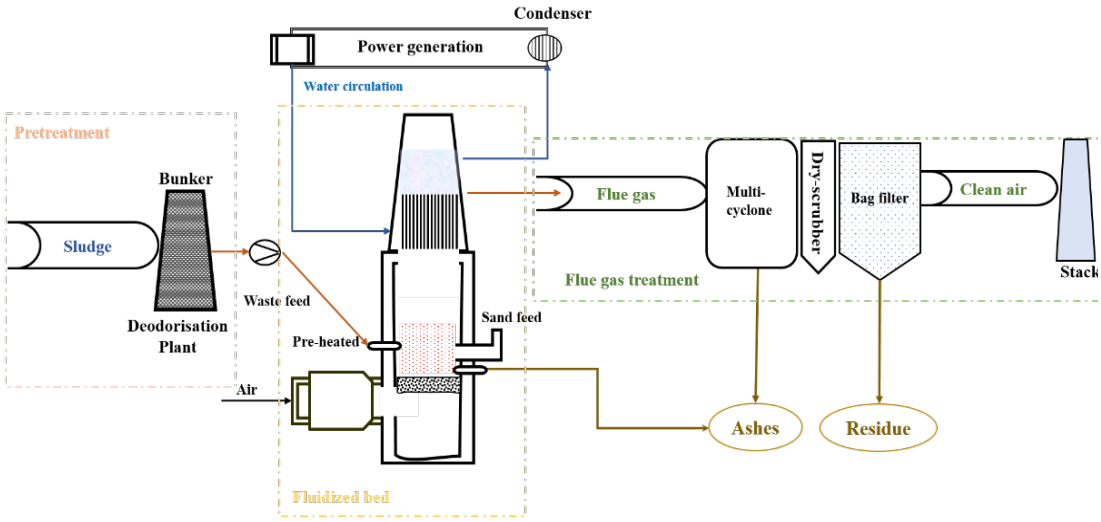

Figure 2-3 SS incineration process at Hong Kong T-Park

The physicochemical environment in the incinerator results in full combustion of sewage sludge to produce an organic-free ash (ISSA) and flue gas in a matter of seconds [58]. Based on P speciation results from NMR, after incineration, orthophosphate, orthophosphate monoesters, orthophosphate diesters, and pyrophosphate in a kind of sewage sludge were transformed into orthophosphate and pyrophosphate in low temperature (400 – 600 °C) which can be attributed to the dehydration of $M_2(HPO_4)_x$ (or $M(H_2PO_4)_x$) in the sludge [57]. The P speciation results from the SMT procedure showed that a complete transformation of OP to IP occurred at 450 °C [54]. Thus, OP can be almost completely transformed into IP below 450 °C. With the increasing of temperature from 600 °C to 800 °C, the formation of pyrophosphate was completely prohibited because a large proportion of various phosphates can react with some metal ions

(M^{x+}) in the sludge resulting in the formation of P–containing minerals [57]. In addition, AP was observed to be more stable than NAIP at an incineration temperature range of 550 – 950 °C since the content of NAIP was reduced slightly at an incineration temperature of 500 – 850 °C and reduced significantly at 950 °C because NAIP volatilizes [54]. To avoid the volatilization of P, the incineration temperature is recommended to be lower than 900 °C [64, 65].

The results from the sequential extraction procedure for P speciation in sewage sludge/ISSA can be quite different. Some typical P compounds found in sewage sludge are selected to showcase their stability towards heating. Figure 2-4 shows the thermal behavior of an exemplar OP compound ($C_{18}H_{15}O_4P$) and two potential IP compounds ($Ca_3(PO_4)_2$ and $CaHPO_4•2H_2O$) over the incineration temperature up to 900 °C [58]. With OP ($C_{18}H_{15}O_4P$) decomposition begins at 160 °C and finishes until 370 °C. After this point, OP can be considered to be completely transformed to IP. $CaHPO_4•2H_2O$ is unstable, it goes through dehydration and decomposition when the temperature increases to 150 °C and 160 °C respectively [58]. $Ca_3(PO_4)_2$ is quite resistant to decomposation up to 950 °C [54, 58]. Apart from AP, NAIP such as vivianite ($Fe_3(PO_4)_2·8H_2O$) can be present in raw sewage sludge as well [66]. The complete dehydration of vivianite to form graftonite ($Fe_3(PO_4)_2$) occurs at a temperature of 450 °C, which can further undergo the oxidation process and be transformed into iron orthophosphate

($FePO_4$) above 625 °C [67]. Moreover, a longer residence time and higher incineration temperature would lead to the formation of a glassy ISSA which resists acid extraction [38, 68].

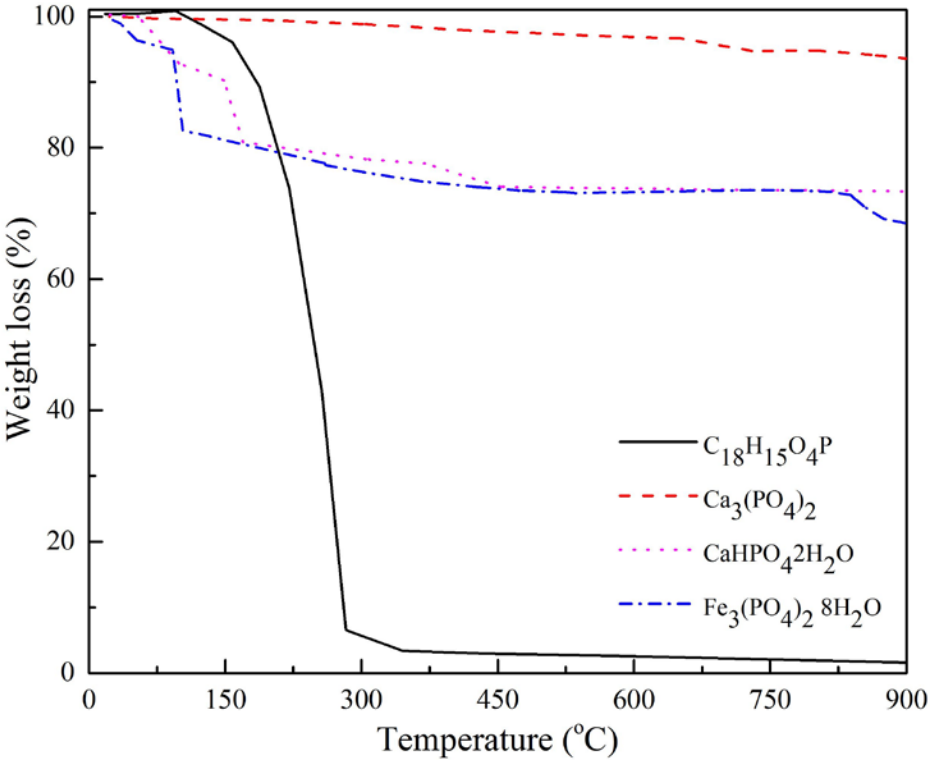

Figure 2-4 Weight loss of $C_{18}H_{15}O_4P$, $Ca_3(PO_4)_2$, $Fe_3(PO_4)_2 \cdot 8H_2O$ and $CaHPO_4 \cdot 2H_2O$ during heating to 900 °C in nitrogen [58]

2.2.3 Characteristics of ISSA

The characteristics of ISSA are determined by the composition of the ingoing sewage sludge and the incineration process (e.g., burner technology, combustion zone temperature and residence time). Differences in the incineration techniques cause different degrees of burnout of sewage

sludge and therefore carbonization of the resultant ashes [69, 70]. Table 2-2 shows the chemical distinctions between the ISSA produced by the cyclone burner and fluidized bed combustion system [69]. Although the sludges burned were different, it is interesting to compare the residual carbon contents, which estimate the degree of burnout achieved. The fluidized bed reactor achieved a high degree of burnout (0.2% carbon) while the cyclone furnace achieved a significantly lower degree of burnout (6.0% carbon). Another interesting comparison was the significantly higher content of Si in fluidized bed ashes (16.0%) compared to 6.8% in the ashes from the cyclone furnace. Apart from potential differences in the feed sludge, the additional Si content may be attributed to the continual loss of sand fines from the fluidized bed material [69].

The contents of elements that can bind with P (especially Ca, Mg, Al and Fe) will depend on the nature of the feed sludge and the choice of any inorganic flocculants or sludge dewatering aids. Higher contents of Ca and Al, which would significantly decrease the P extraction efficiency [71]. Moreover, due to the lower costs, the higher efficiency and improved environmental performance in comparison to the conventional multiple hearth type incinerator, fluidized bed combustors are considered to be the best available technology for incineration of sewage sludge worldwide [9, 72]. Table 3 compares the characteristics of ISSAs from several countries with varying incoming sewage sludge compositions and incineration

technologies [6, 10, 73, 74]. Comparing sewage sludge and ISSA, it can be seen that incineration causes the concentration of certain metals to increase by a factor of between 4 and 5. Particular concern should be given to As, Cd, Hg, Ni and Pb, for which the maximum concentrations in fertilizer are controlled by regulations [6]

Table 2-2 Characteristics of various ISSAs

Country	Combustion technology	P (%)	Concentration of major contaminant elements of concern in case of fertilizer application (mg/kg)									Reference
			As	Cd	Co	Cr	Cu	Hg	Ni	Pb	Zn	
German (24 incinerators)	Fluidized bed/ grate firing/ multiple hearth firing/ fluidized bed gasification	4.9-11.9;	5- 19	2.1-2.9				0.08-0.47	58.6-72.2	96.2-124		[10]
UK (7 incinerators)	Fluidized bed	5.3-7.6	7.1-42.5	0.1-9.4	.	91.7-1031	492-828	0-3.9	4-351	130-627	1226-2737	[6]
France	Fluidized bed	6.5	23	14	669	2636	2483	-	621	720	7103	[73]
Denmark	Fluidized bed	7.0/9.9	-	-	-	-	540/690	-	29/72	85/112		[75]
Netherlands (2 mono-incinerators)	Fluidized bed	11.8	35	3.8				-	67	250		[76]
Taiwan	Brick-firing kiln	7.8	-	8.9	-	75.7	432.6	-	-	199.4		[74]
Korea	-	10.7	29.8	12.5				-	86.9	823.9	2236	[77]
China	Muffle furnace	5.2-5.4	703-937	122-141	-	458-492	406-436	-	194-220	410-564	867-909	[78]

Krüger & Adam (2015) studied the ISSA produced from 24 facilities in Germany, which accounted for 97% of all ISSA produced in Germany. It was found sewage sources primarily determined the P content in ISSA produced, while the combustion technology mainly affected the carbon content in ISSA. To be specific, the P content in ISSA produced from municipal sewage sludge (mean value of 8.9%) was about 75% higher than that produced from industrial sludge (mean of 2.2%) [10]. The heavy metals of concern varied depending on the region. For examples, the ISSA produced in European countries had Ni and Pb as the most significant heavy metals, while those from Asia had Cd and As as the primary concern.

In comparison, the presence of metal(loid)s such as As, Cd, Hg, Ni and Pb are concern in ISSA, while the P-rock is associated with some radioactive elements [30, 79]. Apart from radioactive elements, P-rock also contains comparable contents of As, Cd and Cr to that of ISSA [40, 80, 81]. Therefore, both ISSA and P-rock need some processing before application in P fertilizer production. An advantage of using ISSA is the saving on extraction of raw materials as ISSA is readily available in urban districts.

ISSA is an amorphous, glassy material containing crystalline quartz (SiO_2) and hematite (Fe_2O_3) [6, 73]. This has led to ISSA being used in construction materials although this does generally represent a waste of P [6, 26, 82-86].

2.3 Recovery of phosphorus from ISSA through wet-extraction for fertilizer application

2.3.1 Wet-extraction of phosphorus from ISSA

P-recovery from ISSA for use as fertilizer requires three important processes: 1) extraction of P from ISSA; 2) separation of P from harmful heavy metals; 3) transformation of P into plant-available forms. The first process is of crucial importance because the efficient extraction of P determines the overall P recovery efficiency. Wet-extraction methods have received extensive attention due to high P extraction efficiency, simple operation and low cost [22]. However, in most cases, methods can cause the co-leaching of heavy metals from ISSA which inhibits use of the recovered P as fertilizers. Purification of the P leachate can be achieved by chemical precipitation, ion exchange or adsorption [87, 88]. The P containing extract can be directly used as a liquid fertilizer or recovered as other P precipitates which need to exhibit plant availability to be beneficial.

Wet extraction processes use different extraction reagents to dissolve P from the ISSA. These extraction reagents can be acid, base and a range of other reagents. Acid and base reagents have been the most extensively studied [41]. The reagents used and the corresponding superior P extraction conditions and efficiencies are summarized in Table 2-3.

(1) Acid extraction of P from ISSA

Acids are the most frequently applied agents used to extract P from ISSA. P is released through the acid-breakage of metal-P bonds, especially under strong acidic conditions (pH range of 1~2) [25]. The applied acids include both organic and inorganic acids such as H_2SO_4, HNO_3, HCl, H_3PO_4, citric and oxalic acids, as indicated in Table 2-3. Extraction processes employing H_2SO_4 are low-cost while those using H_3PO_4 are expensive [12].

Table 2-3 Optimal P extraction efficiency by various extracts

Extractant	Region		Major contents of ISSA (%)				Extractant Concentration (mol/L)	Liquid to solid ratio (mL/g)	Equilibrium time (hour)	P extraction efficiency (%)	Reference
			P_2O_5	CaO	Al_2O_3	Fe_2O_3					
H_2SO_4	Switzerland	Basel	8.9	22.8	9.1	15.6	1.4	2	10	99	[26]
		Winterthur	21.0	22.7	6.5	20.0	1.4	2	10	67/84	
	England	Blackburn Meadows	15.1	11.9	13.7	10.1	0.19	20	2	85	[89]
		Esholt	14.2	7.6	27.9	20.7	0.19	20	2	86	
		Calder Valley	13.5	9.2	15.0	24.3	0.19	20	2	72	
		Knostrop	17.6	8.8	32.0	6.8	0.19	20	2	88	
		Shell Green	13.0	10.4	13.3	23.3	0.19	20	2	75	
		Beckton	17.8	17.1	13.1	6.9	0.19	20	2	90	
		Crossness	16.0	18.9	12.1	6.7	0.19	20	2	91	
	China	Hong Kong	9.3	7.5	15.2	16.4	0.2	20	2	88	[90]
	Sweden	Mora	15.6	25.1	17.5	2.3	1.0	8	2	89	[91]
		Uppsala	13.3	9.1	5.8	15.1	0.8	7.5	2	91	
		Gävle	22.4	11.1	6.2	10.4	1.0	6	2	95	
	China	Wuhan	13.2	4.6	22.4	7.5	0.05	30	2	82	[78]
	Japan	Kumamoto	20.1	7.9	11.6	7.4	0.05	150	4	≈100	[25]
	United Kingdom	London (Crossnes)s	16.4	20.0	5.6	4.3	0.5	20	0.5	93	[19]
		London (Beckton)	17.2	15.3	6.6	5.3	0.6	20	0.5	90	

Table 2-3 Optimal P extraction efficiency by various extracts

Extractant	Region		Major contents of ISSA (%)				Extractant Concentration (mol/L)	Liquid to solid ratio (mL/g)	Equilibrium time (hour)	P extraction efficiency (%)	Reference
			P_2O_5	CaO	Al_2O_3	Fe_2O_3					
HCl	Japan	Kumamoto	20.1	7.9	11.6	7.4	0.1	150	4	≈100	[25]
	China	Shanghai	15.2	7.8	15.1	6.4	0.2	50	2	98	[65]
			27.4	10.3	9.9	5.7	0.5	50	2	95	
	China	Hangzhou	21.0	5.4	9.3	20.9	0.8	20	4	99.7	[92]
	Denmark	Avedore	13.4	20.6	5	2.2	12	3	-	62	[93]
	China	Wuhan	13.2	3.3	11.6	5.2	0.1	30	2	92.8	[78]
NaOH	China	Hong Kong	9.3	7.5	15.2	16.4	2.0	20	24	9.1	[90]
	China	Shanghai	15.2	7.8	15.1	6.4	0.8	150	2	28	[65]
			27.4	10.3	9.9	5.7	0.8	50	2	25.5	

There are many factors which can affect the P extraction efficiency and the most critical are acid concentration, liquid to solid ratio (L/S ratio) and reaction time [94]. Increasing the acid concentration increases P extraction efficiency because more intense conditions producing more available protons to break the metal-P bonds [95]. Similarly, a higher L/S ratio is favored because it allows improved P-extract separation and a higher P extraction efficiency is achieved by having more available protons [25]. However, higher P extraction efficiency is not only due to more H^+. Ottosen et al. (2013) found that when the concentration of acid (mole H^+ per g ash) was the same in the two extractions with different L/S ratio (0.19 M H_2SO_4 at L/S 20 and 0.38 M H_2SO_4 at L/S ratio 10), the extracted percentage of P was considerably less in the latter, demonstrating that P extraction is dependent on L/S ratio [75].

Reaction time is also an important parameter affecting the extraction process in practice. Kinetic studies of P leaching from ISSA using acid show that P leaching increases rapidly initially and then eventually reaches a slow increasing??? state (around 2 h), and slightly decreases afterwards [25]. In most cases, 2 h is selected as the optimal extraction time. Some studies show that 0.5 h was sufficient to extract P from ISSA [19]. Furthermore, an excessive leaching time can be detrimental due to increased metal(loid)s dissolution and P re-precipitation [75].

Due to differences in ISSA characteristics, the optimal P extraction conditions vary. Generally, a high content of Ca in ISSA causes a reduction in P recovery efficiency due to the rapid dissolution of Ca, resulting in a low ratio of P/Ca in the extract [68]. The highest P recovery efficiency of ISSA may occur at mass ratio of P/Ca in range of 0.74-0.92 g/g, which corresponds to a P/Al higher than 3.3 g/g [68]. In addition, the dissolution of Fe is strongly affected by the chemical phases present in ISSA, for example, hematite is fairly soluble in acids. P-phases that are encapsulated in unreactive materials such as a glassy phases can resist P extraction by impeding acid contact. Increased glassy phases are formed by a longer incineration times and higher incineration temperatures [68].

(2) Alkaline extraction of P from ISSA

The co-dissolution of heavy metals in acid leaching is inevitable because the extraction of heavy metals at the same or higher pH than P [75]. For fertilizer application, a complex separation process of P from the metal(loid)s is needed [41]. Alkaline extraction of P from ISSA has therefore also been investigated [65, 90]. The rationale behind P extraction from ISSA using alkalis includes a) amphoteric aluminum phosphate compounds present in ISSA can be dissolved in alkalis and b) only amphoteric heavy metals can be dissolved under alkaline conditions [41].

The alkali concentration, L/S ratio and extraction time influence the P

extraction efficiency. Not all ISSAs are suitable for alkaline treatment due to the varied forms of P present in the ISSA, which normally include whitlockite($Ca_3(PO_4)_2$), aluminum calcium phosphate ($Ca_9Al(PO_4)_7$), hydroxyapatite ($Ca_5(PO_4)_3(OH)$, aluminum phosphate($AlPO_4$) and iron phosphate ($FePO_4$). These are produced from the reaction of the P in sewage and inorganic flocculants during incineration [26, 89]. Only amorphous aluminum phosphate in the ISSA is reported to be extracted under alkaline conditions, while many aluminum phosphate are crystalline [34, 96]. In addition, the alkaline leachable amount of aluminum phosphate is affected by both the Ca and Al contents [41]. The alkaline P extraction efficiency is reported to be higher with a lower Ca content in ISSA [96]. The statistical data present in the study of Petzet et al. (2011) showed that when the molar ratio of P/Ca of ISSA exceeds 1.0, the alkaline leachable P can be more than 30% of the total P in ISSA [41]. For example, ISSA from the WWTP in Gifu (Japan) achieved a P extraction efficiency of 75% by direct alkali leaching because the ISSA had a high P/Ca molar ratio (2.0) [41]. However, in most cases, P extraction efficiencies from ISSA by alkalis are low (shown in Table 2-4), due to the presence of a high content of calcium phosphates (derived from potable water with a high hardness) [39, 41].

(3) Other extraction processes

Apart from acids and alkalis, other reagents have also been used to extract

P from ISSA. The combined use of acid and base for P recovery had attracted significant attention [41, 77]. This involved acid leaching with a fixed pH value of around pH 3.0~4.0 which transforms the calcium phosphate to aluminum phosphate in ISSA. The aluminum phosphate rich residue is then dissolved by alkali to achieve high P extraction efficiency and heavy metal removal, although this method is only efficient for Al-rich ISSA.

2.3.2 Production of P fertilizers

(1) Recovered as liquid P fertilizer

Liquid fertilizers account for 30% of the fertilizer market and are particularly used in developed regions [97]. Liquid fertilizer can be categorized into solution fertilizer, and suspension fertilizers according to Regulation (EC) No 2003/2003 of the European Commission [98]. Solution fertilizers have no solid particles in the fertilizer, while suspension fertilizers contain suspended particles.

Liquid P fertilizer can outperform granular P fertilizer because the improved mobility of a liquid fertilizer creats a uniform distribution of P in soil [99]. The high solubility, lability and diffusion of P from the liquid P fertilizer produces high P-fixing in calcareous soils but this is not significant in non-calcareous soil [100].

The liquid P-extract from ISSA produced by wet-extraction processes can be used as a liquid P fertilizer. However acidic P-extract need be purified, pH adjusted and additional nutrients added to give around 18% of $N+P_2O_5$ [68].

The composition of liquid fertilizers from ISSA will be determined by the composition of the ISSA, the chemical/thermal P extraction process and the purification method used. If the purity is sufficient high then the liquid P-extract can be processed into H_3PO_4, which is the most favored product for its various usage compared with other P fertilizers for the recovery of P in ISSA. Donatello (2010) developed a cation exchange column to purify the P-extracts and recover technical grade H_3PO_4, but the cost-effectiveness of the process is not clear [89]. Other studies also found that producing H_3PO_4 from ISSA requires a purifying process such as nanofiltration [101] and more studies are required to develop simple and low cost process.

(2) Recovered as solid P fertilizers

Solid P fertilizers are widely used and are produced using various kinds of P-precipitation processes. The solid mineral P-fertilizers contain $AlPO_4$, $FePO_4$, $Ca_3(PO_4)_2$, mono-ammonium phosphate and struvite ($Mg(NH_4)PO_4 \cdot 6H_2O$) [9]. Other than these, the liquid P can be absorb by absorption media, such as biochar, activated carbon, chelating agents, and

so on, thus recovering as solid P fertilizer.

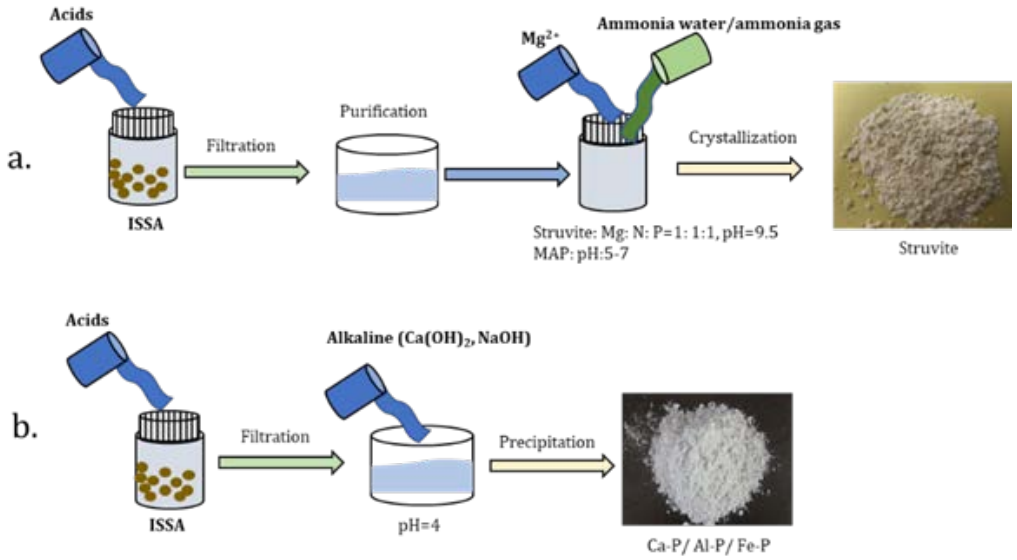

Figure 2-5 Production process of two major kinds of solid P fertilizer (a: MAP/struvite; b: Ca-P/Al-P/Fe-P) [102]

The production of process for mono-ammonium phosphate and struvite similar (Figure 2-5a), while the production of calcium phosphate and aluminum phosphate are also similar (Figure 2-5b). Struvite is a slow release fertilizer. During the production process, the P-extract is obtained by acid leaching of ISSA and the impurities are purified using various methods such as cation exchange [90]. Impurities such as metal cations (Al, Na, K, etc.) and anions (SO_4^{2-}, NO_3^-, Cl^-, etc.) inhibit the growth of struvite crystals by forming hydroxide salts or other non-struvite compounds in the alkaline environment and compete for PO_4^{3-} [102]. The crystallization of struvite is molar ratios of Mg^{2+}, NH^{4+} and PO_4^{3-} approaching 1:1:1 at pH 9.5 [90]. However, the disadvantages of this method is the requirement of

high purity P-extract and the high ammonium demand [12, 103]. Similarly to struvite, MAP is produced by adding ammonia solution or ammonia gas into a high-purity P-extract at a pH between 5 and 7 [14].

For aluminum phosphate, iron phosphate and calcium phosphate, selective precipitation of $Al_3(PO_4)_2(OH)_3(H_2O)_5$ and $Fe(II)_3(PO_4)_2(H_2O)_8$ by maintaining the P-extract pH between 3 and 4. Calcium phosphate ($Ca_3(PO_4)_2$) precipitates above pH 4 [71]. Because the P-extract has only a marginal Fe content, the resulted precipitately majorly consists of aluminum phosphate and calcium phosphate. The formation of the target P-precipitates can thus be achieved by pH control and stoichiometric dosing of Al, Ca or Fe to the P-extract.

The complex purification process required for P-extracts and the precipitation/crystallization process for P fertilizer production, has led to research investigating the use of plant-available media (such as biochar), to selectively sorb P from the acid-extract of ISSA. Biochar is a carbon based sorbent with high porosity, specific area and surface functional groups [104, 105]. Compared with other sorption media, biochar is more favored because it can be used as a soil conditioner to retain and release nutrients thus improving soil fertility, increasing seed germination rates and enhancing crop yields [106]. However, the biochar needs proper modification to alter its negatively charged surface and improve its surface area [107]. To recover P from liquid, modifying biochar with Mg and Ca

was favorable for producing plant-available modified biochar with formation of Mg-P and Ca-P particles [108, 109]. After sorption, the P-laden media can then be directly used as a P fertilizer.

2.3.3 Feasibility of agronomic application of recovered P fertilizers (RPF) from ISSA

Table 2-4 summarizes the P and heavy metal contents in recovered P products from ISSA. Not all the recovered P products can be utilized as fertilizers because the heavy metal contents of recovered P products may exceed the limits set by local authorities (see Table 2-5) or the plant availability of the recovered P product might be poor. It is therefore necessary to assess the agronomic effectiveness of recovered P products as fertilizers using plant cultivation experiments.

Table 2-4 P and heavy metal contents in RFPs from ISSA

Recovered P product	P content (%)	Heavy metals contents (mg/Kg) Reference							Reference
		Zn	Cu	As	Ni	Pb	Cr	Cd	
Aluminum and hydroyphosphates	7.9	2.2	30.5						[110]
Aluminum phosphate	19.2	160.7	399.5						[110]
Aluminum and calcium phosphates mixture	10.4	321.4	479.4						[65]
Calcium phosphate	15.3	4500	20730	27930	203	3374		74	[41]
Crystals of $CaClH_2PO_4 \bullet H_2O$	15	5.4	2.8	1.0	0.94	1.1	0.2	0.013	[93]
Reco Phos P38	Not clear	1580	663	9.1	47.3	51.4	118	2.2	[40]
Struvite	10.1	28	22	16		12			[90]
Struvite	14.2	5.4	10.6						[78]

Struvite	22.8	290.6	45.2		29.7	2.2	6.0	[92]
Thermochemically treated ISSA (with $MgCl_2$)	9.7	1110	220					[111]

Note：only the average value is shown in this table.

Franz (2008) conducted pot experiments to test the agronomic effectiveness of the RPF on the cultivation of Swiss chard, kohlrabi and corn in greenhouse. The results showed that the RPF had no adverse effect on the plants and the nutrients in RPF were effectively adsorbed by the plants. RPF was concluded to exhibit comparable agronomic effectiveness to commercial phosphate fertilizer [40]. Weigand et al. (2013) compared the fertilizing effect of RecoPhos P 38 (RPF) from ISSA to that of a conventional P-fertilizer (Triple Superphosphate) through cultivating maize (var. Lukas) and rapeseed (var. Ability) in soil [40]. The results showed that although the water-soluble and citrate-extractable phosphates from RPF were lower than those of the commercial P-fertilizer, the RPF exhibited comparable or superior fertilizing effects to the commercial P-fertilizer in term of the mass yield per pot.

Table 2-5 Legal limited values for trace elements in fertilizer [65]

Trace element	Germany	Austria	China	Switzerland	Turkey	Japan
As (mg/kg)	40	-				50
Cd (mg/kg)	4	15	10	3		5
Cr (mg/kg)	-	667	500	200	270	500
Cu (mg/kg)	70	778	-	400		
Hg (mg/kg)	1	1	5	3		2

Ni (mg/kg)	80		-	50	120	300
Pb (mg/kg)	150	100	150	200		100
Zn (mg/kg)	1000	3333	-	1300	1100	
Co (mg/kg)				40		

Cabeza et al. (2011) used ISSA (SI-ash) after heavy metals removal as a P source to cultivate maize in a 2-year experiment [112]. The proportions of total water-soluble P and 2% citric acid-soluble P were 6.4% and 31.4%, respectively, which were lower than that of triple superphosphate (water soluble ~90%) but higher than phosphate rock (water soluble: <0.01%, 2% citric soluble: 17.0%). When applied to an acidic sandy soil, the fertilizer efficiency of SI-ash was lower than that of phosphate rock although the opposite effect was observed when two fertilizers were applied to neutral loamy soil. This study showed that the effectiveness of RPFs is not well indicated by P solubility in water or citric acid, but is determined by the dissolution in soil. The relative fertilizer efficiency of SI-ash was significantly lower than that of triple superphosphate.

Lemming et al. (2017) directly utilized ISSA and thermally treated ISSA as P sources to cultivate spring barley in pot experiments [111]. The P solubility in water of both the ISSAs was less than 1%, which was significantly lower than that of triple superphosphate (46.2%). However, the water exchangeable P in the soil from thermally treated ISSA was higher than that of raw ISSA. As a result, the thermally treated ISSA had

higher agronomic effectiveness in terms of dry mass yield per pot and P uptake by plant. The plant available P for raw ISSA and thermally treated ISSA were 3.4 and 6.9%, respectively, which is significantly lower than that of triple superphosphate (12.8%). Both the ISSAs were not as effective as triple superphosphate for fertilizing spring barley.

The fertilizing effects of the RPFs remains controversial. It is hard to compare literature results due to different characteristics of RPFs and the different cultivation methods used in experiments. However, it can be stated that the agronomic effectiveness of RPFs cannot be determined simply by testing their P solubility in water or citric acid and P solubility in soil is a much better indicator.

There are too few studies on the agronomic effectiveness of the RPFs from ISSA produced by wet extraction methods. In addition, research has often ignored the high content of heavy metals present in the RPFs and the potential detrimental effect of this on plants [111]. Additionally, most plant cultivation tests were conducted using pot experiment and no long-term field experiments to test the agronomic effectiveness of RPF has been completed. This is because the complex P recovery processes make the production of large amounts of RPFs costly and time-consuming and the heavy metal contents in some RPFs exceed legal limits. It is recommended that more attention should be paid to address these issues in the future.

2.3.4 P recovery from ISSA as fertilizer in practice

The pilot- or full-scale applications of wet-extraction processes for P recovery from ISSA are mainly found in some developed regions that have no or limited P resources. The scarcity of P in these regions has motivated their people to recover P from secondary sources. Phosphoric acid is the most favorable product because it can be further processed to produce many P-fertilizers products . Table 2-6 gives a brief summary of some full-scale applications of P recovery from ISSA, which will be introduced detailly in the following part.

1) REMONDIS TetraPhos® [113]

A sewage sludge incineration plant located in Werdohl Germany commenced P recovery from ISSA in May 2018. The process adopted in this plant is mainly composed of two parts: a) leaching P from ISSA by phosphorus acid; b) purification of the P concentrated acid leachate as shown in Figure 2-6a. The phosphoric acid can extract more than 80 % of the P from the ISSA. After purification of the acid leachate by sulfuric acid to remove calcium ions, ion-exchange and selective nano-filtration to remove other heavy metals, a phosphorus acid named as RePacid® can be produced as the main final product. This product is suitable to be directly applied in industries or further processed to make other products including P-fertilizers, animal feed, and food supplements and so on. The process

also generates some byproducts like gypsum, salts ions, and residual ash as well. Some can find their application, for example gypsum can be used for the production of building materials; the aluminium and iron salts can be used coagulants in wastewater treatment. The application of the residual ash however is uncertain. Overall, the process can obtain around 18 kg H_3PO_4/h when ISSA is fed at around 50 kg DM/h.

2) A wet extraction process in Gifu, Japan [114]

In Japan, a full-scale plant located at a wastewater treatment plant in Gifu City started to recover P ISSA in April 2010. The process adopted in this plant is illustrated in Figure 2-6b. The P in ISSA is leached by alkaline under 50-70 ^oC. After solid liquid separation by a membrane-type separator, $Ca(OH)_2$ is added into the P enriched leachate and reacted under 20-50 ^oC to produce calcium hydroxyapatite (HAP). The final product named as Gifu-no-daichi® is a popular fertilizer among the local farmers. The insoluble residue can be applied as a soil improver after heavy metal elimination by acid washing. Overall, the process achieved a 30-40% of P recovery efficiency from the ISSA generated in Gifu City and produced around 300-400 t HAP per year.

3) A wet extraction process in Achi, Japan [115]

Nippon Phosphoric Acid Co. Ltd (NPA) is a famous phosphoric acid production company in Japan. In 2009, NPA started to study the feasibility

of substituting phosphate rock with ISSA to produce phosphoric acid by a wet acid process due to the sudden increase of phosphoric rock cost in 2007-2008. The commercial application of ISSA as a partial substitute of phosphate rock begun in Nov. 2012. The production process is briefly shown in Figure 2-6c, the phosphoric acid is obtained by acid extraction of the ISSA/phosphate rock, followed by filtration of the acid slurry and purification of the filtrate. Except from the phosphoric acid, gypsum is obtained that finds its application in cement, plasterboard and soil improvers. To ensure the quality of both phosphoric acid and gypsum, ISSA is fed at a low mass ratio (ISSA: PHOSPHATE ROCK) around 2.5%.

4) Phos4life® [116]

The scarcity of P reserves promoted the Switzerland government to recover P from ISSA. The major problem is the harmful substance present in the ISSA. A technical grade of phosphoric acid (74 %) can be obtained through a solvent-extraction process called Phos4life, which is illustrated in Figure 2-6d. The P is extracted from the ISSA by H_2SO_4. Iron present in the leachate is first removed as $FeCl_3$ solution. The P is then separated from the heavy metals by a solvent extraction process, and phosphoric acid is finally obtained by a concentration step. The generated residue can find its application in cement industry. The $FeCl_3$ solution can be reused as precipitates to remove P from wastewater. The process is predicated to be able to recover more than 95% of P from the ISSA as phosphoric acid and

simultaneously recycle other valuable substances.

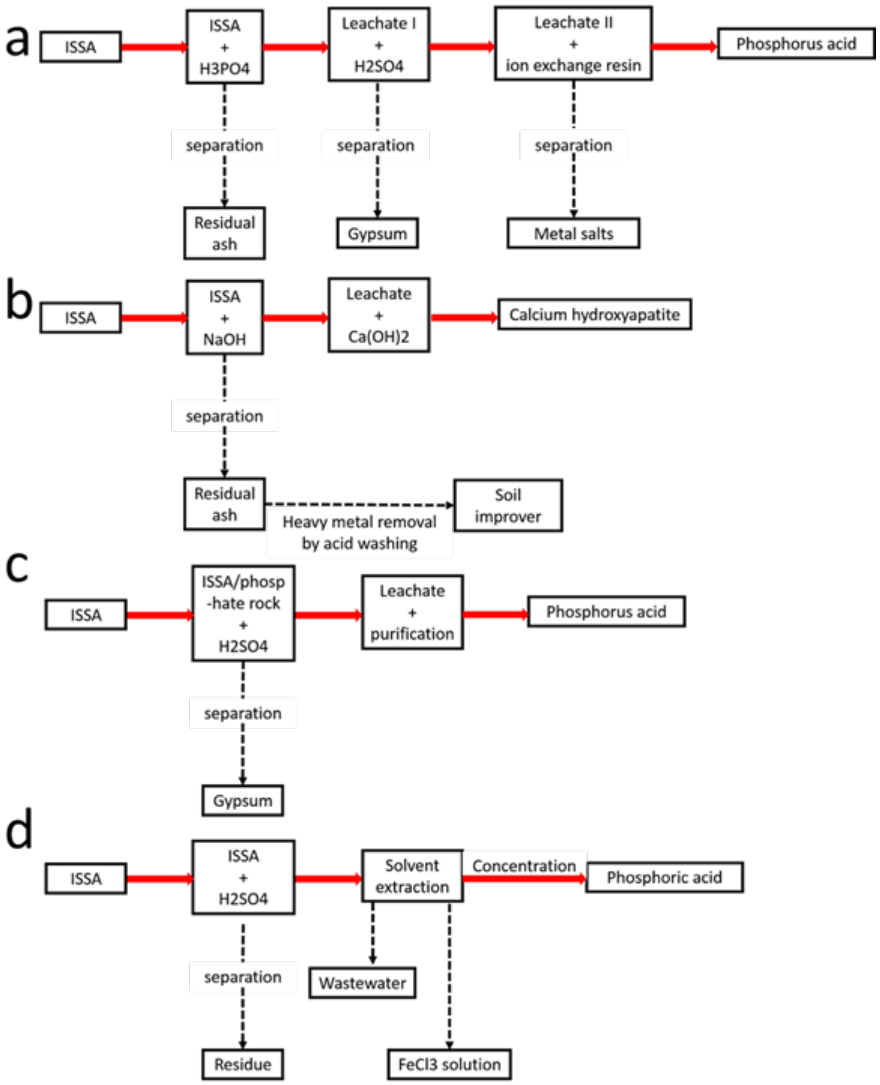

Figure 2-6 Schematic diagram of the a) REMONDIS TETRAPHOS® process; b) a wet P recovery process in Gifu City; c) a wet P recovery process in NPA; and d) Phos4life®

Table 2-6 Summary of the full-scale phosphorus recovery processes for ISSA

Location	Processes	Designer	Description	Products	Market	Reference
Germany (Sewage sludge incineration plant WFA Elverlingsen GmbH, Werdohl Germany)	REMONDIS TetraPhos®	Lippeverband with REMONDIS Aqua	The ash is reacted with phosphoric acid. The obtained leachate is purified by using sulphuric acid, ion-exchange and selective nano-filtration to get an industrial quality phosphoric acid.	Main product: phosphoric acid By-products: a) Coagulants: aluminium and iron salts; b) gypsum; c)Residue	Phosphoric acid: industrial application or further processed to make industrial products like P-fertilizers;	[113]
Japan (at a wastewater treatment plant in Gifu City)	A wet acid process	Local government and Metawater Co.	The ash is reacted with heated alkaline solution several times. Then leachate is obtained by a membrane-type liquid-solid separator. The leachate is then mixed with Ca(OH)2 to produce calcium hydroxyapatite.	Main product: calcium hydroxyapatite By-product: Residue	Local farmers	[114]
Japan (one production factory of NPA in Aichi)	A wet acid process	Nippon Phosphoric Acid Co., Ltd	The ISSA is mixed with phosphate rock at a mass ratio of 2.5%. The mixture is reacted with concentrated H2SO4, the slurry is filtrated and processed to obtain phosphoric acid and gypsum.	Main product: phosphoric acid By-product: gypsum	Available online	[115]
Switzerland (Canton of Zurich)	Phos4life®	Center for Sustainable Waste and Resource Management (ZAR) and the Technicas Reunidas (Spain)	P in ISSA is extracted by H2SO4. Iron is first isolated from the leachate and recovered as FeCl3 solution. Technical phosphoric is obtained via a solvent extraction process.	Main product: phosphoric acid By-products: a) acid insoluble ISSA residue; b) FeCl3 solution	Not mentioned.	[116]

2.4 Summary

The global P scarcity is aggravated by a lack of P recovery from waste, essentially resulting in a one-way flux of P-resources from concentrated P-rock deposits, to P-based products and then to the unrecoverable concentrations in the aquatic environment. Sewage sludge is a major source of P containing waste and its incineration produces ISSA, an inorganic ash in which P is concentrated. The presence of other elements in the sludge (Ca, Mg, Fe, Al and Cl especially), as well as incineration conditions (e.g. temperature and residence time) will influence the speciation and subsequent availability of P in ISSA.

A number of different techniques have been developed to convert the P in ISSA into a useful P fertilizer product. While each method has its advantages and disadvantages, the wet extraction method seems to be the most popular method investigated, due to its potential simplicity and low-cost. The major challenge with wet extraction methods is the subsequent purification of the extract to the point that it complies with any relevant limits for residual heavy metals in plant fertilizers. An alternative to purification is to use media with high P adsorption selectivities. The development of plant-available P adsorption media which can selectivity adsorb P from the P-extract and be directly used as P fertilizer is required. In addition, the quality and value of the final P-products need to increase

significantly to over-come the costs inherent to the extraction process. Agronomic evaluation of RPFs should be completed to identify harmful effects on plants and the ecology as the criteria for recovered fertilizer are currently inadequate.

The transition from using P-rock to recovery from P-waste may require a change in mindset and the associated business model needs to be modified and refined. Technology bottlenecks need to be overcome and governments need to develop effective policy to assist the development of P recovery from wastes. Researchers, decision-makers and industries should work together to find sustainable solutions to the future issues associated with the finite supply of P.

Chapter 3 Experimental Program

3.1 Introduction

This chapter presents the materials, research techniques and experimental process in characterization of ISSA, acid extraction of P from ISSA, plant-available P fertilizer and evaluation of agronomic effectiveness of recovered phosphate fertilizer produced in the recovery and fertilizer production experiments.

3.2 Phosphorus recovery and leaching of trace elements

3.2.1 ISSA characterization

ISSA was obtained from the T-Park sludge treatment facility in Tuen Men, HK. Prior to testing, the collected sample was coned and quartered to give representative samples and oven dried at 105 °C. Table 3-1 shows the physical properties and chemical composition of T-Park ISSA. The specific gravity was determined by water pycnometer method and the pH was determined at a weight ratio of 1:5 dry sample: distilled water. Drying ISSA resulted in a brown powder, which had a loss of ignition (LOI) of 0.99% on heating to 1000 °C for 30 min [117]. LOI is reported to vary between 0.9% and 2.1% in the United Kingdom's ISSAs [89], and the low LOI of HK's ISSA indicates good combustion of the organic content [118]. The mean particle diameter was very fine compared to previously reported

ISSA samples which had a mean particle diameter of ~250 μm [38]. The elemental P content was ~4.0 wt.%, which was lower than the ~6 wt.% reported in some European ISSAs [89].

Table 3-1 Characteristics of Hong Kong ISSA [119]

Parameter					
Specific gravity	2.49				
pH	8.45				
Mean particle size (μm)	56.0				
Specific surface area (m^2/g)	1.83				
Loss on ignition (%)	0.99				
Major elements (%)	Fe	Al	Si	Na	Mg
	15.82	6.12	15.56	1.64	0.93
	P	S	K	Ca	Cl
	3.99	1.61	2.90	6.82	0.281
Trace elements (%)	Cr	Ti	Mn	Ni	Cu
	0.059	0.330	0.096	0.026	0.145
	Zn	Rb	Sr	Y	Zr
	0.553	0.029	0.067	0.015	0.013

The total heavy metal content in the ISSA was determined by aqua-regia digestion following EN 13657 (2002). The total concentrations of P, Zn, Cu, Pb, As and Ni are shown in Table 3-1. Residues produced from different leaching tests were dried at 105°C and subjected to X-ray

diffraction (XRD, Rigaku SmartLab, Japan) for crystalline-phase mineralogy analysis using CuK α radiation (λ= 1.54059 Å) at 40 kV and 30 mA. The main crystalline phases were analysed by MDI Jade 5.0. Angles from 5 to 80° 2θ were scanned to identify peaks with increments of 0.02° and a counting time of 2 s per step. Chemical compositions of residues were analyzed by X-ray fluorescence (XRF) (Rigaku Supermini200). Specific surface area was measured by BET method which was carried out using nitrogen adsorption at a range of relative pressure p/p0 from 0.06 to 0.3. The morphology of gold-coated was determined using a Tescan-vega3 scanning electron microscope with energy dispersive X-ray spectroscopy (SEM-EDX).

3.2.2 Leaching experiments

The same leaching conditions were used for all leaching tests. A total of 20 g of dry ISSA was transferred to a 500 ml polypropylene bottle, 400 ml of leachant added, the lid sealed, and the bottle rotated end-over-end at 30 rpm for 2 h. Table 3-2 summarizes the six different types of leachants with the concentration gradients selected based on previous research [25, 89]. After leaching, the samples were centrifuged at 4,000 rpm for 10 min to allow solid-liquid separation. The leachates were then filtered through a 0.45 μm mixed cellulose esters membrane filters and diluted into the detection range of colorimetric testing for P analysis, using ammonium

molybdate to develop ‘molybdenum blue’ of which the absorbance was measured at 882 nm in a spectrophotometer and was directly proportional to the amount of phosphorus concentration. For trace element testing, the leachates were acid digested using concentrated HNO_3 at a volume ratio of 5:2 (sample:HNO_3) followed by inductively coupled plasma optical emission spectrometry (ICP-OES) (Perkin Elmer Optima 3300DV) analysis. The superior reaction conditions are given in Table 3-3 following the same leaching process as above. Under the fixed reaction conditions, the leachants were applied with various conditions, thus the optimal reaction condition was selected.

Table 3-2 Experimental design of comparison leaching abilities by different leaching agents

Agents		Concentration (mol/L)	Leachant pH
Inorganic acids	Nitric acid (HNO_3)	0.1	1.20
		0.2	0.88
		0.5	0.85
	Sulfuric acid (H_2SO_4)	0.1	1.3
		0.2	1.26
		0.5	0.89
Organic acids	Citric acid ($H_3C_6H_5O_7$)	0.1	2.03
		0.2	1.85
		0.5	1.70
	Oxalic acid ($H_2C_2O_4$)	0.1	1.35

Table 3-2 Experimental design of comparison leaching abilities by different leaching agents

Agents		Concentration (mol/L)	Leachant pH
		0.2	1.12
		0.5	1.01
Chelating agents	EDTA($C_{10}H_{16}N_2O_8$)	0.01	4.84
		0.02	4.74
		0.05	4.72
	EDTMP($C_6H_{20}N_2O_{12}P_4$)	0.01	2.12
		0.02	1.60
		0.05	1.32

Table 3-3 Experiment design of reaction condition optimization of sulfuric acid and EDTA

Agents	Condition optimized	Fix quantify	Variate
Sulfuric acid	Leaching time	Concentration: 0.2 mol/L, liquid to solid ratio 20:1.	10 min, 30 min, 60 min, 120 min, 240 min, 360 min and 1440 min.
	Concentration	Leaching time: 120 min, liquid to solid ratio 20:1.	0.1 mol/L, 0.2 mol/L, 0.3 mol/L. 0.4 mol/L, 0.5 mol/L, 0.7 mol/L and 1 mol/L.
	pH values	Leaching time: 120min, concentration is related to pH value, liquid to solid ratio 20:1.	1, 2, 3, 4 and 5.
	Liquid to solid ratio	Leaching time: 120 min, concentration 0.2 mol/L.	L/S ratios of 10, 15, 20, 25, 30, 40 and 50.

Table 3-3 Experiment design of reaction condition optimization of sulfuric acid and EDTA

Agents	Condition optimized	Fix quantify	Variate
EDTA	Leaching time	Concentration: 0.02 mol/L, liquid to solid ratio 20:1.	10 min, 30 min, 60 min, 120 min, 240 min, 360 min and 1440 min.
	Concentration	Leaching time: 120 min, liquid to solid ratio 20:1.	0.01 mol/L, 0.02 mol/L, 0.03 mol/L, 0.04 mol/L and 0.05 mol/L.
	pH values	Leaching time: 120 min, concentration is 0.02 mol/L, liquid to solid ratio 20:1.	pH of 1.7, 2.9, 7, 9.3 and 12.6.
	Liquid to solid ratio	Leaching time: 120 min, concentration 0.02 mol/L.	L/S ratios of 10, 15, 20, 25, 30, 40 and 50.

3.3 P recovery by combined two-step extraction and selective precipitation

3.3.1 Extraction process by two-step and single-step methods

The optimized conditions for metal(loid)s removal and P extraction using only EDTA or only sulphuric acid have been investigated [120]. However, when considering these extractions in sequence, it is evident that the first step with EDTA influences the mobility of heavy metals in the solids that are fed to the second step [121, 122]. It therefore becomes necessary to optimize the conditions for both steps, with the aim of achieving the highest

P recovery with the lowest metal(loid) impurities.

The two-step extraction method is illustrated in Figure 3-1. The variables of the EDTA (1st step) single-factor optimization conditions are shown in Table 3-4, which includes concentration, liquid to solid ratio and reaction time. For extraction experiments, 1.0 g of dried and homogenized ISSA was weighed (±0.005) and transferred into a 50 ml centrifuge tube. The EDTA reagent (concentration and volume according to Table 3-4) was added, and the tube placed on an end-over-end mechanical rotator at 30 rpm for continuous mixing (contact times are given in Table 3-4). After the EDTA extraction, the mixture was centrifuged at 4000 rpm for 10 minutes. The supernatant was withdrawn, filtered using a 0.45-µm mixed cellulose ester membrane filter paper and analyzed for metal(loids) by inductively coupled plasma optical emission spectroscopy (ICP-OES, SPECTROBLUE FMX 36) and for P by colorimetry after molybdenum blue complex formation. Prior to the second step, the solid residues were washed with deionized water to remove excess EDTA and then dried at 105 °C overnight.

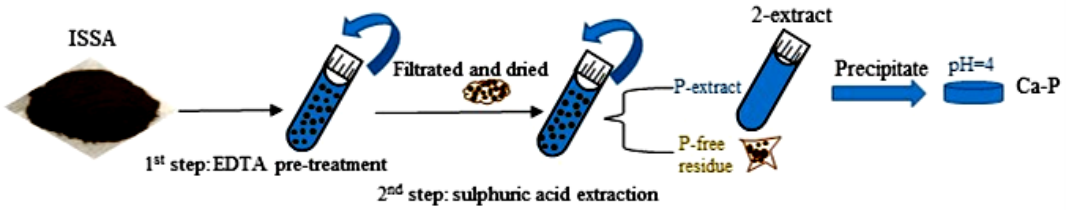

Figure 3-1 Process of two-step extraction

Table 3-4 Mix design for single-factor conditions optimization of EDTA pretreatment of two-step extraction

Agents	Condition optimized	Fix quantify	Variate
1st step: EDTA	Concentration	Reaction time: 120 min, liquid to solid ratio 20:1.	0.01, 0.02, 0.03, 0.04 and 0.05 mol/L.
	Liquid to solid ratio	Reaction time: 120 min, concentration 0.02 mol/L.	Liquid to solid ratios of 5:1, 10:1, 20:1, and 40:1.
	Reaction time	Concentration: 0.02 mol/L, liquid to solid ratio 20:1.	10 min, 30 min, 60 min, 120 min, 240 min, 420 min and 1440 min.
2nd step: sulphuric acid	-	Concentration is 0.2 mol/L, 20:1 of liquid to solid ratio and 120 min of reaction time.	-

The second step involved adding sulphuric acid under the optimized conditions (0.2 mol/L, 2 hours, 20:1 of liquid to solid ratio) as identified [120]. For comparison, a single step extraction was also carried out, also using 0.2 mol/L H_2SO_4, 2 hours contact time and liquid to solid ratio of 20:1, as in chapter 4. All the tests were carried out in triplicate and the average results were reported, and the error bars in the respective figures indicate the standard deviations.

The extracted mass of P and metal(loid)s were calculated using the equation:

$$\text{Extracted mass } (\text{mg} \cdot g^{-1}) = \frac{c \times T \times V}{M_0} \qquad (3-1)$$

Where, *c* is the concentration of the metal(loid)s or P in mg/L, *(c)*; *T* is the

dilution factor; *V* is the volume of extract, *(L)*; and M_0 is the mass of the ISSA before processing, *(g)*.

3.3.2 pH adjustment for obtaining the P-precipitates

Final extracts were subjected to pH adjustments to precipitate P from solution. A 40 ml aliquot of the extract was added to a beaker with a magnetic stirrer and continuously mixed. The pH was increased incrementally by addition of NaOH or $Ca(OH)_2$ while a pH electrode was used to continuously monitor the pH. When the target pH was reached, the resulting suspension was centrifuged at 4000 rpm for 10 minutes. The supernatant was filtered through a 0.45-µm mixed cellulose ester membrane filter and tested for P and metal(loid)s. The remaining precipitate was dried at 105 ^{o}C overnight prior to further analysis.

The MINTEQ modelling was used to predict the balancing of cations and anions in liquid. The MINTEQ modelling is a software for calculating ion form, complexation constant and chemical equilibrium.

3.3.3 P-precipitate analysis

The crystalline-phases in the dried and milled precipitate were analysed by X-ray diffraction (XRD, Rigaku Smartlab, Japan). The CuKα radiation (λ= 1.54059 Å) at 40 kV and 30 mA was used for scanning. Peaks were identified in the range from 5 to 70° 2θ with a scanning increment of 0.02°

and a counting time of 2 seconds per step. For qualitative analysis, the Rigaku XRD software (PDXL) was applied for Rietveld refinement phase verification. The elemental composition of the precipitates were analyzed by X-ray fluorescence (XRF, Rigaku Supermini 200). The micro-morphology of the precipitate was observed using scanning electron microscopy (Tescan-vega3) with energy dispersive X-ray spectroscopy (SEM-EDX).

3.4 Production of P-laden biochar

3.4.1 Preparation of biochars

Peanut shells (Ps) and sugarcane bagasse (Sc) were obtained from a food factory in Shenzhen, China. Prior to use they were thoroughly washed in deionized (DI) water, oven-dried at 105 ^{o}C overnight and milled to pass through a 2 mm sieve.

Solutions of $MgCl_2$ and $CaCl_2$ were prepared by dissolving 40 g of $MgCl_2 \cdot 6H_2O$ and 50 g of $CaCl_2 \cdot 2H_2O$ (AR Grade, Fischer Scientific) separately in 60 mL of DI water [108, 123]. The biomass samples were modified by soaking them in the prepared solutions for 1 h (mass to volume ratio of 1:3). The modified biochars were separated by using a vacuum filter with Whatman No. 42 filter papers and then oven-dried at 105 ^{o}C until achieving constant mass. The Mg/Ca modified biomass samples were then

pyrolysed at 450 °C, 700 °C or 850 °C for 1 hour in an inert N_2 atmosphere. Samples were heated to the target temperatures at a heating rate of 10 °C/min and N_2 (99.9 vol. % purity) flow rate of 11 L/min was maintained in order to remove the pyrolysis off-gasses. The biochars formed were ball milled and sealed in vacuum desiccators prior to carrying out the sorption tests.

The biochars produced were labelled based on the biomass (Ps/Sc) used, the modifying solution ($MgCl_2$/$CaCl_2$) and the pyrolysis temperature (450, 700 and 850 °C). For example, Ps modified by $CaCl_2$ at 450 °C was labelled PsC450. Sc modified by $MgCl_2$ at 700 °C was labelled ScM700..

3.4.2 Characteristics of biochars

The zeta potential of the biochars was determined (Brookhaven Instruments, Holtsville, NY) [124]. The organic functional groups on the biochars surfaces before and after sorption were determined by FTIR analysis (Nicolet Nexus 410) in the range 4000-400 cm^{-1}. The pH of the biochars was evaluated at a mass ratio of of 1:5 (dry sample: distilled water) by a pH meter (PHS-3C, LEICI). The surface area of the biochar was measured using the Brunauer-Emmett-Teller (BET) method using N_2 sorption over a range of relative pressures (P/P0) from 0.06 to 0.3. The crystalline phases in the ball-milled biochars were analyzed by using XRD (10-80 °) (Rigaku Smartlab, Japan). The surface morphology and chemical

compositions of the biochars before and after sorption were examined using a Tescan-vega3 SEM-EDX.

In addition, the biochars produced by the optimal modification method were measured by an elemental analyzer (Elementar vario EL) for C, H and N. The total P and metal(loid)s concentrations of the optimal biochar before and after sorption were measured after aqua-regia digestion. The P concentrations were measured using a spectrophotometer and the metal(loid)s were measured using inductively coupled plasma optical emission spectroscopy (ICP-OES, Spectoblue FMX 36), as in previous work [125].

Table 3-5 Characteristics of two kinds of P-extracts

P-extract	pH	Concentration of major metal(loid)s (mg/L)	Concentration of minor metal(loid)s (μg/L)	Zeta potential
1-step method	1.0	Ca (2068), P (1645), Al (1309), Mg (6), Fe (4.6), Zn (0.7), Cu (0.3), Mn (0.16)	As (10.6), Ni (10.8), Pb (10.2), Cr (1.3)	-0.41
2-step method	1.1	Ca (2658), P (1282), Al (819), Mg (3), Fe (3.6), Zn (0.3), Cu (0.1), Mn (0.09)	As (10.6), Ni (10.8), Pb (10.2), Cr (1.3)	-1.29

3.4.3 Selection of the optimal sorbent

The effect of biomass type, pretreatment method and pyrolysis temperature of biochars on P removal from the acid-extract was studied using ten different biochars (Ps700, PsM700, PsC450, PsC700, PsC850, Sc700, ScM450, ScM700, ScM850 and ScC700). Two replicates were carried out

for each test and additional replicates were performed whenever the deviation was higher than 5%. To avoid the influencing effect of P-extract characteristics and increase the effect of the biochar types on P sorption, the P-extract was diluted 4 times and adjusted to pH 2 prior to the sorption tests.

A mixture of 0.1 g of biochar and 10 mL of P-extract was continuously agitated using an end-to-end shaker at room temperature (23±2 ^{o}C) for 24 h. The mixture was then centrifuged at 4000 rpm for 5 min and the supernatant was filtered through a 0.45 μm mixed cellulose ester membrane filter prior to P and metal(loid)s analysis by ICP-OES.

The removal capacity (Q_e in mg-P/g dry biochar) of P or meta(loid)s was calculated according to Eq. (6-1):

$$Q_e = \frac{(C_0 - C_e)V}{\mathrm{m}} \qquad (3\text{-}2)$$

where, C_0 (mg/L) is the initial concentration of P or metals in the P-extract, C_e (mg/L) is the equilibrium concentration of P or metal(loid)s in the P-extract adsorption, V (L) is the volume of P-extract and m (g) is the mass of biochar used.

3.4.4 Sorption tests

(1) Effect of initial pH of P-extract

Based on the results in part 3.4.2, biochars of PsM700 and ScM700 were

selected as the optimal P sorbents and they were used in the sorption tests carried out at room temperature. The 4 times diluted P-extracts with different pH (1, 1.3, 1.6 and 2) were used to evaluate the effect of pH on P sorption. The pH of the extract was adjusted by adding either 1 M NaOH or HCl. Transformation between different forms of phosphate (H_3PO_4, $H_2PO_4^-$ and HPO_4^{2-}) in the pH range studied was assessed using Visual Minteq 3.1. The supernatants were collected after 24 h of sorption for P and metal(loid)s analysis.

(2) Kinetic sorption

The P-extract was diluted 4 times and adjusted to pH 2. The sorption process was the same as in the batch sorption experiments except that the solution samples were collected after sorption for 5, 10, 20, 40, 60, 80, 120, 240, 360, and 720 min.

Three common models were applied to fit the experimental data, which are pseudo-first-order, pseudo-second-order and intra-particle-diffusion (IPD) model [126]. These models are described by Eqs. (3-3), (3-4) and (3-5) respectively.

$$\ln(Q_e - Q_t) = \ln Q_e - K_1 t \qquad (3-3)$$

$$\frac{t}{Q_t} = \frac{1}{K_2 Q_e^2} + \frac{t}{Q_e} \qquad (3-4)$$

$$Q_t = K_{id} t^{0.5} + C \qquad (3-5)$$

where, Q_e (mg/g) is the P sorption capacity at equilibrium; Q_t (mg/g) represents the P uptake at time t; K_1 (min^{-1}), K_2 ($g \cdot mg^{-1}min^{-1}$) and K_{id} ($mg \cdot g^{-1}min^{-1/2}$) are rate constants.

(3) Sorption isotherms analysis

Sorption isotherms were obtained using a range of different concentrations (3-5800 mg/L) of the P-extract. To obtain higher concentration of P-extract compared with the alluded P-extract, 2.5 g of ISSA was dissolved in 20 mL of acid. While a lower concentration of P-extract was produced by dilution. Supernatants were collected after 24 h.

Langmuir, Freundlich and Sips models (Eqs. (3-6), (3-7) and (3-8) respectively) were applied to fit the sorption isotherms results.

$$Q_e = \frac{Q_m K_L C_e}{1 + K_L C_e} \qquad (3-6)$$

$$Q_e = K_F {C_e}^{1/n} \qquad (3-7)$$

$$Q_e = \frac{Q_m K_s C_e^{1/n}}{1 + K_s C_e^{1/n}} \qquad (3-8)$$

where, Q_e (mg/g) and C_e (mg/L) are the sorbed capacity of biochars and concentration of P-extracts at equilibrium, respectively; K_L (L/mg), K_F ($(L/mg)^{1/n}$) and K_s ($(L/mg)^{1/n}$) are constants of these three models; and n is the heterogeneity factor.

The biomasses were twice washed by distilled water then oven dried at 105

^{o}C for 24 hours. Then dried biomass was milled to pass a 2 mm sieve amendment. The modification reagents, $MgCl_2$ and $CaCl_2$, were separately prepared by dissolving 40 g of $MCl_2 \cdot 6H_2O$ and 50 g of $CaCl_2 \cdot 2H_2O$ into 60 m distilled water, with referring to relevant studies [108, 123]. Modification was carried out through soaking biomass into prepared regent by solid to liquid ratio of 1:3 for 1 h and oven-drying for 48 h.

The Mg/Ca biomass underwent carbonization at the denoted pyrolysis temperature (450, 700 or 850 ^{o}C) by heating at a rate of 10 ^{o}C/min and maintained for 1 h under N_2 flow. Nitrogen (99.9 vol. % purity) with a flow rate of 111/min was used to keep an inert atmosphere during the pyrolysis process and elute pyrolysis off-gasses from the chamber. Finally, the produced biochars were stored separately in vacuum desiccators before use in sorption tests.

0.1 g of biochar was added into 10 ml of the produced P-extract and the mixture was mixed in an end-to-end rotary extractor at room temperature for 24 h. Then the mixture was centrifuged at 4000 rpm for 5 min and the supernatant was filtered through a 0.45-μm mixed cellulose ester membrane filter for P and metal(loid)s analysis. After solid-liquid separation, the precipitate was the P-laden biochar.

3.5 Agronomic effectiveness evaluation of recovered RPFs

3.5.1 Characteristics of RPFs

Three kinds of RPFs, P-loaded biochar (BP), P-precipitate (CaP) and struvite (SP), are produced from Hong Kong ISSA by different methods and processes, as previous alluded [125, 127, 128].

For characterization of RPFs, they were digested using aqua-regia, then P and heavy metal concentrations in the filtrates were measured using spectrophotometer and inductively coupled plasma/optical emission spectroscopy (ICP-OES, FMX 36, SPECTROBLUE), respectively. The chemical compositions of these three fertilizers are showed in Table 3-6.

Table 3-6 P and heavy metal contents in SP, MP and BP

Items	P	Heavy metal (mg/kg)				
	(mg/g)	As	Cd	Cu	Pb	Zn
SP	63.1	9.3	N.D.	26.6	54.7	37.6
CaP	61.9	18.0	19.0	48.0	120.0	136.0
BP	30.8	13.0	10.0	60.5	130.0	215.5

3.5.2 Pot experiment

Hydroponics: The choy sum, one of the major and most favorable vegetable crops in southern China, which has a low variation in growth [129], was cultivated in hydroponics using Hoagland's nutrient solution with P substituted by RPFs under indoor environments for a 30-day period

in Hong Kong Polytechnic University from September 30 to October 29 in 2018 [130]. Because of the short growth period for leafy vegetables, fertilizers were commonly applied one time for choy sum growth [131]. The RPFs and monopotassium phosphate (MP, KH_2PO_4) were applied at the beginning of the cultivation at a rate of 31 mg P/L, with an unfertilized blank control (BC) as a reference. Each treatment was conducted in triplicate.

To be more specific, firstly the seeds of choy sum were disinfected using 95% ethanol and germinated on moistened filter paper in the dark at 22 ^{o}C. After a 7-day germination period, two seedlings of uniform growth were selected and transferred into a pot (height:11 cm, bottom 10 cm and mouth 12 cm) containing 500 mL Hoagland's nutrient solution with P from RPFs and MP. The water level was recorded at the beginning and the nutrient solution without P was provided once every 2~3 days according to the water level. The group name of pots was based on the applied fertilizer.

Soil cultivation: Ryegrass used in this experiment is a kind of hardy grass. A round plastic pot with a diameter of 27 cm and a depth of 20 cm were used. Prior to sowing, the seeds of the ryegrass were sterilized with 95% ethanol for half of an hour and soaked in deionized water for 3 hours. The sowing was carried out by spreading 20 g of urea evenly into the 1.5 kg sieved soil followed by covering with 1 kg of the sieved soil. (This soil was sampled from the campus of the Southern University of Science and

Technology, Shenzhen, China.) Then P fertilizer was applied separately with the same P content (5 g P-precipitate and struvite, 10 g P-loaded biochar and 1 g compound fertilizer) and then again covered with 0.5 kg sieved soil (the control group, blank controlled group, only covered soil). Finally, an aliquot of sterilized seeds (around 100 grains) was sowed uniformly and carefully and covered with another 0.5 kg of the sieved soil. During the cultivation, distilled water was added to each pot once every two days. The effect of RPFs on growing of ryegrass was compared with the compound fertilizer group and the blank controlled group. The experiment of each group was conducted in triplicate. These five of experiments were separately and synchronously carried out outdoor under natural sunshine conditions over 40 day in the campus of the Southern University of Science and Technology from September 1 to October 10.

3.5.3 Determination of physicochemical characteristics of the plants

The visual growth conditions of choy sum/ryegrass were recorded using the cameras of smart phones. For the choy sum, the number of leaf and the maximum leaf size were recorded at 7^{th}, 13^{th}, 21^{st} and 30^{th} day. For the ryegrass, conditions were recorded at day 30 and 40 and finally harvested at day 40.

The length (distance from the leaf base to the leaf tip) of leaf, fresh weight and dry weight (105 ℃ for 2 hours, and 60 ℃ until constant weight) of

the shoot were measured [132]. The chlorophyll contents of the plants was determined using spectrophotometer after 24-hour extraction of the cut leaf using 95% ethanol. Referring to the NIST SRM 2711a [133, 134], the total digestion was carried out on a ball-milled plant samples by using concentrated $HNO_3/HClO_4$ (4:1) on a hot plate, then the elemental concentrations in the filtrates were analyzed, as in previous ICP analyzation process.

3.5.4 Data analysis

Statistical analysis (one-way analysis of variance, ANOVA, Fisher Least-Significant Difference--LSD) were conducted using Origin 8.0 (OriginLab, USA). In all cases, a value of $p<0.05$ was considered to be statistically significant, compared to the control group.

Choy sum, one of the major and most favorable vegetable crops in southern China [129], was cultivated in hydroponics using Hoagland's nutrient solution with P substituted by RPFs under indoor environments for a 30-day period in the laboratory of the Hong Kong Polytechnic University. Because of the frequent cultivation and short growth period for leafy vegetables, fertilizers are commonly applied one time for choy sum growth [131]. Three kinds of RPFs: struvite (SP), calcium phosphate compounds (CaP) and P-loaded biochar (BP) along with monophosphate fertilizer (MP) were applied at the beginning of the cultivation at a rate of 31 mg P/L, with

an unfertilized blank control (BC) as a reference. Each treatment was conducted in triplicate.

To be more specific, firstly the seeds of the choy sum were disinfected using 95% ethanol and germinated on moistened filter paper in the dark at 22 ^{o}C. After a 7-day germination period, two seedlings of uniform growth were selected and transferred into pots (height:11 cm, bottom 10 cm and mouth 12 cm) containing 500 mL Hoagland's nutrient solution with P from RPFs and MP. The water level was recorded at the beginning and the nutrient solution without P was provided once every 2~3 days according to the water level. And the group name of the pots was based on the applied fertilizer.

Chapter 4 P and metal extraction from ISSA

4.1 Introduction

The daily produced ~1,200 tonnes of sewage in Hong Kong is transported to the T-Park sludge treatment facility. The combustion gases generated are maintained at >850°C for >2 seconds to inhibit formation of organic pollutants, and the resulting ISSA is currently landfilled. Increasing production of ISSA will place an additional burden on the already limited landfill capacity available in HK. The government claimed that all of the landfill capacity in HK will be exhausted in 2019 if there is no landfill extension.

During sewage sludge incineration ~75-98% of the P is retained in the ISSA [135]. The P content in ISSA is typically in the range of 10.0-25.7% as P_2O_5 [77, 136], which is comparable to the P content in commercially exploited phosphate minerals (5-40 wt.% P_2O_5) [137]. The demand for P fertilizers is increasing and economically extractable P-containing reserves are shrinking [77, 138]. It is therefore critical to either recover P from waste streams wherever possible or develop alternative P sources [139]. Extracting P from ISSA has several advantages as this does not involve mining, and the primary by-product is a Si-rich residue that has potential for use as a pozzolan in concrete [89]. ISSA is a P-rich solid waste and should be used to conserve P-containing mineral resources [25, 135, 140].

Various methods can extract P from ISSA. These include thermo-chemical extraction [136, 141], electro-dialytic [142, 143], and chemical extraction methods [89, 144]. Chemical extraction is the most widely used method for its high efficiency and low cost, but it also leaches metal/metalloids contaminants present in ISSA [75]. For P recovery from the P-containing leachate, P can be precipitated by adjusting to pH 4 but it is necessary to transform the metal-P precipitates into plant-available fertilizer by adding Ca^{2+}, NH^{4+}, Mg^{2+} and other kind of cations [26, 144, 145]. Thus, the conventional method for P extraction results in low P recovery because P losses in complicated purification process[144].

For separating P from metals/metalloids by different types of leachants, it is necessary to find suitable leaching agents for P extraction and metals/metalloids removal, respectively. Inorganic acids leach alkali metal oxides and most of P-containing phases [26, 144], of which sulphuric acid and nitric acid have been proven to be most effective. Organic acids induce chelating effects that greatly increase leaching of metals/metalloids from ash and soil and they are widely used in washing [146-149] and flushing / heap leaching technologies [150, 151]. Citric acid and oxalic acid were found to have relatively high P extraction and metal leaching capacities, whereas synthetic chelating agents such as EDTA and EDTMP were effective for metal removal by complex formation [152-155]. They may be applied as a pre-treatment to P recovery from ISSA.

Impurities of Cu, Zn, Pb, Ni and As should not be in phosphate fertilizers and these were the targeted metal/metalloids in this part. The presence of Cu, Zn and Ni is toxic for plant growth, while Pb and As are toxic for cells [156-158]. Previous work evaluated the characteristics of ISSA generated in HK and found high concentrations of heavy metals but with relatively low leachability, thus ISSA in HK is classified as a non-hazardous material [159]. The P in ISSA has a high mass ratio and good leachability thus is suitable for extraction and recycling.

This chapter investigated the effects of two inorganic acids (sulphuric acid, nitric acid), two organic acids (oxalic acid, citric acid), and two chelating agents (EDTMP and EDTA) on the leaching characteristics of P and trace elements in ISSA. The leaching behaviour of Cu, Zn, Pb, Ni and As were compared to the leaching of P. The aim of this chapter was to select a suitable P leaching regent and a metal(loid)s leaching agent. The residues produced after different leaching procedures were analyzed to determine composition, microstructure and BET surface area. The combined use of a superior pre-leaching agent and a superior P leaching agent would suggest a new P leaching route. The leachate of the leaching route would be the P-containing resource for P fertilizer production.

4.2 Results and discussion

4.2.1 P leaching

The P leaching data using different leachants are shown in Figure 4-1, given as mean values (expressed in mg P/g ISSA) and standard deviations derived from three replicates. Increasing the concentration gradient increased P leaching, especially for nitric acid, which increased from 2 mg P/g ISSA to 36 mg P/g ISSA. Despite the variation of phosphate speciation (e.g., aluminium phosphate, iron phosphate, and calcium phosphate), inorganic acids can extract all these phases of P penetrating and dissolving the ISSA gradually with high concentration (higher than 0.5 mol/L) [75, 160, 161]. Sulphuric acid gave better results compared to nitric acid probably because it released more P at the same concentration due to the double concentration of H^+ ions. Organic acids also produced good P leaching, with 0.2 mol/L of oxalic acid leaching >95% of P and citric acid leaching about 80% of P with same concentration [25, 162]. The chelating agents had limited ability to leach P from ISSA. As they have high affinity to metal ions, the partial dissolution of P may be related to the dissolution of metals and the destabilization of metal-phosphate bonds, thus P was released into leachate [163]. The 0.05 mol/L EDTA leachant released ~40% of P content of ISSA, but reducing the EDTA concentration to 0.02 mol/L reduced leaching by 50% (5 mg P/g ISSA). In comparison, EDTMP only

leached a maximum of ~25% P.

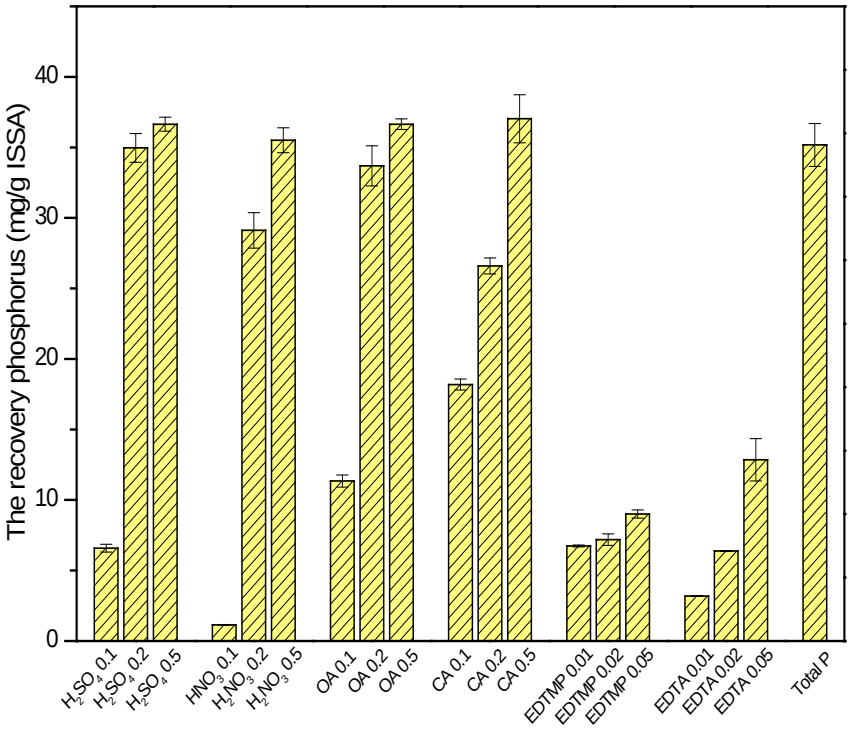

Figure 4-1 Recovery of P from ISSA using leachants. Oxalic acid is abbreviated to 'OA' and citric acid to 'CA'

The variations in the pH of leaching solutions during the tests are shown in Figure 4-2. Because HK ISSA is alkaline ash, it neutralize the acidic pH but this effect depleted by strong acids. When concentrations higher than 0.2 mol/L (such as 0.5 mol/L of nitric acid and oxalic acid), the small difference in pH value before and after leaching suggests the presence of some redundant acids in the leachate. Both inorganic and organic acids are able to extract all of the P at sufficiently concentrations while sulphuric acid performed best, but the suitable leachant should be selected considering the metal leaching capacities, which will be discussed in the

following section. From the economic point of view, sulphuric acid was the most efficient leachant because the sulphuric acid was the cheapest of all used agents.

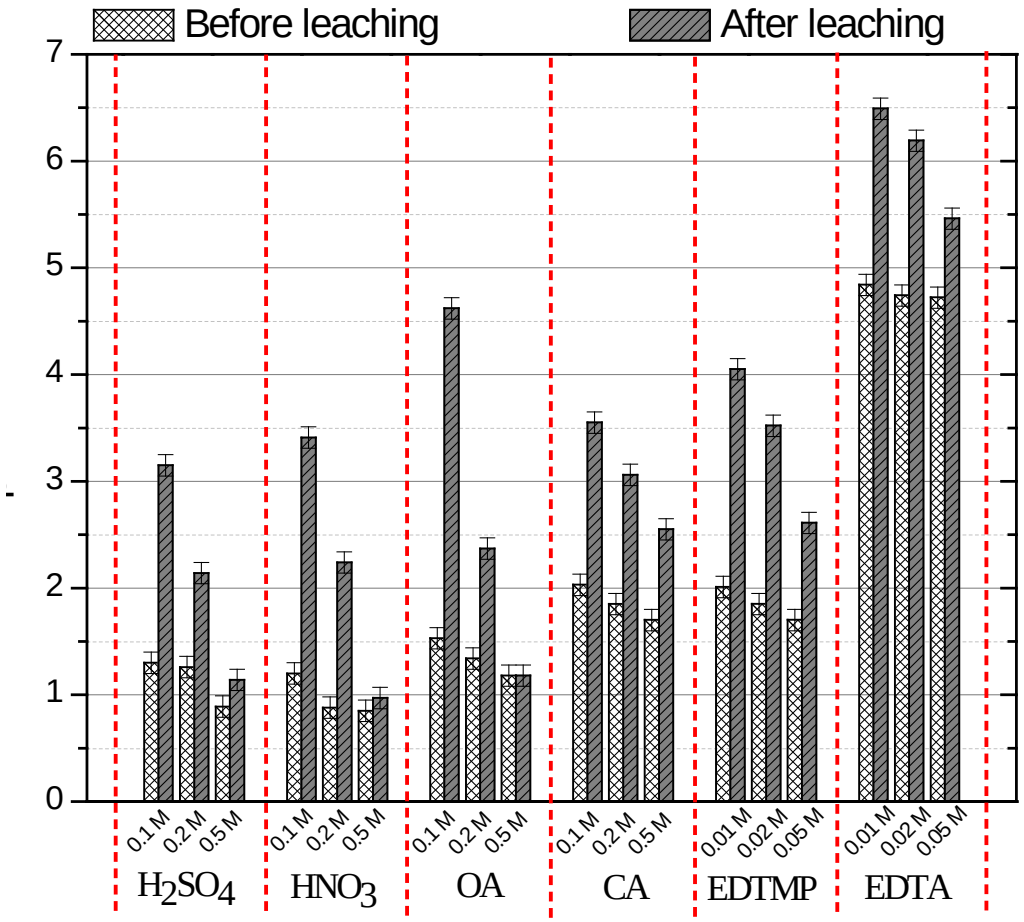

Figure 4-2 pH variations in different agents before and after leaching

Almost complete P extraction was obtained from ISSA using 0.19 and 0.38 mol/L H_2SO_4 at liquid-to-solid ratio of 20 [75]. According to calculations of acid requirement [26], 20 ml of 0.2 mol/L H_2SO_4 should be sufficient to dissolve all phases containing P, which exist as $FePO_4$, $AlPO_4$, $Ca_3(PO_4)_2$ or mixed forms of these compounds [89]. Hence, optimum P leaching was

obtained using 0.2 mol/L H_2SO_4. Chelating agents gave limited P leaching, especially at concentrations below 0.02 mol/L.

4.2.2 Trace element leaching characteristics

Co-dissolution of metals/metalloids occurs when metal-phosphate bonds are disrupted during P leaching process [25]. Figure 4-3 shows leaching of Cu, Zn, Pb, Ni and As from ISSA using six different leachants. Table 4-1 shows the total concentrations of Cu, Zn, Pb, Ni and As for reference. Except As, the extraction efficiency of the selected metals/metalloids by sulphuric and nitric acids, where the highest extraction efficiencies were 21% and 23% for Cu and Zn, respectively. It was reported that Cu and Zn gave similar leaching results [6], with both exhibiting high leaching in acid solutions. Organic acids produced the highest leaching of metals among the leachants used, and citric acid achieved extractions of 73.6% and 73.7% for Cu and Zn, respectively, whereas 0.5 mol/L of oxalic acid caused the highest leaching of Pb (40%). Chelating agents had relatively high leaching ability for Pb, where EDTMP and EDTA showed similar Pb leaching ability (~32% Pb) in ISSA. Most of the acids and chelating agents resulted in low leaching of Ni, except citric acid. Arsenic was highly leachable in all leachants, which dissolved nearly all the As even at low concentrations, except for nitric acid (dissolving about 42%). This may be because As in ISSA was mainly in the form of non-silicate phases, which have high

solubility [164, 165].

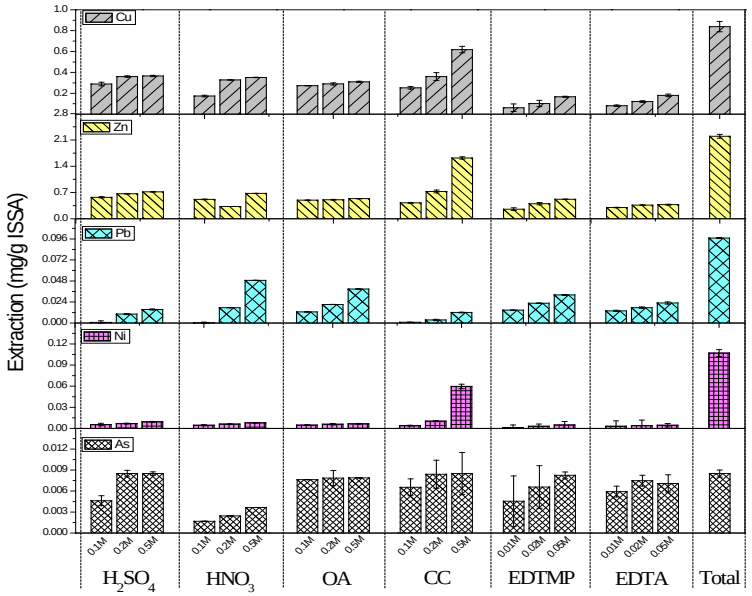

Figure 4-3 Leaching of trace elements from ISSA using different leachants

Trace element leaching by chelates is highly pH-dependent and affected by the forms of the functional groups [166]. EDTA used in this study is a strong organic ligand with high complexing capacity to many metals [167, 168]. EDTA performed better than EDTMP not only for the five trace elements investigated in this study, but also for other trace elements, such as Al (EDTA: 2400 mg/kg ISSA, EDTMP: 124 mg/kg ISSA), Zn (EDTA: 400 mg/kg ISSA, EDTMP: 350 mg/kg ISSA), Fe (EDTA: 1200 mg/kg ISSA, EDTMP: 98 mg/kg ISSA), etc. This is attributed to more ternary surface sites for cation adsorption present in EDTA than EDTMP [163].

Based on the experimental results, sulphuric acid has the highest P extraction efficiency with inevitable co-dissolution of metals/metalloids

while EDTA can leach out metals/metalloids with limited P extraction capacity. Moreover, the precipitate of some metal-sulphate would decrease metal concentrations in the leachate and thus improve its purity. Meanwhile, organic acids not only dissolve much more metals/metalloids than sulphuric acid but also significant amount of P, which is disadvantageous for P recovery. Overall, sulphuric acid was selected as the optimal P leachant, while EDTA was selected for pre-treatment to remove trace elements before P leaching. The EDTA pre-leaching conditions and sulphuric acid extraction conditions will be further optimized in the following section.

4.2.3 EDTA and sulphuric acid leaching conditions for P and heavy metal leaching

(1) EDTA

The leaching of P and co-dissolution of trace elements using EDTA are shown in Figure 4-4 and 4-5. As discussed above, EDTA gave relatively low P removal under a range of leaching conditions. The P leaching by EDTA was rapid and it almost reached the P leaching capacity within 30 min. Between 30 and 240 min there was a slow increase in P concentration. Metals/metalloids were gradually leached out during the first 120 min with concentrations becoming stable after 180 min. After 360 min, re-precipitation of metalloids such as As, Cu and Zn occurred. All the

‘available’ amounts of metals/metalloids were leached within 20 h by chelates. The longer leaching time of 24 h used in this research was sufficient to obtain reproducible results [152]. Therefore, 180 min was determined as the superior time for EDTA pre-leaching.

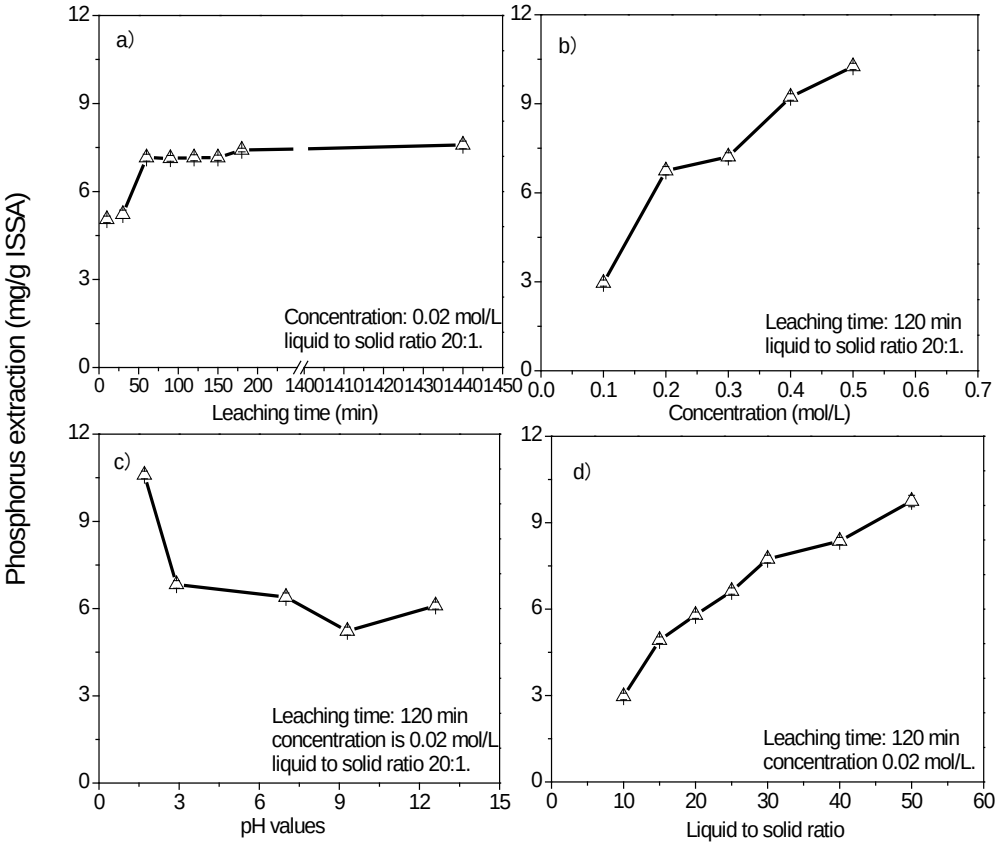

Figure 4-4 Effect of leaching conditions on P extraction using EDTA. a: effect of leaching time; b: effect of EDTA concentration; c: effect of leaching pH; d: effect of liquid to solids ratio on P leaching

With increasing EDTA concentration, P leaching by EDTA increased and the same trend was observed for trace elements. However, when the concentration of EDTA was higher than 0.02 mol/L, co-dissolution of trace

elements did not significantly increase with increasing EDTA concentration. Therefore, 0.02 mol/L EDTA was the optimum leachant concentration.

Solution pH is a key factor that controls leaching of P and metals [169]. In this study, five different pH values (1.7, 2.9, 7.0, 9.3 and 12.6) were prepared by adding nitric acid and sodium hydroxide to determine the optimal pH for EDTA leaching. It can be found that the more acidic of the EDTA leachant the more of metals/metalloids can leach out. Yet, a more intense acidic environment was not used because when the pH is below 1.7, EDTA re-precipitates. As P was marginally leached at pH ≥ 2 [26], EDTA only marginally increased P leaching while the concentrations of trace elements in the leachate doubled. When pH is lower than 1, both EDTA and acid can facilitate metal dissolution and thus enhance metals/metalloids pre-extraction from ISSA. Alkaline leachants leached 12% and 36% of Cu and Zn, respectively, due to their amphoteric characteristic. The superior reaction pH for EDTA was determined to be ~2.0.

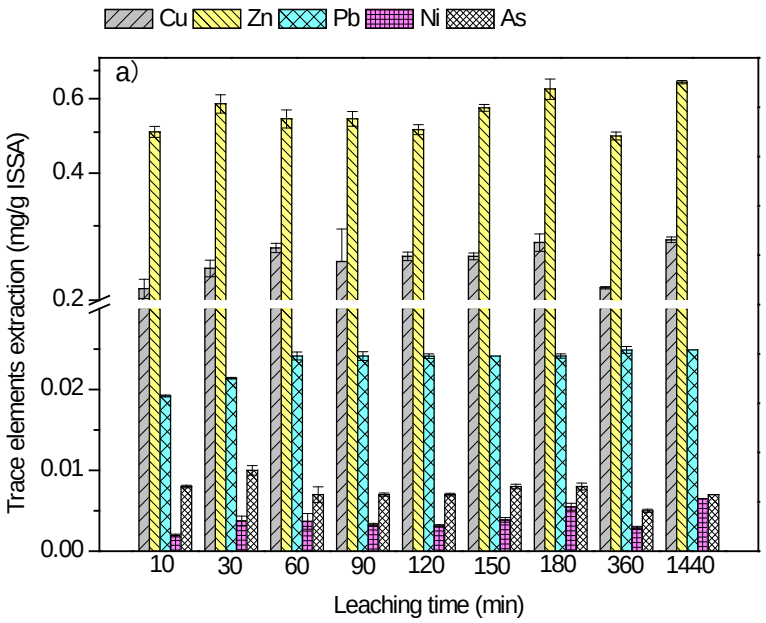
Cu
Zn
Pb
Ni
As
a)
Trace elements extraction (mg/g ISSA)
0.6
0.4
0.2
0.02
0.01
0.00
10
30
60
90
120
150
180
360
1440
Leaching time (min)

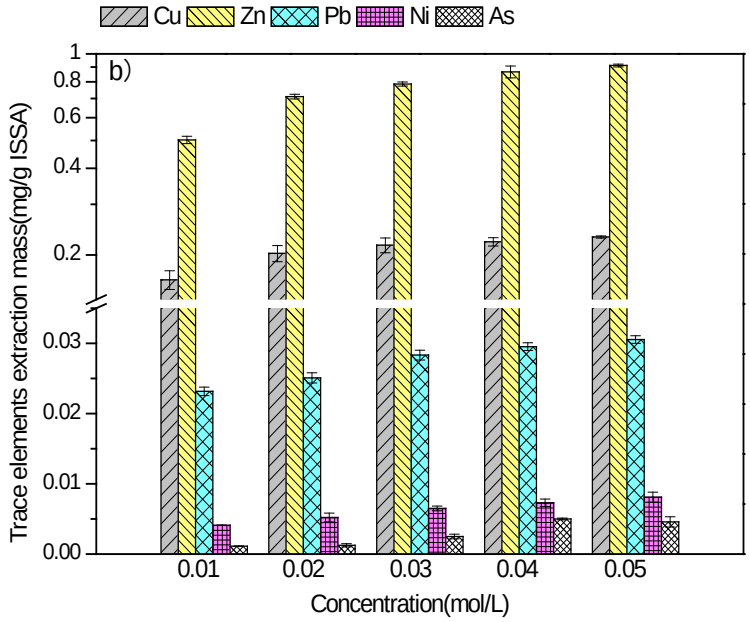
Cu
Zn
Pb
Ni
As
b)
Trace elements extraction mass(mg/g ISSA)
1
0.8
0.6
0.4
0.2
0.03
0.02
0.01
0.00
0.01
0.02
0.03
0.04
0.05
Concentration(mol/L)

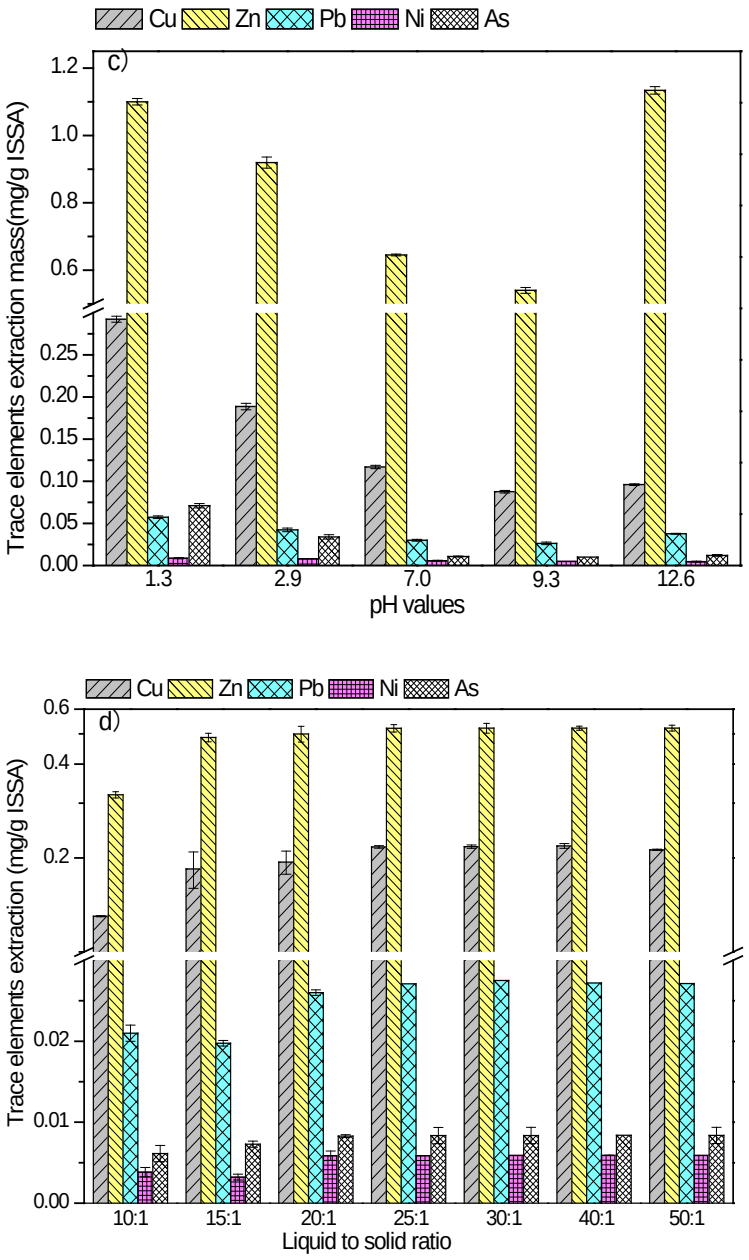

Figure 4-5 Trace element leaching using EDTA under different leaching conditions (a: effect of leaching time; b: effect of concentration; c: effect of leachant pH; d: effect of liquid to solid ratio)

Increasing the liquid-to-solid ratio gave a continued increase in leaching of P while the leaching of trace elements was not increased. However, at liquid-to-solid ratios ranging from 10:1 to 20:1, all the metal/metalloids

leached significantly. Thus the liquid-to-solid ratio was determined to be 20:1.

(2) Sulphuric acid

It should be noted that P leaching from ISSA using sulphuric acid is rapid. Figure 4-6a shows that in the first 10 min, 72% of the total P was leached and the remaining P was leached within 120 min. This is consistent with other studies [89]. Steric hindrance caused by the formation of gypsum crystals and/or acid-insoluble haematite and quartz phases may restrict acid from contacting whitlockite crystals [89]. After 120 min, additional P leaching was negligible. Figure 4-7a shows that longer leaching time leached more trace elements into the P leachate. Thus, the superior reaction time for high efficiency of P leaching and relatively low trace element leaching was 120 min. The results showed that P could not be leached at pH > 2, in agreement with previous reports that a pH range of 0.5-1.0 extracted significant P from ash [135, 144, 170].

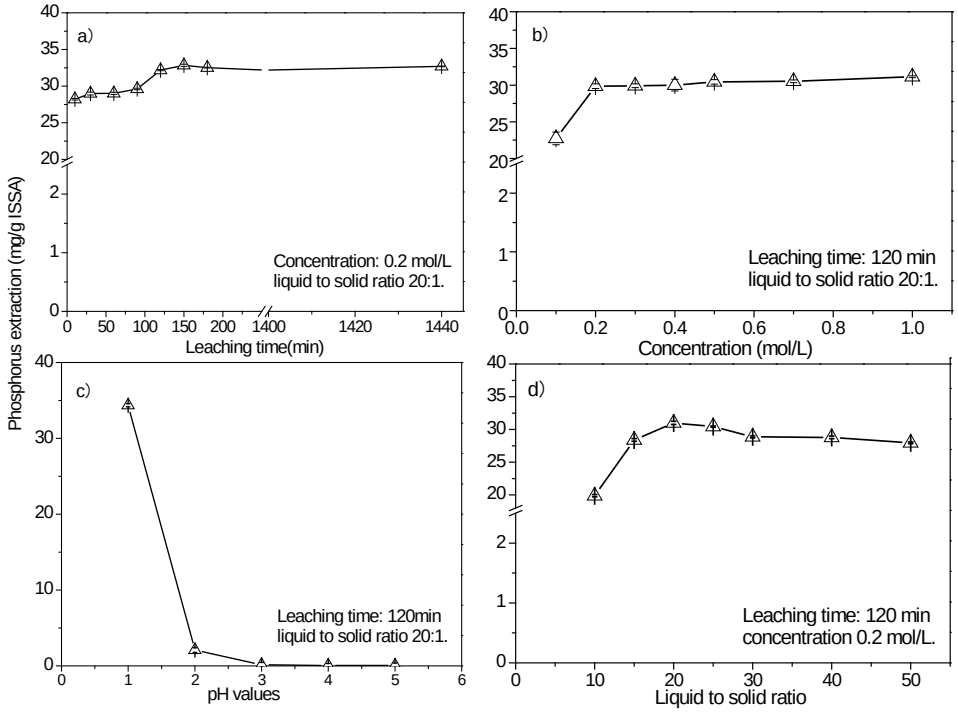

Figure 4-6 P extraction from ISSA under different leaching conditions using sulfuric acid. a: effect of leaching time on P extraction; b: effect of leachant concentrations on P leaching; c: effect of pH on P leaching; d: effect of liquid to solid ratio on P leaching

The leached P (Figure 4-6b) and trace elements (Figure 4-7b) gradually increased as H_2SO_4 concentration increased from 0.1 to 0.5 mol/L, corresponding to the decrease of solution pH from 1.3 to 0.3 as shown in Figure 4-7b. Given that P leaching showed a sharp increase from 0.1 mol/L to 0.2 mol/L of sulphuric acid and a marginal increase from 0.2 mol/L to 0.5 mol/L, 0.2 mol/L (pH = 0.8) of sulphuric acid was selected as the superior P leaching concentration. With increasing concentrations of sulphuric acid, Ni and Pb were more significantly extracted while Cu, Zn

and As extraction remained stable. Acid treatment at the lower pH increased Ni and Pb leaching mainly through dissolution of acid-soluble minerals. Therefore, P extraction by high concentration of sulphuric acid is not favourable for P purity in the leachate. Taking into account both the higher P recovery and lower trace element leaching, 0.2 mol/L of sulphuric acid was selected as the superior concentration for P extraction from ISSA.

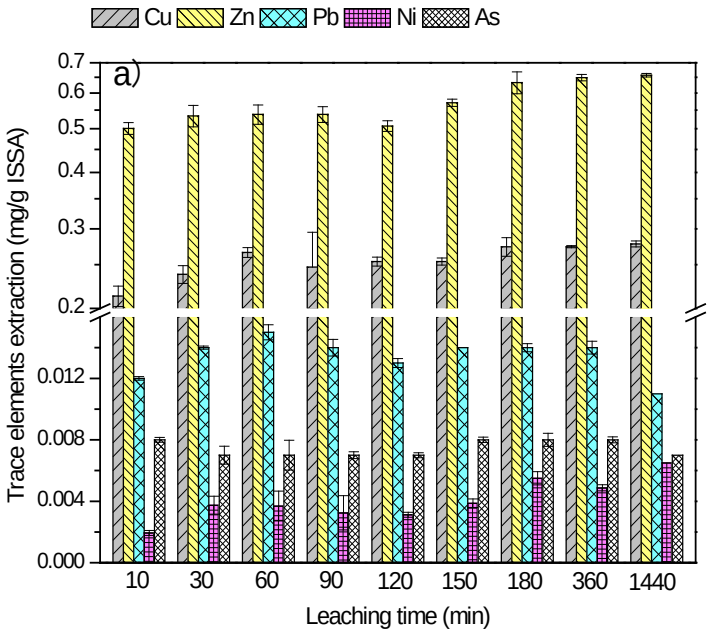

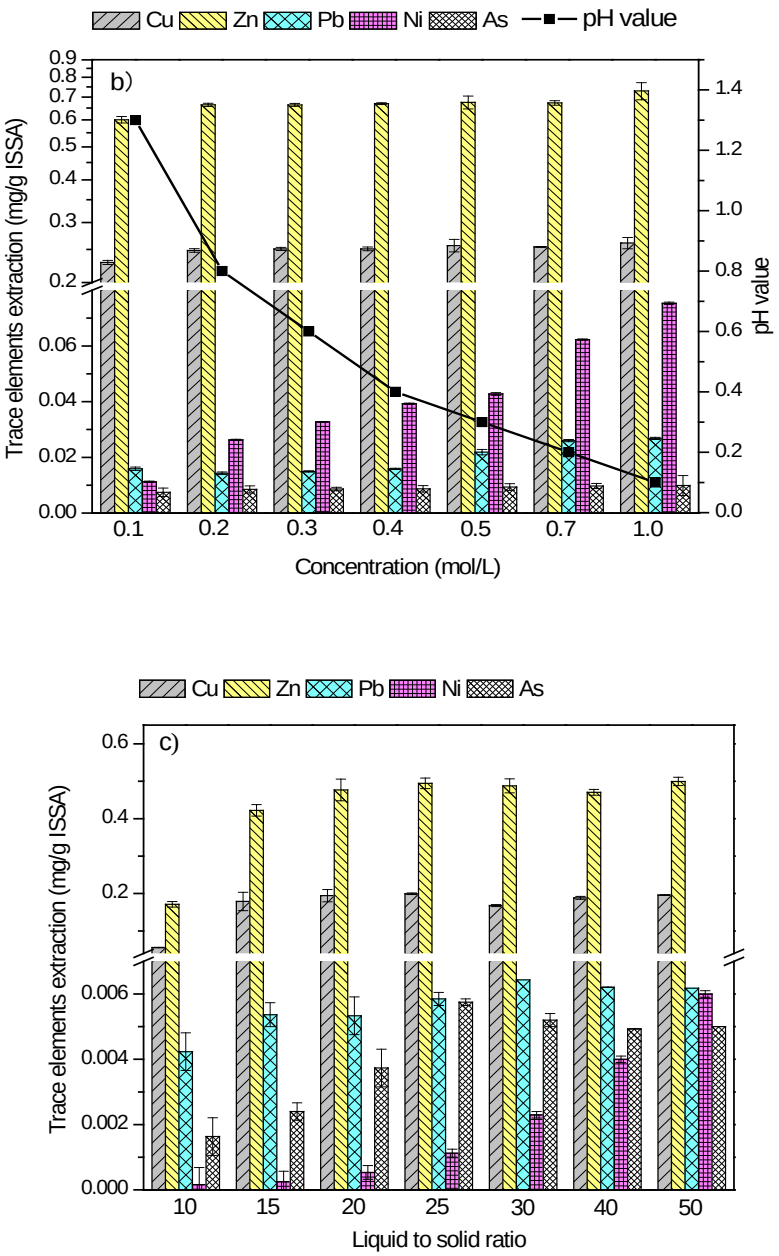

Figure 4-7 Trace elements leaching under different conditions using sulfuric acid. a: effect of leaching time; b: effect of acid concentration on leaching and pH; c: effect of liquid to solid ratio

Figure 4-7c shows that a liquid-to-solid ratio of 20:1 was sufficient for P leaching because there was a steep rise in P concentration before this ratio and it reached a plateau afterwards. Co-dissolution of trace metals showed

a significant increase with increasing liquid-to-solid ratio, except As leaching, which agrees with previous findings [165]. Taken together, the superior liquid-to-solid ratio of 20:1 was selected to give high P leaching and low leaching of trace elements.

4.2.4 Characterization of leached ISSA residues

The XRD data are shown in Figure 4-8, and XRF and BET data are summarized in Tables 4-4 and 4-5. SEM-EDX (Figure 4-9) analysis was conducted before and after different leaching processes to investigate changes in the morphology of ISSA and to identify compounds that were leached or formed during leaching. The as-received ISSA was poorly crystalline as indicated by the broad background hump between 15 and 40° 2θ (Figure 4-8). The plot of identified phases of XRD were shown in Figure 4-10, which included albite ($NaAlSi_3O_8$), anorthite ($CaAl_2Si_2O_8$), calcium silicate (Ca_2SiO_4), hematite (Fe_2O_3), quartz (SiO_2) and whitlockite ($Ca_9(MgFe)(PO_4)_6PO_3OH$). Calcium silicate phases are reported to form during the sewage sludge combustion process [159].

Table 4-1 XRF results of residues (% dry weight of sample)

Oxides	Origin ISSA	H_2SO_4 0.5 mol/L	HNO_3 0.5 mol/L	EDTA 0.05 mol/L	EDTMP 0.05 mol/L	OA 0.5 mol/L	CA 0.5 mol/L
Na_2O	2.42	0.34	1.75	1.69	0.98	0.57	0.81
MgO	1.66	1.98	1.13	1.24	1.14	0.63	1.29
Al_2O_3	11.88	4.90	8.91	12.14	12.22	7.88	8.68
SiO_2	31.15	26.60	41.02	36.26	31.16	42.54	43.29
P_2O_5	9.27	1.35	1.83	8.22	18.04	1.53	5.29
SO_3	4.08	25.96	1.15	0.48	0.64	0.59	0.32
Cl	0.24	0.02	0.05	0.05	0.05	0.032	0.06
CaO	9.73	9.34	1.78	7.32	5.61	15.48	5.46
Fe_2O_3	23.95	25.07	36.02	26.69	24.94	25.11	29.09
NiO	0.04	0.04	0.05	ND	0.035	0.04	0.03
CuO	0.24	0.17	0.24	0.22	0.21	0.12	0.17
ZnO	0.77	0.76	1.05	0.78	0.71	0.58	0.64
As_2O_3	0.02	ND	ND	ND	ND	ND	ND
Others[a]	4.56	3.48	5.02	4.92	4.26	4.89	4.86

ND replace for not detectable. 'Others[a]' contains: K_2O, Rb_2O, SrO, Y_2O_3, MnO, Cr_2O_3 and TiO_2.

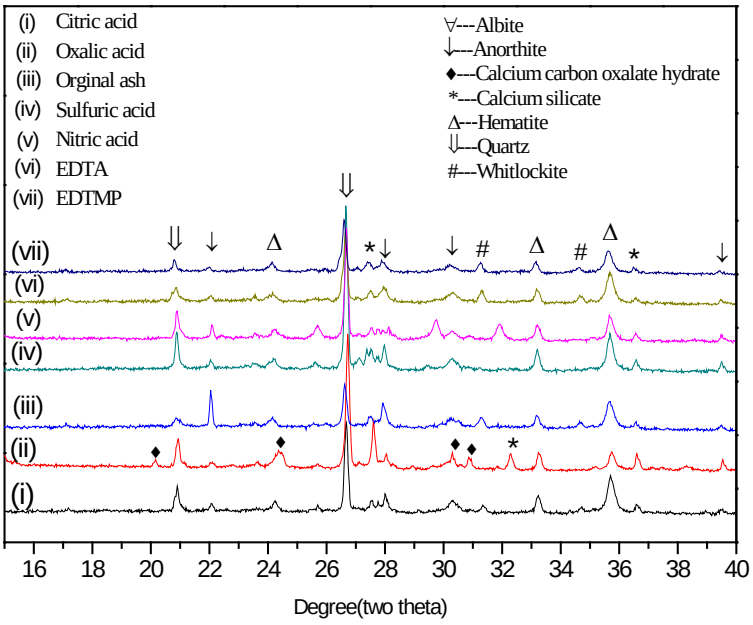

Figure 4-8 XRD results of leached residues of ISSA using different leachants (0.2 mol/L of acids and 0.02 mol/L of chelating agents)

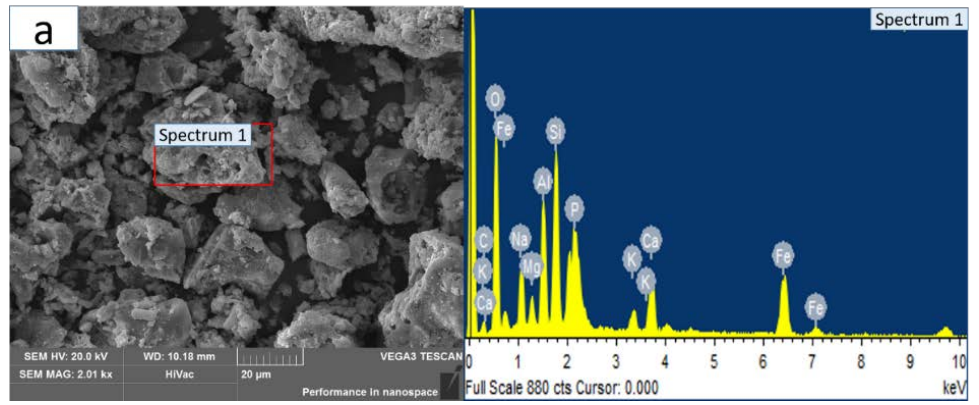

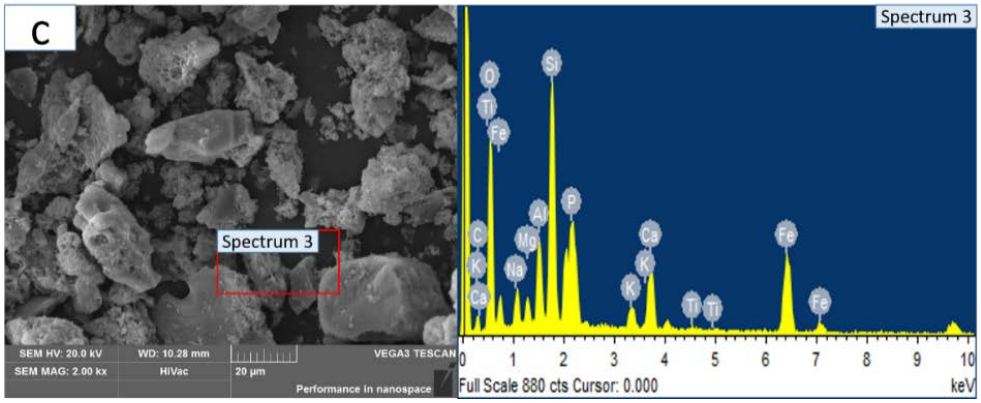

Figure 4-9 SEM micrographs of a: as-received ISSA, b: residue after leaching with 0.2 mol/L of sulphuric acid c: residue after leaching with 0.02 mol/L EDTA. The EDS spectra show analysis from the area within the square.

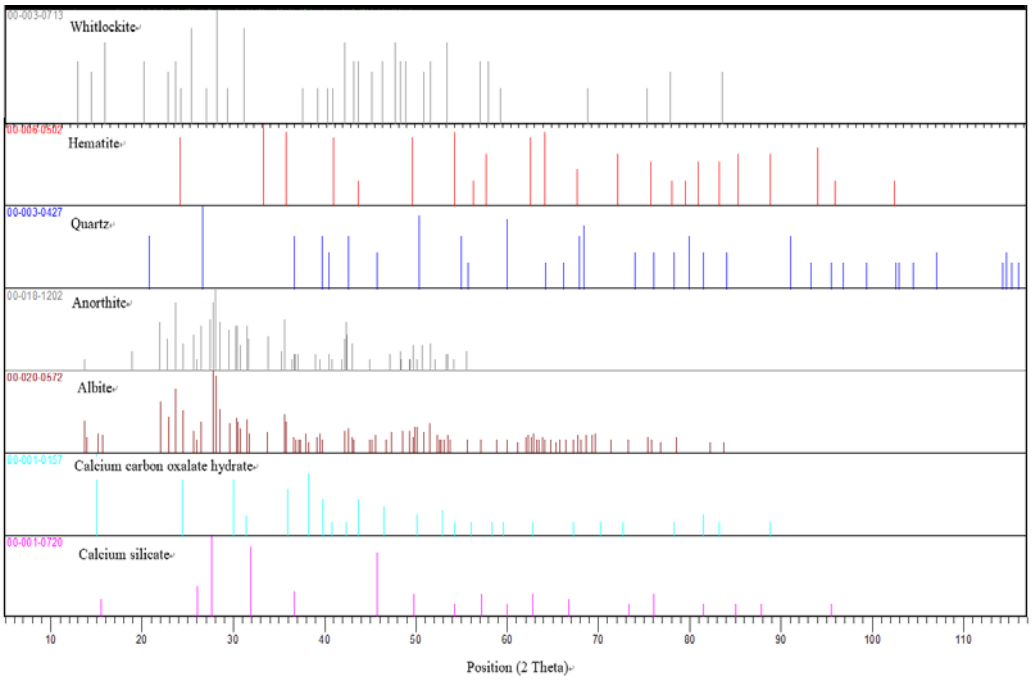

Figure 4-10 Identified phases of XRD

Whitlockite was readily dissolved in both organic and inorganic acids, but

was not leached by chelating agents. This was confirmed by a decrease in the mass ratio of P_2O_5 to CaO, except for sulphuric acid and oxalic acid leaching where calcium sulphate and calcium oxalate formed. The ISSA residues after leaching by organic and inorganic acids were similar, with the main crystalline phases being quartz, hematite, and albite. The phosphate content was low in inorganic acid-treated residues. Anorthite was present in the residues after leaching by inorganic acids but was barely detected in the residues after leaching by organic acids, indicating that transformation of Ca and Al was caused by inorganic acids. The relative amount of hematite in ISSA residues increased after the treatment with organic and inorganic acids. In contrast, Fe was dissolved more readily by chelating agents than organic and inorganic acids.

During sulphuric acid leaching $CaSO_4$ can form and precipitate in the leachate. Compared to nitric acid leachate, sulphuric acid leachate contained more Ca in the residues, as seen in the XRD data. Similarly, there was considerable Ca from dissolving calcium phosphate in the oxalic acid because calcium oxalate was formed and precipitated, as observed by XRD in the formation of calcium carbon oxalate hydrate. Because EDTMP contains P itself, thus the P content in its residue increased after leaching. However, the dissolving mechanism of organic acid is different from inorganic acid. Organic acids facilitate dissolution of amorphous oxides via surface complexation and reduction of Fe^{3+} [169]. Therefore,

metals/metalloids dissolved more intensively in organic acids, as reflected in the XRF data for these residues. The concentrations of Mg, Pb, As, Mn, Cu and Zn were low compared to other residues, which is in consistent with the leaching results, especially for oxalic acid. The XRF results also showed that in the residues treated by EDTA and EDTMP the phosphorus oxide was decreased.

The ISSA particles had a porous and loosely bound structure similar to previous findings [171]. After extraction with sulphuric acid, the morphology of the ISSA residue particles were more irregular and porous as corroborated by the significant increase of BET surface area in Table 4-5. Therefore, the surface-bound chemicals in ISSA would largely be dissolved by sulphuric acid, which partially destructed surface structure and created more loose structure [172]. Organic acid caused the most significant structural change to ISSA, suggesting their high dissolving capability and deep invasion into ISSA structure. While for the residues of the EDTA-treated samples, the structures of the residues were similar to the original ISSA. The marginal structural change may reflect that EDTA complexed with heavy metals on the ISSA surface [173], and the EDX analysis showed phosphorus was not washed out. This indicates that EDTA is a good pre-treatment agent to remove heavy metals from the ash before P extraction.

Table 4-2 BET value comparison of residues

Ash	Origin ISSA	OA	CA	H_2SO_4	HNO_3	EDTA	EDTMP
BET surface area m^2/g	3.42±0.03	31.34±0.00	43.91±0.86	10.18±0.42	19.92±0.26	2.80±0.05	8.77±0.00

4.3 Summary

Both organic and inorganic acids can extract P from ISSA, while chelating agents extract relatively small amounts of P. Sulphuric acid was selected as the superior P leachant. The superior P leaching conditions using sulphuric acid were 0.2 mol/L with pH ~ 0.9 at a liquid-to-solid ratio of 20:1 using a 120-min reaction time. EDTA leached high amounts of metals/metalloids from ISSA but low concentrations of P, and thus it was considered the superior pre-treatment leaching agent. The superior ISSA pre-treatment leaching conditions using EDTA were 0.02 mol/L at a liquid-to-solid ratio of 20:1 and 180 min of reaction time at pH 2. Pre-treatment by EDTA did not change the microstructure of the ISSA as shown by BET and SEM analysis. Studying of P leachant and pre-treatment metal/metalloid leachant are significant for obtaining higher purity of P-containing leachate for subsequent P-fertilizer production. Further investigation into a simpler P recovery method and potential hurdles (e.g., competition ions in leachate) should be performed and compared with traditional P recovery routes in the future research.

Chapter 5 Recovery of P from ISSA by Combined Two-step Extraction and Selective Precipitation

5.1 Introduction

The exhaustion of limited natural phosphate rock resources and the one-way flux of phosphate rock from highly concentrated ores to diffuse low level concentrations in the environment stimulate the motivation of recycling P from waste streams and convert a linear consumption of P resources into a partially circular consumption mode [26, 27, 174]. After consumed by human activities, the consumed-P and waste-P are disposed of as wastes [175]. If properly collected, these P-wastes typically end up in the sewage of waste-water treatment plants, where the vast majority of P is removed in the sewage sludge [176]. Although land-spreading remains the dominant form of sewage sludge disposal, during the last 20 years there has been a trend at a global level away from landfilling and sea disposal towards incineration of sewage sludge [177]. Incineration is especially attractive in densely-populated regions and effectively reduces the volume of waste, eliminates odour problems, produces a sterile ash and allows for potential energy recovery from the organic solids in the sludge [38, 178]. Almost all of the P in sewage sludge remains in the inorganic fly ash produced by sewage sludge incineration [27, 179, 180].

ISSA consists of small glassy particles partially sintered together into

irregularly shaped porous agglomerates containing Fe, Al, Si and P [120, 181]. The P is preferentially deposited on the surface of particles, thus facilitating recovery [159, 178, 182]. The main crystalline phases containing P in ISSA are whitlockite, beta-tricalcium phosphate mineral and $AlPO_4$ [29, 182, 183]. However, the presence of Mg and Fe can also influence the type of P phases formed.

According to previous studies, either thermal treatment or wet-extraction is used to recover P from ISSA [178, 184, 185]. Thermal methods have limitations due to high energy consumption and unsatisfactory removal results for non-volatile metals (Ni, As, Mo, etc) [186]. Wet-extraction is more common and mineral acids have been shown to be the best recovery agents because they readily dissolve P but the co-dissolution of metal(loid)s is a problem [10] . However, alkaline solutions induce a low P solubility although the co-dissolution of metal(loid)s is also low [20-24]. The presence of metals such as Zn, Cd, Mg and Pb, reduce the quality of phosphate fertilizer [187]. Efforts to eliminate these metal(loid)s have included adsorption by organic and inorganic media (activated carbon, biochar, modified silicate, etc.) [119, 188-190], cation-exchange resins [27], solvent extraction [178] and ion migration in electric fields [25].

Each purification method has specific limitations. For example, removal efficiencies by cation adsorption in a highly acidic solution are impeded by the high concentration of H^+ ions. Organic solvent extraction is not

sufficiently efficient and also requires an additional step for P extraction from the solvent and solvent recovery before a phosphoric acid product can be obtained [59, 178]. The removal of metal ions by direct current was found to be limited by high energy consumption and low efficiency [143, 191]. Hence, it is necessary to find new methods which can effectively extract P with high purity through a simple process route.

Our previous study has identified that EDTA and sulphuric acid could effectively leach metal(loid)s and P, respectively [120]. EDTA is applied mostly in soil washing and can remove metal(loid)s effectively [192-194], while sulphuric acid was found to be a P superior extraction agent [120]. Consequently, it makes sense to combine the properties of these two extractants in a sequential procedure.

Obtaining a solution with low concentrations of metalloids and a high concentration of P is only part of the challenge. The next step is to convert that solution in a useful P-based product. Previous studies have demonstrated that P co-precipitates with Al, Fe and Ca at pH above 4 [41, 110]. Of the three kinds of P-precipitation, only calcium phosphate is an effective constituent for fertilizer application and therefore significant efforts have been made to recover calcium phosphate directly or produce it from other P-phases. However, direct recovering of calcium phosphate has low efficiency while the complex transforming process would result in P loss [41, 110].

Consequently, this study has assessed the feasibility and efficiency of generating a solid CaP-based product by pH adjustment (by addition of NaOH or $Ca(OH)_2$) of the less contaminated solution obtained from the two-step extraction procedure. The overall aim of the research is to develop a commercially viable process for extracting P from sewage sludge ash so that P can become part of a circular economy.

5.2 Results and discussion

5.2.1 Optimization of two-step extraction conditions

(1) Phosphorus extraction

A limited fraction of P in the ISSA can be extracted by EDTA and the majority of the P was extracted by sulphuric acid. Both the extracted mass of P in the 1st step (EDTA pre-treatment) and the 2nd step (sulphuric acid extraction) are shown in the first row of Figure 5-1. The mass of extracted P by the single-step extraction is shown in the right column for reference. The low pH of EDTA solution increased the solubility of P, the EDTA was found to be able to release P by breaking the bonds of Ca-P to form EDTA-Ca (Eq. (5-2) and (5-3)) [195].

$$\mathrm{H_4EDTA} \leftrightarrow 4H^+ + EDTA^{4-} \qquad (5-1)$$

$$M^{2+} + EDTA^{4-} \leftrightarrow M-EDTA^{2-} \qquad (5-2)$$

$$M^{3+} + EDTA^{4-} \leftrightarrow M-EDTA^{-} \qquad (5-3)$$

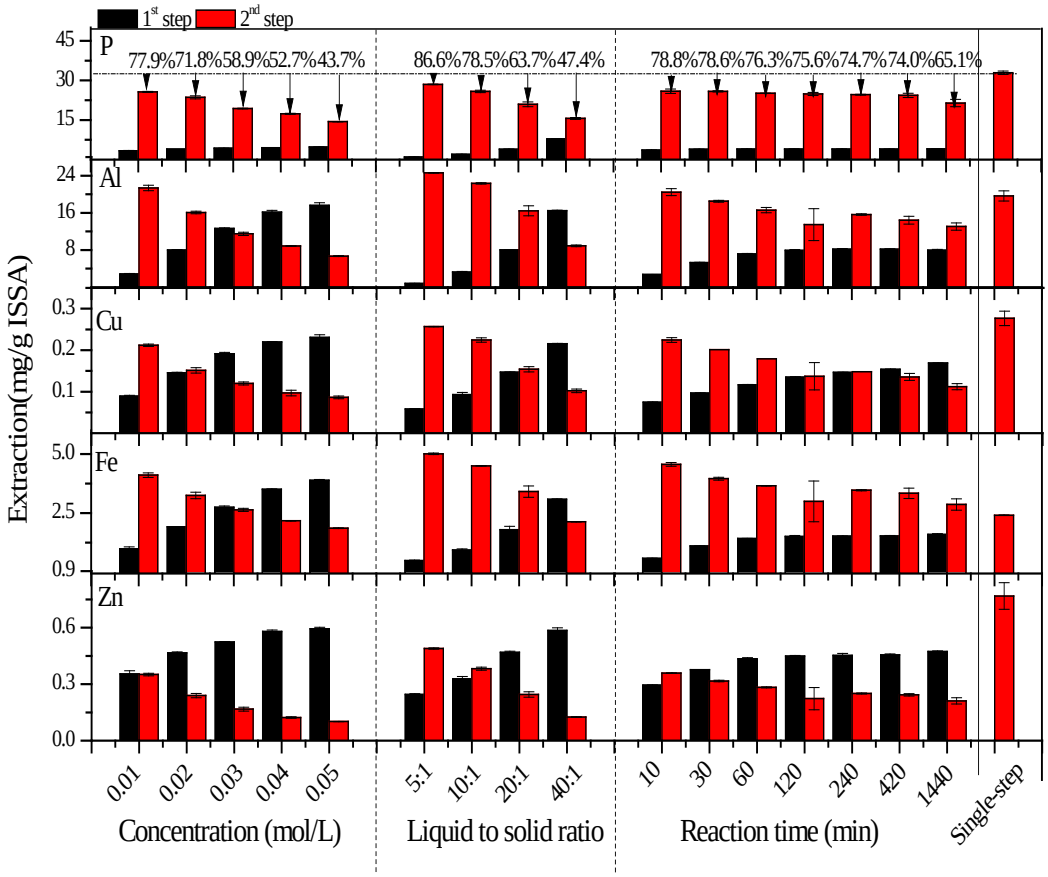

Figure 5-1 Optimization of EDTA pretreatment conditions

The results in Figure 5-1, show that an increase in EDTA concentration (0.01 to 0.05 mol/L) or in liquid to solid ratio (from 5:1 to 40:1) considerably increased undesirable P extraction in the 1st step, as in Chapter 4. This resulting in an inevitable decrease in the quantity of P extracted in the 2nd step. Increasing the EDTA concentration or liquid to solid ratio would decrease the molar ratio of P:EDTA significantly in the extracts (by about 20%) over the ranges studied as shown in Figure 5-2. The molar ratio of P:EDTA was increasing up to the reaction time of 120 minutes but then became constant. For a given quantity of EDTA used, the P recovery in the 2nd step gradually decreased as reaction time increased. To ensure recovery

of P > 70% in the 2nd step, the concentration of EDTA in the 1st step should not be higher than 0.02 mol/L and the L/S ratio no higher than 20:1. Lowering the L/S ratio and reducing the reaction time of the 1st step improved P recovery in the 2nd step. However, the optimum conditions must be based on minimizing the co-dissolution of metal(loid)s in the 2nd step.

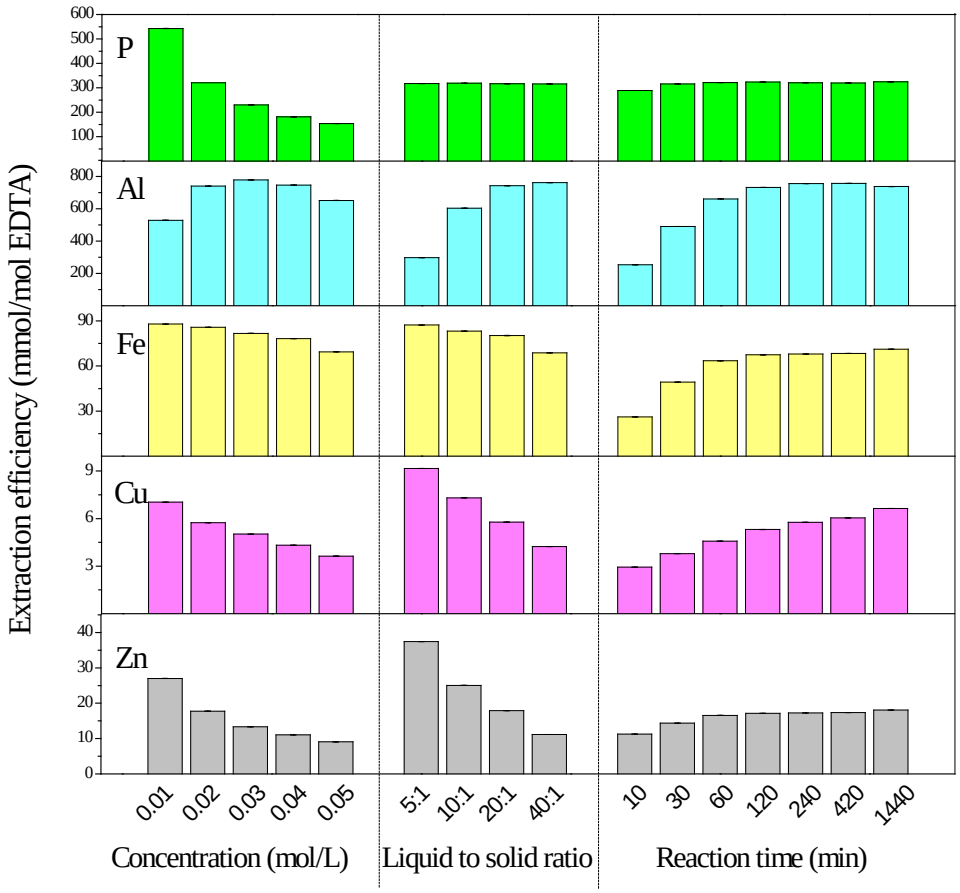

Figure 5-2 EDTA removal efficiency in 1st step of two-step extraction

(2) Co-dissolution of major metal(loid)s

Any soluble metal(loid)s in the ISSA forming multi-valent cations can potentially compete for the complexing sites on EDTA (see Eq. (5-3) and

(5-4)) and the metal(loid)s removal in the 1st and 2nd step of the two-step extraction method shown in Figure 5-2. Additionally, free H^+ from EDTA (see Eq. (5-1)) would also enhance the dissolution of metal(loid)s by attacking alkaline oxides because the ISSA used in this research was slightly alkaline [120]. If not removed previously, metal(loid)s such as Al, Cu, Fe and Zn can co-precipitate with P when the pH is raised, reducing the purity and potential commercial value of the P precipitate.

These metal(loid)s can be easily dissolved by acids or chelates [159, 196], while the effect of chelates was mainly related to the dissolution of metallic carbonates or sulfides by the chelating effect [197]. When using EDTA to remove undesirable impurities, it is necessary to consider (i) the molar ratios of impurities: EDTA, (ii) the potential solubilities of these impurities in the pH range studied and (iii) different affinities (chelating coefficients) of different impurities for chelation by EDTA. Due to the importance in analytical chemistry, the relative stabilities of different metal cation-EDTA complexes (under standard conditions) are well known. The general order of preference for the most relevant leachable cations from ISSA is $Fe^{3+}/Fe^{2+}/Mn^{3+} > Cu^{2+}/Ni^{2+}/Pb^{2+} > Zn^{2+}/Al^{3+} >> Ca^{2+} > Mg^{2+} >>> Na^+ > K^+$. Kim and Ong [198] used the much greater affinity of Fe^{3+} than Pb^{2+} to effectively recycle EDTA used to treat Pb contaminated wastewaters. In researches with contaminated soils, the Pb^{2+} removal by EDTA was strongly influenced by pH [199]. Finzgar and Lestan [192] found that Pb^{2+}

removal was generally more efficient than Zn^{2+} but that further increases in removal efficiency were hampered by the presence of Fe cations. Similar results were found by Sawai et al. [199] that, under acidic conditions, even though the apparent stability constant of Cu-EDTA was greater than that of the corresponding Zn complex under the same pH conditions, the Zn-EDTA was dominant. In order to ensure the cost-effective use of EDTA, it is important to assess the efficacy of metal(loid) removal under different conditions.

Although Figure 5-2 shows that decreasing the molar ratio of metal(loid):EDTA (either by increasing the EDTA concentration or the L/S ratio at a fixed concentration) had a direct benefit on the removal efficiencies of Al, Cu, Fe and Zn, it was also clear that this came at the cost of undesirable co-dissolution of P in 1st step. In the EDTA concentration ranges studied, the extraction rate of Fe, Cu and Zn fell significantly between 0.01 and 0.02 mol/L indicating the highest efficiency can be obtained using 0.02 mol/L EDTA. Al extraction rate remained constant after 0.02 mol/L EDTA. In considering P extraction, increasing the concentration of EDTA decreased the removal efficiency The optimal concentration was selected as 0.02 mol/L. Similarly, increasing the volume of EDTA induces more metal(loid)s dissolution resulting in more impurities in the final extract. However, the extraction efficiency of EDTA fell with increased L/S. Considering that the higher L/S ratio was

unfavorable for P recovery nor practical, a L/S of 20:1 was selected as the optimized for EDTA pretreatment. The contact time study indicated that taking the balance of P and metal(loid) extraction, the optimal contact time was 120 min. Additionally, residue EDTA in the second step was favorable to purity, because EDTA would form stable phases with metal(loid)s. The washing by deionized water after 1st step in the applied two-step extraction method would be removed in future applications.

5.2.2 Comparison of two-step extraction and single-step extraction

The final extract of the two-step method and the only extract of the single-step method were analyzed respectively under optimized reaction conditions and the results are shown in Figure 5-3. According to the total digestion results from previous studies on raw ISSA [120], the extracted mass ratios of major elements are shown in Table 5-1.

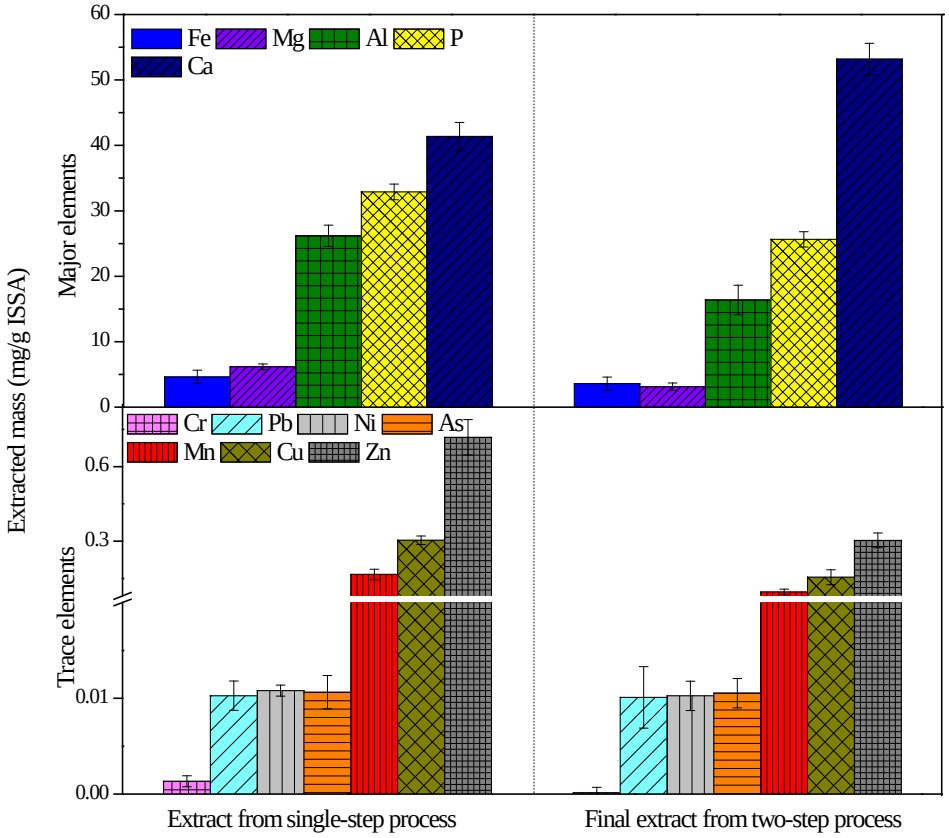

Figure 5-3 Extracted mass of metal(loid)s and P from ISSA by two-step extraction and single-step extraction

Of the 11 metal(loid)s studied, the two-step method, with the notable exception of Ca, effectively decreased concentrations in the final extracts when compared with the single-step method. The unusual results for Ca can be at least partially attributed to the lower stability of Ca-EDTA complex compared with other EDTA complexes such as Fe^{3+}, Cu^{2+}, Zn^{2+} and Al^{3+}. This effect would explain why Ca is not so effectively removed during the first step. However, the same effect does seem to apply to Mg^{2+}, which could be expected to have an even lower stability than Ca^{2+} in EDTA complexes, yet the two step process succeeded in reducing Mg^{2+} levels in

the final extract but not Ca^{2+}. The basic observation is that EDTA has a direct or indirect effect on the (sulphuric) acid solubility of Ca. One logical explanation would be that the residual EDTA from the first step is still present on the surface of dried ISSA particles when they are used in the second step. This residual EDTA then inhibits the formation of gypsum precipitates (from reaction with SO_4^{2-} ions from sulphuric acid) allowing Ca to remain in solution as Ca-EDTA complexes. This results in the higher concentration of soluble Ca when compared to the single step, where no EDTA residues are present and gypsum precipitation is uninhibited.

The presence of metal(loid)s in fertilizers is legally restricted in most countries [65]. In this context, the decreases in Cr (92%), Zn (58%), Cu (49%) and Al (38%) shown in Table 5-1 are especially helpful in ensuring that the extractant can be used to generate a fertilizer with low problematic impurities. Arguably of greatest concern is the content of Al due to its proven effects on plant toxicity in acidic soils. Followed by Cu, which is very phytotoxic, and the accumulation of Cd is toxic for soil in the long term. The decrease in Mn (50%), Mg (49%) and Fe (23%) are of benefit in terms of permitting a much purer phosphate product to be produced (either as fertilizer or an intermediate for further processing). Interestingly, the EDTA pre-treatment did not significantly affect the extractability of Pb (3%), Ni (1%) or As (1%). The most probable explanation for this observation is that these metals are present only in non-soluble forms in

ISSA particles, where they may be immobilized in a glassy matrix [6].

Table 5-1 Extracted mass ratio of major elements by single-step extraction and two-step extraction methods

Extraction mass ratio	Cr	Zn	Mn	Mg	Cu	Al	Fe	P	Pb	Ni	As	Ca
	(%)											
Single-step	1.3	32.7	16	35.4	36.1	55.0	4.8	94.0	10.3	15.4	9.8	75.2
Two-step	0.1	13.8	8	17.9	18.5	34.4	3.7	73.3	10.0	15.3	9.9	96.7
Difference	92.3	57.8	50	49.4	48.8	37.5	22.9	22.0	0.3	0.1	0.1	-22.2

Overall, by using the two-step method, the purity of the final extracts can be improved. To be specific, 5.16 mmol/kg ISSA of metal(loid)s was removed by the treatment of 1st step, although 2.34 mmol/kg ISSA of P was lost at the same time, when compared to the single-step method. These results indicated that the two-step method can produce an extract with a higher application value.

5.2.3 Precipitation of metals and phosphates by pH adjustment

As the pH of the acidic extract is increased, it causes precipitation of different phosphate, silicate, sulphate and hydroxide solid-phases. The presence of Al, Ca and Fe essentially influent phosphate precipitation [200]. Graphs of the extract concentrations of Al, Ca and Fe against pH are shown in Figure 5-4 and similar plots for As, Cu, Ni and Zn are shown in Figure 5-5.

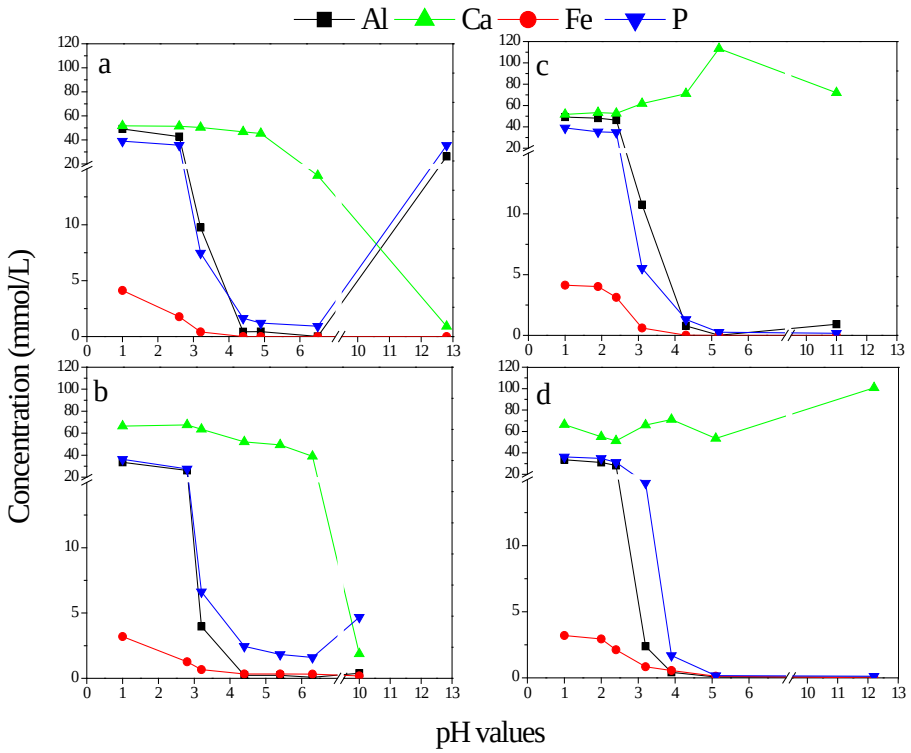

Figure 5-4 Variation of main metals (Fe, Al and Ca) and P concentration in extract when pH adjusting: a. extract of single-step method by NaOH; b. extract of two-step method by NaOH; c. extract of single-step method by $Ca(OH)_2$; d. extract of two-step method by $Ca(OH)_2$

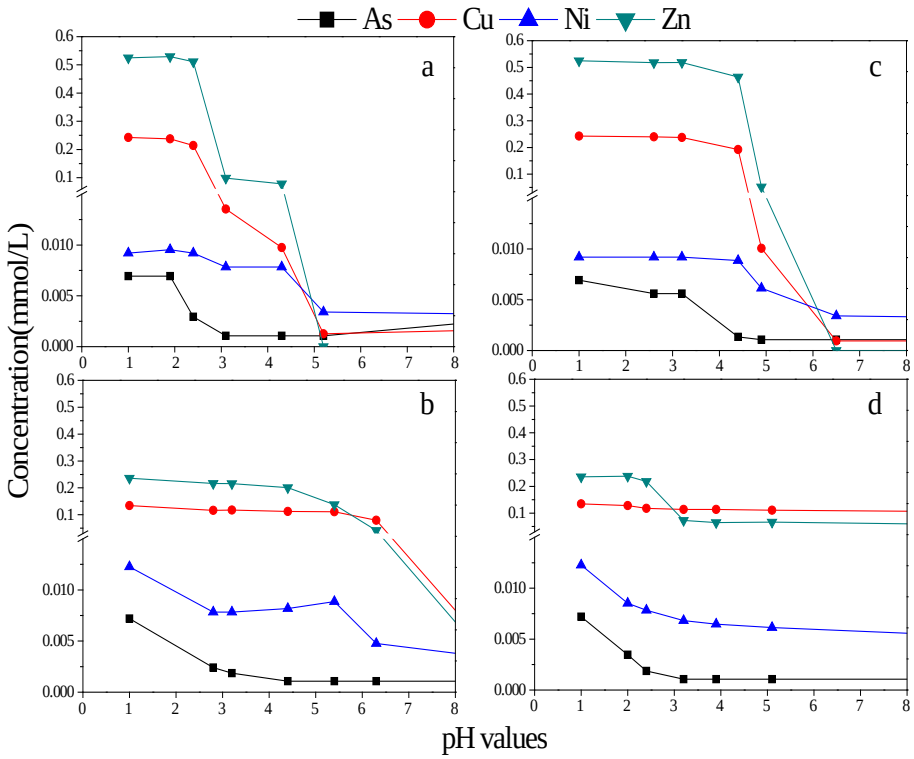

Figure 5-5 Variation of trace metals (As, Cu, Ni and Zn) concentration in extract when pH adjusting: a. extract of single-step method by NaOH; b. extract of two-step method by NaOH; c. extract of single-step method by $Ca(OH)_2$; d. extract of two-step method by $Ca(OH)_2$

(1) Predicted precipitation reactions

The type of P-precipitates and saturation indexes have been simulated by MINTEQ (as shown in Figure 5-6 and Table 5-2) to predict the main precipitates at specific pH values following the addition of NaOH. Gypsum ($CaSO_4 \cdot 2H_2O$), strengite ($FePO_4 \cdot 2H_2O$), variscite ($AlPO_4 \cdot 2H_2O$) and hematite (Fe_2O_3) are predicted to be the main precipitates. As the pH increases, P would precipitate as predominantly Al or Fe phosphates.

However, there is potential for Ca-P formation at high pH and to a much greater extent in the extract from the two-step process. Nevertheless, it is worth highlighting some of the limitations regarding values from the MINTEQ equilibrium calculations:

(a) The input SO_4^{2-} concentration used was the concentration of extractant (sulphuric acid). However, some of this would precipitate with the metals (with Ca^{2+} → gypsum) and not be available in the aqueous phase. Thus, the concentration of SO_4^{2-} in the extract may be overestimated.

(b) Anions like SiO_2^{2-} were released from the ISSA when contacting with sulphuric acid. However, they could not be detected by the ICP and were excluded from the simulation calculation. Silicates were not the focus of this study.

(c) Although the residues were washed using deionized water twice prior to the 2nd step, some EDTA might still be adsorbed onto the residues of the 1st step and these EDTA residues would affect the equilibrium to some extent.

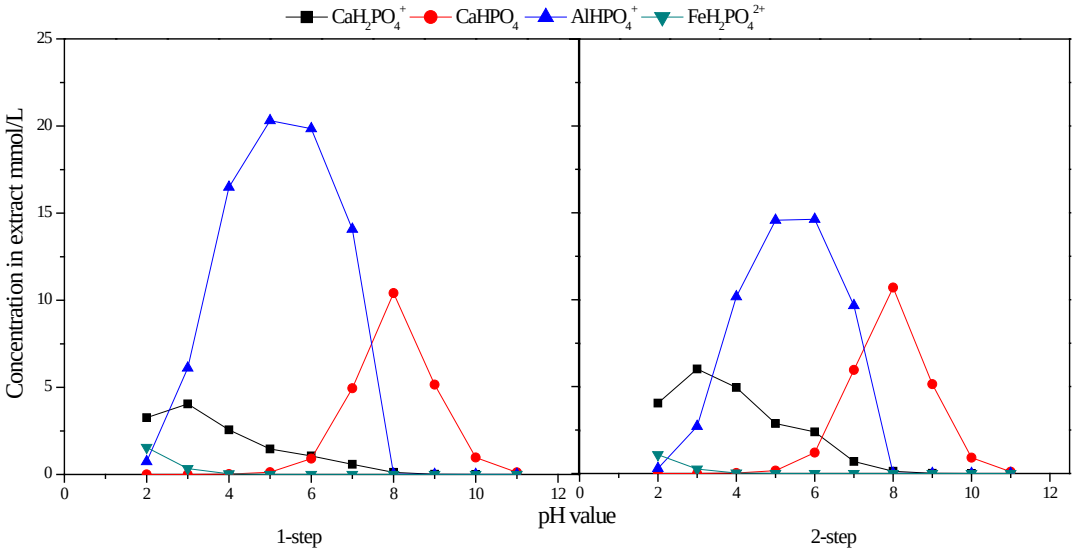

Figure 5-6 Concentration of P-precipitate in 1-step and 2-step extracts with pH change (mmol/L) (MINTEQ results)

Table 5-2 Equilibrium of two kinds of extracts (extract of single-step method and two-step method) when adjusting pH values by NaOH (MINTEQ results)

Single-step								Two-step						
pH=3								pH=3						
$AlOHSO_4$(s)	0.491	-1	H^+	1	Al^{3+}	1	SO_4^{2-}	$AlPO_4x1.5H_2O$	0.742	1	Al^{3+}	1	PO_4^{3-}	1.5	H_2O
$AlPO_4x1.5H_2O$	0.983	1	Al^{3+}	1	PO_4^{3-}	1.5	H_2O	Gypsum	0.883	1	Ca^2	1	SO_4^{2-}	2	H_2O
Cupric Ferrite	0.315	-8	H^+	1	Cu^{2+}	2	Fe^{3+}	Goethite	1.767	1	Fe^{3+}	2	H_2O	-3	H^+
Goethite	1.948	1	Fe^{3+}	2	H_2O	-3	H^+	Hematite	5.939	2	Fe^{3+}	3	H_2O	-6	H^+
Gypsum	0.752	1	Ca^{2+}	1	SO_4^{2-}	2	H_2O	Lepidocrocite	0.887	-3	H^+	1	Fe^{3+}	2	H_2O
Hematite	6.299	2	Fe^{3+}	3	H_2O	-6	H^+	Strengite	4.443	1	Fe^{3+}	1	PO_4^{3-}	2	H_2O
Lepidocrocite	1.068	-3	H^+	1	Fe^{3+}	2	H_2O	Variscite	3.029	1	Al^{3+}	1	PO_4^{3-}	2	H_2O
MnHPO4(s)	2.37	1	Mn^{2+}	1	PO_4^{3-}	1	H^+	Anhydrite	0.654	1	Ca^{2+}	1	SO_4^{2-}		
Strengite	4.524	1	Fe^{3+}	1	PO_4^{3-}	2	H_2O	$AlOHSO_4$(s)	0.25	1	Al+3	1	SO4-2	1	H_2O
Variscite	2.591	1	Al^{3+}	1	PO_4^{3-}	2	H_2O								
pH=4								pH=4							
AlOHSO4(s)	1.225	-1	H^+	1	Al^{3+}	1	SO_4^{2-}	$AlPO_4x1.5H_2O$	2.45	1	Al^{3+}	1	PO_4^{3-}	1.5	H_2O
AlPO4x1.5H2O	2.421	1	Al^{3+}	1	PO_4^{3-}	1.5	H_2O	Cupric Ferrite	7.498	-8	H^+	1	Cu^{2+}	2	Fe^{3+}
Anhydrite	0.555	1	Ca^{2+}	1	SO_4^{2-}			Diaspore	0.978	-3	H^+	1	Al^{3+}	2	H_2O
Cupric Ferrite	6.755	-8	H^+	1	Cu^{2+}	2	Fe^{3+}	Ferrihydrite	1.736	1	Fe^{3+}	3	H_2O	-3	H^+
Diaspore	0.602	-3	H^+	1	Al^{3+}	2	H_2O	Ferrihydrite (aged)	2.246	1	Fe^{3+}	-3	H^+	3	H_2O
Ferrihydrite	1.485	1	Fe^{3+}	3	H_2O	-3	H^+	Gibbsite (C)	0.108	1	Al^{3+}	3	H_2O	-3	H^+
Ferrihydrite (aged)	1.995	1	Fe^{3+}	-3	H^+	3	H_2O	Goethite	4.448	1	Fe^{3+}	2	H_2O	-3	H^+
Goethite	4.199	1	Fe^{3+}	2	H_2O	-3	H^+	Hematite	11.298	2	Fe^{3+}	3	H_2O	-6	H^+
Gypsum	0.795	1	Ca^{2+}	1	SO_4^{2-}	2	H_2O	Lepidocrocite	3.568	-3	H^+	1	Fe^{3+}	2	H_2O
Hematite	10.803	2	Fe^{3+}	3	H_2O	-6	H^+	Maghemite	3.494	-6	H^+	2	Fe^{3+}	3	H_2O
H-Jarosite	0.486	3	Fe^{3+}	2	SO_4^{2-}	-5	H^+	Strengite	5.476	1	Fe^{3+}	1	PO_4^{3-}	2	H_2O
Lepidocrocite	3.319	-3	H^+	1	Fe^{3+}	2	H_2O	Variscite	4.058	1	Al^{3+}	1	PO_4^{3-}	2	H_2O
Maghemite	2.999	-6	H^+	2	Fe^{3+}	3	H_2O	Anhydrite	0.465	1	Ca^{2+}	1	SO_4^{2-}		

Table 5-2 Equilibrium of two kinds of extracts (extract of single-step method and two-step method) when adjusting pH values by NaOH (MINTEQ results)

Single-step								Two-step							
$MnHPO_4$(s)	3.112	1	Mn^{2+}	1	PO_4^{3-}	1	H^+	$Ca_3(PO_4)_2$ (am1)	7.482	3	Ca^{2+}	2	PO_4^{3-}		
Strengite	5.573	1	Fe^{3+}	1	PO_4^{3-}	2	H_2O								
Variscite	4.028	1	Al^{3+}	1	PO_4^{3-}	2	H_2O								
pH=12								pH=12							
$Al(OH)_3$ (Soil)	1.255	1	Al^{3+}	3	H_2O	-3	H^+	$Al(OH)_3$ (Soil)	1.126	1	Al^{3+}	3	H_2O	-3	H^+
Anhydrite	0.042	1	Ca^{2+}	1	SO_4^{2-}			Boehmite	0.84	-3	H^+	1	Al^{3+}	2	H_2O
Boehmite	0.973	-3	H^+	1	Al^{3+}	2	H_2O	Brucite	3.827	1	Mg^{2+}	2	H_2O	-2	H^+
Brochantite	2.696	4	Cu^{2+}	6	H_2O	-6	H^+	$Ca_3(PO_4)_2$ (am1)	7.482	3	Ca^{2+}	2	PO_4^{3-}		
Brucite	3.723	1	Mg^{2+}	2	H_2O	-2	H^+	$Ca_3(PO_4)_2$ (am2)	10.232	3	Ca^{2+}	2	PO_4^{3-}		
$Ca_3(PO_4)_2$ (am1)	6.435	3	Ca^{2+}	2	PO_4^{3-}			$Ca_3(PO_4)_2$ (beta)	10.902	3	Ca^{2+}	2	PO_4^{3-}		
$Ca_3(PO_4)_2$ (am2)	9.185	3	Ca^{2+}	2	PO_4^{3-}			$Ca_4H(PO_4)_3$:3H_2O(s)	9.916	4	Ca^{2+}	1	H^+	3	PO_4^{3-}
$Ca_3(PO_4)_2$ (beta)	9.855	3	Ca^{2+}	2	PO_4^{3-}			$Cu(OH)_2$(s)	1.288	1	Cu^{2+}	2	H_2O	-2	H^+
$Ca_4H(PO_4)_3$:3H_2O(s)	8.852	4	Ca^{2+}	1	H^+	3	PO_4^{3-}	Cupric Ferrite	20.787	-8	H^+	1	Cu^{2+}	2	Fe^{3+}
Cu(OH)2(s)	1.506	1	Cu^{2+}	2	H_2O	-2	H^+	Diaspore	2.545	-3	H^+	1	Al^{3+}	2	H_2O
Cupric Ferrite	21.178	-8	H^+	1	Cu^{2+}	2	Fe^{3+}	Ferrihydrite	4.895	1	Fe^{3+}	3	H_2O	-3	H^+
Diaspore	2.678	-3	H^+	1	Al^{3+}	2	H_2O	Ferrihydrite (aged)	5.405	1	Fe^{3+}	-3	H^+	3	H_2O
Ettringite	11.967	6	Ca^{2+}	2	Al^{3+}	3	SO_4^{2-}	Gibbsite (C)	1.676	1	Al^{3+}	3	H_2O	-3	H^+
Ferrihydrite	4.972	1	Fe^{3+}	3	H_2O	-3	H^+	Goethite	7.606	1	Fe^{3+}	2	H_2O	-3	H^+
Ferrihydrite (aged)	5.482	1	Fe^{3+}	-3	H^+	3	H_2O	Hematite	17.614	2	Fe^{3+}	3	H_2O	-6	H^+
Gibbsite (C)	1.805	1	Al^{3+}	3	H_2O	-3	H^+	Hydroxyapatite	28.307	5	Ca^{2+}	3	PO_4^{3-}	1	H_2O
Goethite	7.687	1	Fe^{3+}	2	H_2O	-3	H^+	Lepidocrocite	6.726	-3	H^+	1	Fe^{3+}	2	H_2O
Gypsum	0.279	1	Ca^{2+}	1	SO_4^{2-}	2	H_2O	Maghemite	9.81	-6	H^+	2	Fe^{3+}	3	H_2O
Hematite	17.781	2	Fe^{3+}	3	H_2O	-6	H^+	Magnesioferrite	20.264	-8	H^+	1	Mg^{2+}	2	Fe^{3+}
Hydroxyapatite	26.21	5	Ca^{2+}	3	PO_4^{3-}	1	H_2O	$Mg(OH)_2$ (active)	2.133	1	Mg^{2+}	2	H_2O	-2	H^+
Langite	0.423	-6	H^+	4	Cu^{2+}	7	H_2O	$Mg_3(PO_4)_2$(s)	2.038	3	Mg^{2+}	2	PO_4^{3-}	1	H^+
Lepidocrocite	6.807	-3	H^+	1	Fe^{3+}	2	H_2O	Spinel	2.918	-8	H^+	1	Mg^{2+}	2	Al^{3+}

Table 5-2 Equilibrium of two kinds of extracts (extract of single-step method and two-step method) when adjusting pH values by NaOH (MINTEQ results)

Single-step								Two-step							
Maghemite	9.977	-6	H^+	2	Fe^{3+}	3	H_2O	Zincite	1.228	1	Zn^{2+}	1	H_2O	-2	H^+
Magnesioferrite	20.333	-8	H^+	1	Mg^{2+}	2	Fe^{3+}	$Zn(OH)_2$ (beta)	0.702	1	Zn^{2+}	2	H_2O	-2	H^+
$Mg(OH)_2$ (active)	2.029	1	Mg^{2+}	2	H_2O	-2	H^+	$Zn(OH)_2$ (delta)	0.612	1	Zn^{2+}	-2	H^+	2	H_2O
$Mg_3(PO_4)_2$(s)	3.835	3	Mg^{2+}	2	PO_4^{3-}			$Zn(OH)_2$ (epsilon)	0.922	1	Zn^{2+}	2	H_2O	-2	H^+
$MnHPO_4$(s)	0.243	1	Mn^{2+}	1	PO_4^{3-}	1	H^+	$Zn(OH)_2$ (gamma)	0.722	1	Zn^{2+}	2	H_2O	-2	H^+
Pyrochroite	0.613	1	Mn^{2+}	2	H_2O	-2	H^+								
Spinel	3.091	-8	H^+	1	Mg^{2+}	2	Al^{3+}								
Tenorite(am)	2.313	1	Cu^{2+}	1	H_2O	-2	H^+								
Tenorite(c)	3.163	1	Cu^{2+}	-2	H^+	1	H_2O								
Zincite	1.538	1	Zn^{2+}	1	H_2O	-2	H^+								
$Zn(OH)_2$ (am)	0.287	1	Zn^{2+}	2	H_2O	-2	H^+								
$Zn(OH)_2$ (beta)	1.007	1	Zn^{2+}	2	H_2O	-2	H^+								
$Zn(OH)_2$ (delta)	0.917	1	Zn^{2+}	-2	H^+	2	H_2O								
Zn(OH)2 (epsilon)	1.227	1	Zn^{2+}	2	H_2O	-2	H^+								

(2) Experimental observations after pH adjustment with NaOH

Figure 5-4a shows that only a negligible decrease in Al and P concentrations was observed between pH 1.0 and 2.6. A significant decrease in soluble Al and P began when the pH increased from 2.6 to 3.2 and most of the Al and virtually all of the P had precipitated by pH 4.4, suggesting precipitation of Al-P [110, 200]. In contrast, more than half of the soluble Fe precipitated before pH 2.6, suggesting it was not related to phosphate precipitation as strengite ($FePO_4 \cdot 2H_2O$) but to formation of Goethite (FeO(OH) or hematite (Fe_2O_3). By pH 4.4, almost all Fe had precipitated, which could be due to any combination of these phases because P also begins to precipitate at that point. The formation of significant quantities of Ca-P below pH 4.9 is unlikely due to absence of any significant decreases in Ca in the soluble phase. The same behavior was noted with both extracts (Figure 5-4a, b). However, two slight differences are that (i) Fe precipitation was never completed at any pH of the two-step extract and (ii) there was a slight lag in P precipitation after Al precipitation. The first difference could be directly attributed to the continued presence of residual EDTA in the two-step extract, while the second difference could possibly be explained by the increased possibility of Ca (more present) and Fe (more still available in solution at pH 3.2-4.4) contributing to initial P precipitation. It is interesting to note that in (Figure

5-4a, b) P resolubilizes at some point between pH 6.5 and 12.8 and that this coincides with almost complete precipitation of Ca. This observation can be explained by the excess OH^- ions from NaOH forming insoluble Ca, Al and Fe hydroxide precipitates and the Na^+ from NaOH forming soluble Na_3PO_4. Changing the alkali from NaOH to $Ca(OH)_2$ prevents this re-solubilization regardless of whether the extract was from the single-step of two-step process (i.e. comparing Figure 5-5a with 4c and comparing Figure 5-4b with 4d).

The variation in As, Cu, Ni and Zn concentrations with pH adjustment for the single-step and two-step extracts by adding NaOH are shown in the (Figure 5-5a) and (Figure 5-5b) respectively. The behavior of Ni and As were relatively consistent in both the single-step and two-step extracts, except for the redissolution of As noted for the single-step extract at pH 11.0. No such behavior was noted in the two-step extract, even when the pH rose to 12.2. The main difference in the two extracts was the behavior of Zn and Cu. In the single-step extract, virtually all Zn and Cu precipitated between pH 2.4 and 5.2 which coincides with P precipitation. However, with the two-step extract, only very limited precipitation of Zn and negligible precipitation of Cu occurred across the entire pH range. The most logical explanation for such a difference must be linked to the continued presence of residual EDTA in the two-step extract. Additionally,

the stability constants of metal-EDTA varied with the solution pH, which can be confirmed by a the previous research result that Cu-EDTA complexes was a more dominant species than Zn-EDTA in the alkaline pH region [201]. This is an advantage for the two-step process because it means that incorporation of Cu and Zn into the P-precipitate by isomorphic substitution is greatly reduced [201].

(3) Experimental observations after pH adjustment with $Ca(OH)_2$

To study the feasibility of improving the formation of Ca-P, and minimize the formation of Al-P and Fe-P, $Ca(OH)_2$ was used for pH adjustment of the extracts produced by the two extraction methods and the results are shown in Figure 5-4 and Figure 5-5.

The close correlation between Al and P precipitation observed in (Figure 5-4a) (for the single-step, NaOH addition) was affected by using the two-step process (i.e. compare to Figure 5-5c) and the use of both the two-step process and $Ca(OH)_2$ addition instead of NaOH (i.e. compare to Figure 5-4d). Changing to $Ca(OH)_2$ for the single-step extract (Figure 5-4c) delayed both the precipitation of Fe and Al with respect to P precipitation. This implies that Ca had a greater, if still relatively minor role in P precipitation, than when NaOH was used.

When considering the two-step extract (Figure 5-4d), there is a clear break between Al and Fe precipitation which occurs mostly between pH 1.0 and

3.2, and P precipitation which occurs mostly between pH 3.2 and 3.9. Consequently, the use of $Ca(OH)_2$ with the two-step extract appears to facilitate the production of much purer Ca-P precipitate than with the single-step extract if the pH can be carefully controlled between pH 1.0 and 5.0. Looking at the effect of pH adjustment with $Ca(OH)_2$ on the precipitation behavior of heavy metals, Figure 5-5 shows that there was no major effect caused by this change with single-step extracts (i.e. compare Figure 5-5a and 5c). With two-step extracts, the major difference was the ability for $Ca(OH)_2$ to precipitate Zn and Cu between pH 6.3 and 9.3. Following on from the previous explanations in this paper, this effect would mean that $Ca(OH)_2$ was somehow able to successfully compete with residual EDTA for the Zn and Cu (i.e. with excess Ca^{2+} ions). Once released, from the EDTA complex, the Zn and Cu precipitates as insoluble hydroxides. This explanation is further supported by the fact that Na^+ ions from NaOH have an extremely low affinity for EDTA and, even when present in excess, are unable to compete with Zn and Cu for active sites in EDTA complexes. Precipitation of Zn and Cu should not be a concern for contamination of the Ca-P precipitate because the heavy metals only precipitate above pH 6.3 while all the P will have been recovered below pH 5.0.

5.2.4 Identification of crystalline phases in P precipitates

The crystalline components of four different precipitates (formed by addition NaOH or $Ca(OH)_2$ to raise the pH of extracts of the single-step and the optimized two-step method) were determined by XRD (Figure 5-7). No metal(loid) based crystalline phases were present in sufficient quantities to be detected by XRD. However, XRF results (expressed as oxides in Table 5-3) showed consistently detectable levels of Zn and Cu. The precipitates of the two-step method by adding $Ca(OH)_2$ (2-Ca) and the single-step method by adding NaOH (1-Na) were analyzed by SEM-EDX as shown in Figure 5-8.

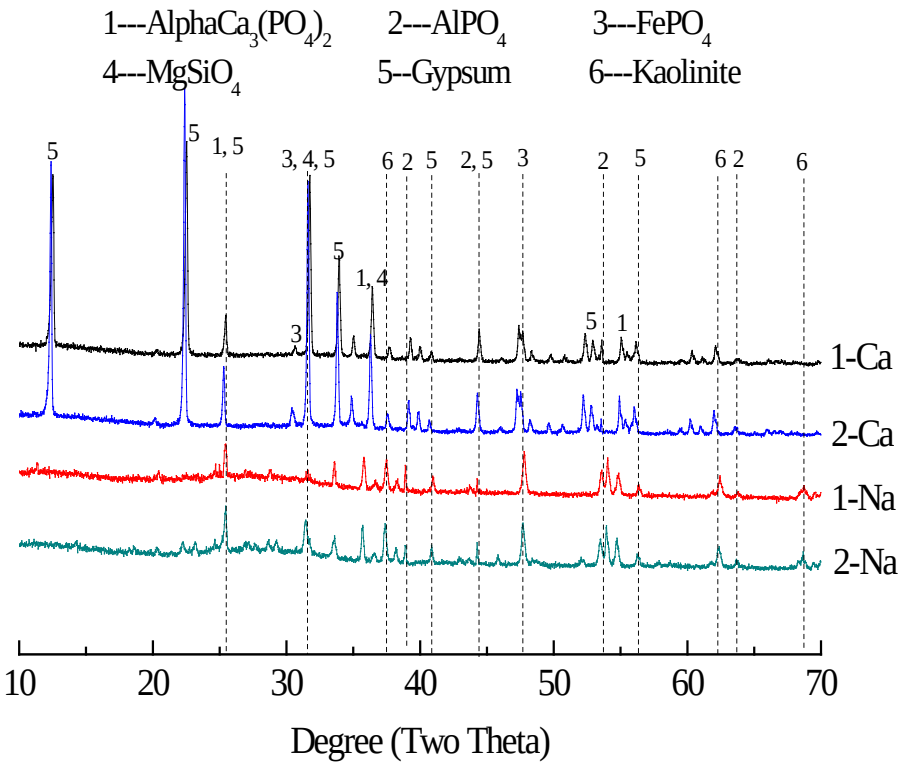

Figure 5-7 XRD patterns of P-precipitate

Table 5-3 Chemical compositions of precipitates produced by changing the pH by adding NaOH and $Ca(OH)_2$ into extracts from the single-step method and the two-step method (%)

Compositions	Raw ISSA	1-Na	2-Na	1-Ca	2-Ca
P_2O_5	9.27	27.154	34.415	9.953	12.907
Al_2O_3	11.88	24.498	26.221	8.893	10.406
SiO_2	31.15	17.431	5.285	8.915	4.918
SO_3	4.08	13.987	19.460	25.321	32.688
Na_2O	2.42	9.484	7.534	ND	ND
Fe_2O_3	23.95	2.836	3.058	1.115	2.294
CaO	9.73	2.310	2.640	43.170	35.384
K_2O	3.50	0.992	0.760	0.377	0.556
MgO	1.66	0.574	0.264	1.905	0.542
ZnO	0.77	0.281	0.056	0.129	0.134
CuO	0.24	0.148	0.021	0.068	0.032
TiO_2	0.55	0.107	0.216	ND	ND
SrO	ND	0.035	0.037	0.038	0.101
Y_2O_3	ND	0.024	0.038	0.012	0.037
As_2O_3	ND	0.008	ND	ND	ND

Ps: ‘1’ is short for ‘single-step extraction’; ‘2’ is short for ‘two-step extraction’; ‘Na’ representing adjusted pH with NaOH; ‘Ca’ representing adjusted pH with $Ca(OH)_2$; ‘ND’ representing not detected.

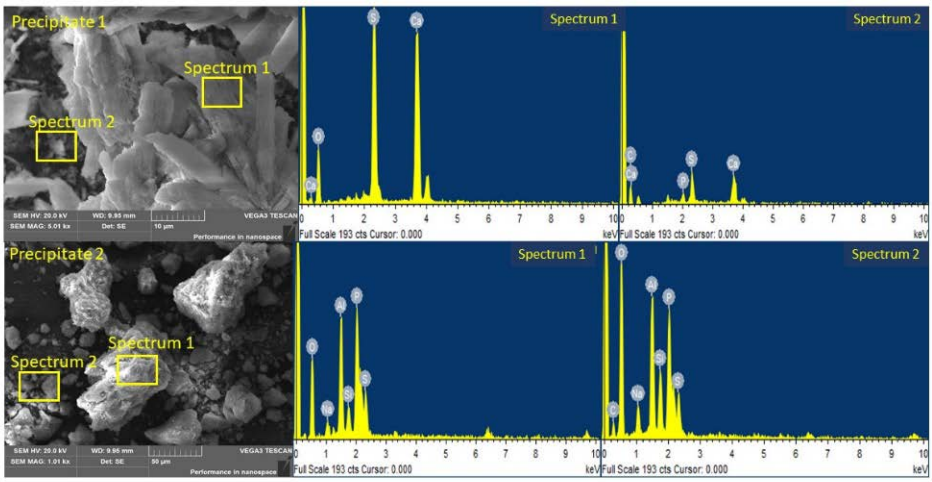

Figure 5-8 SEM-EDX images of precipitates from extract of two-step method by adding $Ca(OH)_2$ (precipitate 1) and extract of single-step method by adding NaOH (precipitate 2) at pH 4

The XRD results show that the main crystalline phases in the precipitates were $Ca_3(PO_4)_2$, $AlPO_4$, $FePO_4$, $MgSiO_4$, gypsum ($CaSO_4$) and kaolinite ($Al_2Si_2O_5(OH)_4$). The peaks of Ca-P were enhanced in 2-Na, 2-Ca and 1-Ca, whereas the peaks of Al-P were reduced in 2-Ca and 2-Na. This indicates that both the two-step method and pH adjusting by $Ca(OH)_2$ could increase the Ca-P formation while the formation of Al-P was averted. The formation of Fe-P precipitate could not be avoided by adding $Ca(OH)_2$ but the peaks were reduced, either due to reduced crystallinity or reduced formation.

The XRF results show that the molar ratio variation of P/Al was related to different P-precipitates. The precipitates from the single-step method using NaOH adjustment had a P/Al of 0.796, while that produced by the two-step

method under the same condition was 0.943. This indicates that the two-step method was beneficial to P-precipitation. When using $Ca(OH)_2$, a large amount of $CaSO_4$ was formed which decreased the mass ratio of other components. For the extract of the single-step method, the P/Al was also decreased from 0.804 to 0.796, but it was increased from 0.891 to 0.943 for the two-step method. These observations indicate that the precipitates of the two-step method formed by adding $Ca(OH)_2$ had the highest efficiency of P-recovery.

SEM-EDX was completed on the precipitate of the two-step method formed by adding $Ca(OH)_2$ (precipitate 1) and the single-step method (precipitate 2) formed by adding NaOH (Figure 5-9). For precipitate 1, large crystals of $CaSO_4$ were observed (chemical compositions detected by EDX). Discrete smaller particles were Ca-P precipitates according to EDX data. For precipitate 2, there were many agglomerates and small irregular particles. EDX verified these were a combination of Al-P with other metal(loid)s.

The main oxide compositions of these four kinds of precipitate are shown in Table 5-4. The mass ratio of MgO, CuO and As_2O_3 were reduced by using the two-step method, indicating improved purity of the P-precipitate. Constituents such as TiO_2 and Y_2O_3 are effective soil restorers, which would improve the properties of soil [202, 203], and the presence of SrO

is also conducive for plant growth [203], thus they provide additional benefits of recovering P precipitates as phosphorus fertilizers. In summary, the two-step extraction method formed Ca-P with improved purity when pH adjustment used NaOH. Using $Ca(OH)_2$ instead of NaOH favors more Ca-P formation but also causes significant precipitation of gypsum. Effective plant grow components including P_2O_5, TiO_2, Y_2O_3, and SrO were enriched in the precipitate of the two-step method which is favorable for valorization of the ISSA for fertilizer applications.

5.2.5 Secondary environmental impact and economic costs

The two-step leaching by EDTA and H_2SO_4 has removed the leachable parts of the ISSA, thus the solid residues mainly consist of immobile glassy phases which pose low risk to the environment. As a result, these residues can be reused as an additive in construction materials, such as concrete, mortar and subbase. However, the liquid extract after P recycling must be treated to meet the local regulation before discharging.

For practical application of this technology, the costs mainly include consumption of EDTA and sulphuric acid. Based on the online quotations afforded by the largest regional supplier in Hong Kong (2017) [203], the costs of EDTA and sulphuric acid are approximately USD 2000/tonne and USD 390/tonne, respectively. As a result, at the optimal extraction condition, the total cost is about USD 386.48/tonne ISSA. However, the

recycled P-fertilizer can be sold at 600 USD/tonne and may provide greater financial return [203].

5.3 Summary

To obtain a high purity P-extract from ISSA a two-step extraction method was developed. This method sequentially leached ISSA with EDTA and then sulphuric acid. The optimal extraction condition was pre-extraction by EDTA (concentration of 0.02 M, L/S ratio of 20:1 and reaction time of 120 min), followed by P extraction with sulphuric acid (concentration of 0.2 M at a 20:1 L/S ratio with a 120-min reaction time). This decreased the final extract concentration of most metal(loids) studied. For example Cr (by 92%), Zn (by 58%), Mn (by 50%), Mg (by 49%), Cu (by 49%), Al (by 37%) and Fe (by 23%). Pre-treatment with EDTA increased the quantity of Ca in the final extract (+22%), which is explained by residual EDTA in ISSA solids restricting the formation of gypsum occurring to the same extent during the single-step extraction. The two-step method produced a precipitate with higher Ca concentration and lower concentrations of Fe and Al impurities. While this favors increased formation of Ca-P, co-precipitation of gypsum makes it difficult to draw a clear conclusion. Detectable levels of desirable minor elements for soil remediation (TiO_2, Y_2O_3 and SrO) were found only in the P-precipitate formed using the two-step method. Therefore, applying the two-step method for P recovery not

only produces a P-extract with higher purity but also produce a P-precipitate which is advantageous for fertilizer applications.

Chapter 6 Use of Mg/Ca modified biochars to take up phosphorus from acid-extract of ISSA for fertilizer application

6.1 Introduction

Large amounts of sewage sludge are produced worldwide every year and they are dominantly agriculture applied and landfilled worldwide [204]. To be specific, in China, approximately landfilled and agriculture take up 31.03% and 44.83%, respectively [205, 206]. However, using of the sewage sludge as fertilizers is increasingly inhibited around the world due to their potential impact to the environment [207]. Incineration of sewage sludge is becoming more popular especially in developed cities due to its better pollution control and potentials for volume reduction, landfill capacity saving and energy recovery [20]. Recently, the T·Park incinerates about 1500 tons of sludge per day and generates about 150 tons of ISSA, which is currently disposed of to landfill [204]. Previous studies have shown that Hong Kong ISSA contains 35 g/kg of P, which is one of the three main inorganic nutrients used in industrial fertilizers that are essential for plant growth (P, N and K) [125, 207]. Meanwhile, P recovery from ISSA is more feasible than that from sewage sludge due to P is dominantly in the form of organic-P [12, 13]. It is well known that economically extractable

P reserves are essentially finite because they form over geological timescales. Consequently, the recovery of P from ISSA for use in fertilizers is a central objective of this study as part of the attempt to develop a circular economy for P.

Previous studies by the authors have developed an effective extraction method to obtain a P-rich acid-extract from ISSA [208]. The acid-extract needs further treatment prior to any application as a P-fertilizer due to the low P concentration and high acidity.

Biochar is a carbonaceous sorbent characterized by high porosity, specific surface area and certain surface functional groups [105]. Biochar can be used as a soil conditioner to retain and progressively release nutrients, improve soil fertility, increase seed germination rates, plant growth and crop yields [106]. An additional advantage of biochars compared to inorganic fertilizers is that their non-carbonized fraction may interact with soil contaminants, thereby improving the properties of soil [104].

The surface of biochar is negatively charged and has a low oxyanion removal capacity [209-211]. P is usually present as an oxyanion (e.g. PO_4^{3-}, HPO_4^{2-}, $H_2PO_4^-$, depending on the pH) and the P sorption capacity of biochar must be improved by modification with metal cations like Mg^{2+}, Ca^{2+}, Fe^{3+} or Al^{3+} [212-215]. Oxyanion removal is governed by positively charged sites formed by protonation of metal oxides in the metal-biochar

composite [209]. Biochars modified with Mg can induce Mg-P particles formation on the surface of the biochars [108, 216] while that with Ca forms brushite ($CaHPO_4 \cdot 2H_2O$) [109, 123]. Additionally, both Mg and Ca are essential mineral elements for plant growth [216]. Therefore Ca and Mg were used in this study to enhance P adsorption on the biochars.

The pyrolysis temperature has a major influence on the porosity of the formed biochar. Numerous meso-pores (between 2~ 50 nm) are generated when the pyrolysis temperature is below 500 ^{o}C but these tend to collapse above 600 ^{o}C [108, 217]. Increasing the pyrolysis temperature changes the mesopore distribution from ordered to disordered, increasing the specific surface area and the number of organic functional groups [108]. Higher pyrolysis temperatures can produce biochars with enhanced physical action and reduce the interference from coexisting ions on P sorption [108]. Pyrolysis temperature of 700 $^{\circ}$C was reported to form biochars with higher aromaticity and lower polarities which improved sorption [104, 218, 219]. Based on the above, pyrolysis temperature of 450 ^{o}C, 700 ^{o}C and 850 ^{o}C were used in this study to determine the most effective biochar for P-sorption.

The acid-extracts from ISSA are usually strong acidic (pH<2). However, information is currently lacking in P-sorption by biochar from acidic solutions. It is necessary to investigate P sorption under acidic conditions

because P can precipitate with metal(loid)s (Al, Fe, Ca, etc.) when the solution pH > 2 [208].

Peanut shells (Ps) and sugarcane bagasse (Sc) are produced as municipal wastes from food processing in China. Biochars based on these materials have been reported to have promising P-sorption capabilities [220, 221].

The overall objective of this study is to investigate how P rich acid extract from ISSA can be used to produce an effective biochar-based P-fertilizer. The P-extracts from ISSA by a 2-step acid-extraction procedure was used based on our previous study [208]. Experiments were performed to determine the optimal biochar production conditions and the optimal pH for P sorption onto the biochar. The sorption mechanisms were investigated using sorption kinetic and isotherm models combined with spectroscopic and microscopic analysis (X-ray diffraction (XRD), scanning electron microscopy with energy dispersive X-ray spectroscopy (SEM-EDX) and Fourier transform infrared (FTIR)).

6.2 Results and discussion

6.2.1 Biochar optimization

The characteristics of the biochar (surface metal deposit, functional group and pH) determined the sorption capacity for anions, oxyanions or cations. The modification method and pyrolysis temperature of biochar were

selected based on previous studies [104, 109, 218, 222]. The optimal P sorption biochar was obtained by comparing biochars produced from two kinds of biomass (Sc and Ps), two kinds of modification methods ($MgCl_2$ and $CaCl_2$) and three pyrolysis temperatures (450, 700 and 850 ^oC).

(1) Characteristics of produced biochars

As shown in Figure 6-1a and 1b, the MgO was produced in the biochars treated with $MgCl_2$ (in range of 30- 80 ^{o}), while for the biochars treated with $CaCl_2$ (in range of 10-60 ^{o}), the CaO was formed only under 850 ^oC. This is because degradation of Mg(OH)Cl occurred with further transformation into MgO in temperature range of 450-650 ^oC [123]. However, thermal stability of $CaCl_2$ is higher than $MgCl_2$ and the formation of CaO requires the pyrolysis temperature greater than 850^oC [223, 224]. In addition, the higher pyrolysis temperature facilitated the crystallization of biochars.

The FTIR data (as shown in Figure 6-1c) detected the peaks at wavenumber of 3400 (O-H stretching), 1613 (C=O stretching), 1373 (C=C aromatic ring modes), 1130 (C-O stretching), 1057 (aliphatic C-O-C) and 850 cm^{-1} (C-Cl bending). Both biomasses were polymer-rich materials and formed biochars had many hydroxyl and aliphatic groups [225]. The C=C peak intensities were increased after the modification of $MgCl_2$/$CaCl_2$. Impregnation with Mg slightly increased the peaks for O-H stretching

which might be attributed to the change in orientation of the O-H groups induced by Mg [226]. Organic functional C-H groups and C-Cl groups were detected at pyrolysis temperature of 700 ºC and these could enhance the P sorption [108].

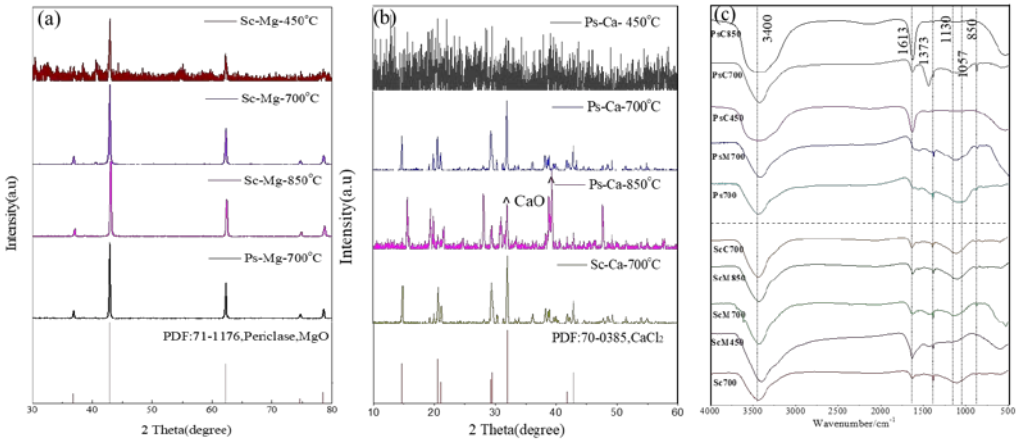

Figure 6-1 XRD and FTIR results of biochars (a: XRD results of biochars modified by $MgCl_2$; b: XRD results of biochars modified by $CaCl_2$; c: FTIR results of biochars)

Treatment with $CaCl_2$ and $MgCl_2$ significantly enhanced the porous structure and biochar surface properties which increased the pH and zeta potential as shown in Table 6-1 (e.g. comparing the results of Ps700 with PsM700 and PsC700). The pyrolysis caused decomposition of organics and the remaining metal oxides led to an increase in the pH (Ps700 from 9.4 to 9.9 and Sc700 from 6.5 to 10.3) [227]. Impregnation with Mg produced positively charged surfaces on the biochar while that with Ca was still slightly negative charged (increased from strong negative charged to

slightly negative charged), as shown by their zeta potential values. Both of the modifications dramatically increased the BET values and pore volumes of the produced biochars. To be specific, treatment with $MgCl_2$ resulted in even higher BET surface areas (+33% and +1340% for PsM700 and ScM700 respectively) and higher pore volumes (+19% and +877% for PsM700 and ScM700 respectively) than the equivalent $CaCl_2$ treated biochar. The superior properties of $MgCl_2$ loaded biochar are related to the activation effect of $MgCl_2$ hydrates [228], while the favorable properties of Sc-based biochar due to the consistent layered porous structure as shown in Figure 6-2.

Table 6-1 Characteristics of ten kinds of biochars

Sample	Zeta potential (mV)	pH	BET (m^2/g)	Pore volume (cm^3/g)	Sample	Zeta potential (mV)	pH	BET (m^2/g)	Pore volume (cm^3/g)
Ps700	-22.73	9.4	7.9	0.009	Sc700	-4.78	6.5	9.1	0.008
PsM700	5.76	9.9	120.6	0.109	ScC700	-0.45	10.3	100.2	0.161
PsC450	-2.97	10.0	6.1	0.030	ScM450	15.55	9.5	40.6	0.031
PsC700	-1.70	10.1	90.2	0.091	ScM700	26.25	9.6	1440.4	1.574
PsC850	-0.52	10.5	74.3	0.072	ScM850	2.85	9.8	228.74	0.243

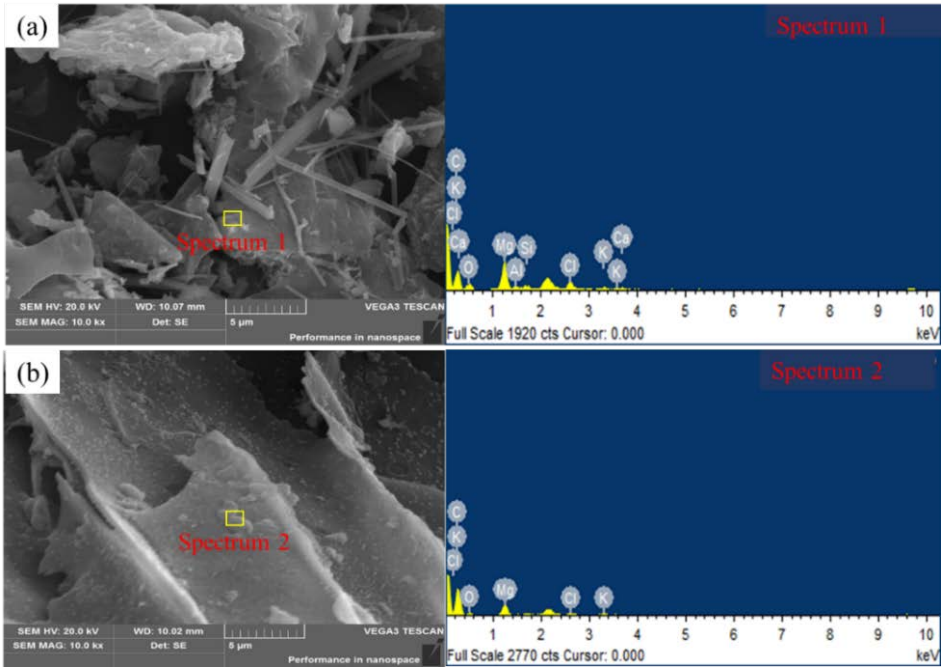

Figure 6-2 SEM-EDX analysis of biochars modified by $MgCl_2$ (a, PsM700; b, ScM700)

The BET value and pore volume of the biochars were increased from 450 to 700 °C and decreased from 700 to 850 °C. This was resulted from increasing decomposition of the biochar causing greater exposure of the

underlying layers and volatilization of HCl which produced more pores as the temperature was increased from 450 ^{o}C to 700 ^{o}C [227]. At higher pyrolysis temperature (>700 ^{o}C) the pore structure formed started to collapse. A pyrolysis temperature of 700 ^{o}C was therefore considered to be optimal.

In summary, the amendment by $MgCl_2$ and pyrolysis at 700 ^{o}C resulted in the optimization of the biochar's physicochemical properties for P sorption. Consequently, subsequent experiments for P sorption used biochars ScM700 and PsM700 as the sorbents.

(2) P sorption efficiency of biochars

The P sorption of P from the P-extract by the biochars is shown in Figure 6-3. As could be expected from the results reported in previous section, amendment with $MgCl_2$ significantly enhanced the P sorption capacity of the biochars, with the highest removal associated with those had the highest BET surface areas and pore volumes. Recovery efficiency of P to these biochars were high (>80%) in acidic solutions (pH<2) and comparable to those in weak acidic solutions [207]. With the presence of SO_4^{2-} and other anions, the biochar modified with $MgCl_2$ showed high selectivity to P. Because phosphate sorption is through the formation of inner sphere complexes with oxides and hydroxides, while the sorption of SO_4^{2-} and other cations is through outer-sphere complexes which could not interfere

with P sorption [105, 207, 229, 230].

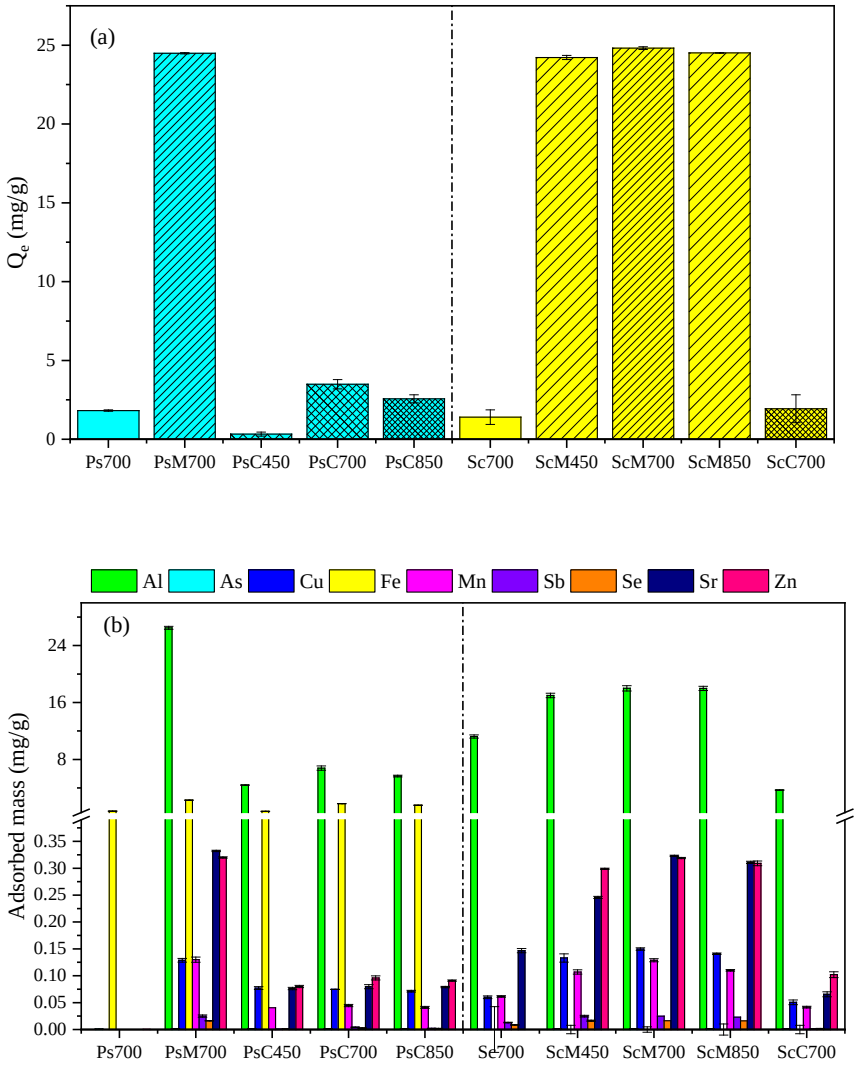

Figure 6-3 Absorption results of 2-step extract by various biochars (a: P; b: metal(loid)s)

Amendment with $MgCl_2$ significantly enhanced the P sorption capacity of biochars. This can be explained by their high porosity, surface area and zeta potential of Mg decorated biochars, which favored the P sorption and precipitation. Additionally, the biochars under pyrolysis temperature of 700

^{o}C achieved the highest P removal efficiency which were in consistent with their highest BET value and pore volume. This high P sorption efficiency (about 80%) of the biochar in acidic solution (pH<2) was comparable to those in weak acidic solutions [207], which implied that the effectivity of the Mg-doped amendment methods for P sorption from acid-extracts of ISSA. Though the existence of SO_4^{2-} and other cations, the biochar modified with $MgCl_2$ showed high selectivity to P. This is because the phosphate sorption is through formation of innersphere complexes with oxides and hydroxides, while the sorption of SO_4^{2-} and other cations is through outersphere complexes which could not interfere the P sorption [105, 207, 229, 230].

Meanwhile, the co-sorption of metal(loid)s was shown in Figure 6-3b. The biochars impregnated with Mg sorbed a number of metal(loid)s from the P-extract synergistically with their P sorption. Massive dissolution of Mg/Ca from the Mg/Ca modified biochars occurred, thus their concentrations are not shown. This implied the significant effect of ion-exchange occurred in the sorption process. For comparison, it is worth noting that, through the same amendment method, biochars produced from the biomass of Sc can sorb more divalent metal ions while those from the biomass of Ps sorb more of trivalent metal ions. This can be related to their different compositions, as shown in the total digestion results in Table 6-4,

which compared biochars of ScM700 and PsM700 before and after sorption. As shown, except the massive existence of Mg and K, Fe was dominant in ScM700 while Ca was dominant in PsM700 before sorption. This also explained why no sorption of Fe was found by Sc-based biochar. Thus, the occurrence of metal(loid)s or ligand exchange was inferred during sorption, which agreed with previous findings that metal(loid)s or ligands exchange played an important role in metal(loid)s sorption [207, 231]. Because many undesirable metal(loid)s are present in the divalent form, especially Zn and Cu, the difference in sorption behavior favors ScM700 over PsM700 in P sorption from the complex acid-extracts [6, 42].

6.2.2 Effect of initial pH of P-extract on P removal

The pH value of the acid-extract controls P sorption onto the biochar by altering the surface charge of the biochar and P-speciation in the extract [216]. The co-precipitation of P with metal(loid)s (e.g. Al, Fe, Ca, etc.) occurs when adjusting the pH of the P-extract to greater than 2. Only at a pH less than 2 is P freely available to interact with the biochar surface, which is supported by the P extraction results from ISSA [6, 125]. Consequently, P sorption on the biochars from the extracts in the pH range of 1 - 2 was studied. In this pH range, H^+ was ionized from H_3PO_4 and induced the formation of $H_2PO_4^-$ as confirmed in the simulated data from Minteq (Figure 6-4).

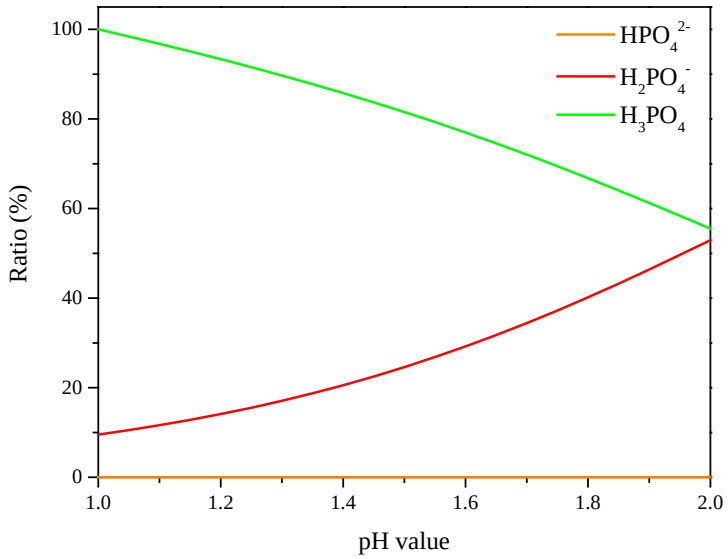

Figure 6-4 Variation of phosphate anion in studied pH range (by Minteq counting)

As shown in Figure 6-5 as the extract pH values increased from pH 1 to 1.6, P sorption by the biochar also increased. At pH 1, phosphate mainly existed as H_3PO_4 in the P-extract. For phosphate to interact with the charged (positive zeta potential) biochar surfaces, it is necessary for them to have a partial negative charge. As the acidic extract interacted with the alkaline biochar, the aqueous environment would become less acidic (final equilibrium pH of around 6 – 7 was observed). As a result, the increasing in P sorption was related to the increased ionization of $H_2PO_4^-$ as the pH increased. In comparison, the P sorption efficiency of ScM700 was higher than PsM700 under the same conditions.

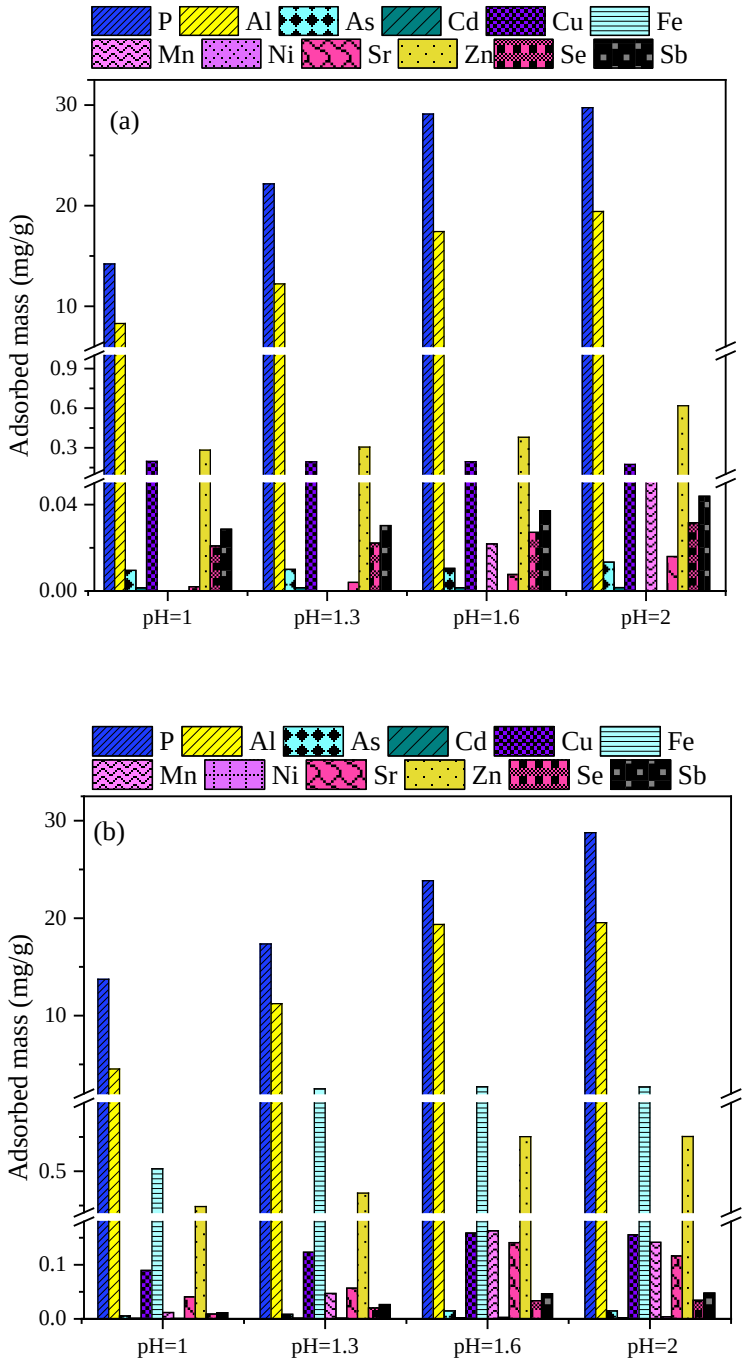

Figure 6-5 Effect of initial pH of the P-extract on sorption by ScM700 and PsM700 (a and b: P and metal(loid)s sorption by ScM700 and PsM700, respectively)

The metal(loid)s removal ratio by the biochars in the pH range studies is shown in Figure 6-5. The higher the pH of the P-extract was, the more metal(loid)s were sorbed by the two kinds of sorption system [126].

Therefore, this can be explained by the greater competition between the generally cationic metalloid ions and H^+ ions in solution. The sorption ratio of these two biochars was at the lowest at pH 1, and slowly increased till pH 1.6 and reached the highest at pH 2. Therefore, the P-extract with a lower pH produced biochars with reduced metal(loid)s. In comparison, biochar ScM700 had the advantage of sorbing P-extract at a low pH (1-1.6). This can be explained by the chelating of metal(loid)s with EDTA that might be easier to be captured by the porous media like ScM700.

To obtain high P recovery and relatively less metal(loid)s on ScM700 for using as a P-fertilizer, the P-extract with an initial pH of 1.6 is recommended as the optimum balance between the increased P sorption and the limited metal(loid)s sorption.

6.2.3 Sorption kinetics

As shown in Figure 6-6a, the sorption kinetics of the two kinds of biochars from the P-extract were a two-stage sorption process, which consisted of a rapid initial sorption phase of a very short duration (around 34 mg/g within a few minutes), and a slow/steady sorption phase (around 35 mg/g during the first 100 minutes). While both biochars achieved the similar total P recovery, and the sorption of the ScM700 material was even more rapid during the initial phase than the PsM700 material that had a lower BET surface area. In the second stage, intra-particle diffusion might impede

further P sorption. Because the reduction of P content in solution and the exhaustion of sorption sites on the biochar, the sorption arrived at an equilibrium [232, 233].

Both of the sorption processes were further studied by fitting with three kinetic models separately. The pseudo-first-order model could not fit these sorption process (coefficient of determination-R^2 was lower than 0.5), thus was not shown. However, the sorption of P from the P-extract could be well fitted by the pseudo-second-order model (Table 6-2). And the fitted sorption rate for ScM700 was higher than that for PsM700. Thus, P sorption was majorly controlled by chemical reaction/chemisorption, which was consistent with other previous findings [234, 235].

Table 6-2 Sorption kinetic parameters of P

	Pseudo-second-order			Intra-particle-diffusion		
	K_2 (g/(mg·min)	Q_e (mg/g)	R^2	K_{id} (mg·g^{-1}min$^{-1/2}$)	C (mg/g)	R^2
SCM700	0.140	30.57	0.894	0.039	29.87	0.375
PSM700	0.049	30.41	0.962	0.106	28.50	0.455

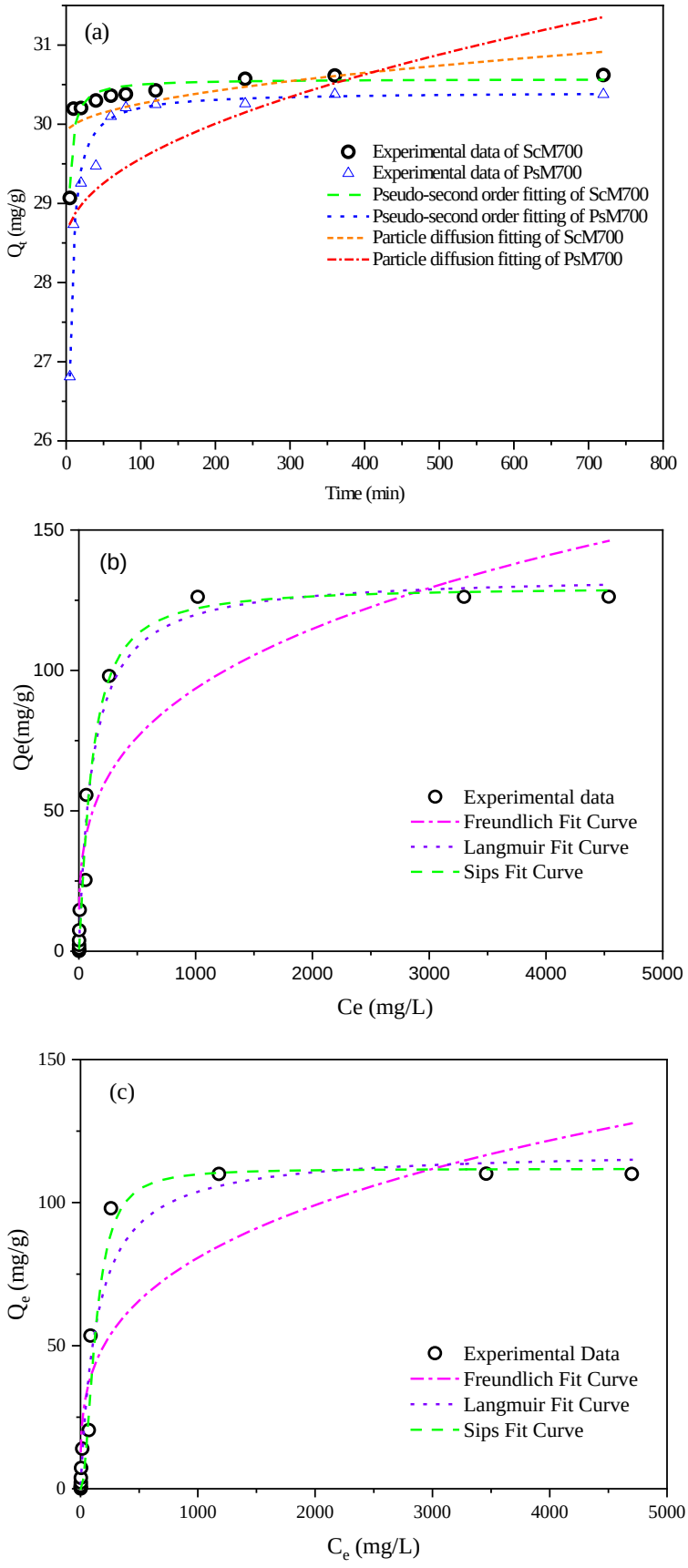

Figure 6-6 Kinetic sorption and sorption isotherm analysis of P removal from the P-

extract (a: Kinetic sorption; b and c: sorption isotherm analysis of ScM700 and PsM700, respectively)

6.2.4 Sorption isotherms

The results of P sorption isotherms are shown in Figure 6-6b and c. When C_e is lower than 85 mg/L, there is a large capacity of biochar available for P sorption. As the C_e approaches around 260mg/L, the available P sorption capacity begins to become saturated and reaches a steady state.

The sorption by both biochars closely fitted the Sips model but did not fit so well with the Langmuir model and showed even poorer agreement with the predictions according to the Freundlich model (Table 6-3). The best fitting by the Sips model suggested that the P sorption process was a multiple process, which was similar to the findings of previous research [233, 236]. The limited fit with the Langmuir equation suggests that one of these processes is a monolayer sorption [237]. According to the prediction of Sips model, the Q_m of ScM700 was 129.79 mg P/g biochar while the PsM700 was 111.80 mg P/g biochar. This further identified the higher sorption capacity of ScM700 compared with PsM700.

Table 6-3 Sorption isotherm parameters of P

	Freundlich			Langmuir			Sips			
Biochar	K_F (L/g)	1/n	R^2	K_L*10^{-2} $(L/g)^{1/n}$	Q_m (mg/g)	R^2	K_s $(L/g)^{1/n}$	1/n	Q_m (mg/g)	R^2
PsM700	10.432	0.2	0.824	0.710	118.42	0.94	0.004	1.142	111.80	0.945

ScM700	12.205	0.2	0.867	0.850	133.89	0.98	0.003	1.233	129.79	0.982

6.2.5 Characteristics of the P-laden biochars and sorption mechanism

As aforementioned, ScM700 was deemed as the optimal P sorption biochar, thus its elemental composition and characteristics were analyzed by XRD, FTIR, SEM/EDX both before and after P sorption.

As shown in Figure 6-7, the XRD results verified the co-precipitation of P with Mg, Ca, Fe and Al on ScM700, which were consistent with the EDX analysis in Figure 6-8, and also agreed with previously implied chemisorption of P sorption. The FTIR detected an obvious newly formed peak at 1100 cm^{-1}, which was attributed to hydro-phosphate (-HPO_4). In addition, the –OH at 3400 cm^{-1} was significantly decreased mostly due to the deprotonation during the sorption of ions from the P-extract. As seen from the images in Figure 6-8, the consistent thin flaked structure of ScM700 before sorption was laden with small globular-like precipitates on the surface which were mainly consisted of Ca, Mg, Al, P and K. The EDX analysis indicated that the molar ratio of P/Mg was about 3, which was much higher than that of $Mg_3(PO_4)_2 \cdot 8H_2O$ (0.67), implying the P was co-precipitated with other elements apart from Mg and/or sorbed to the charge surface sites.

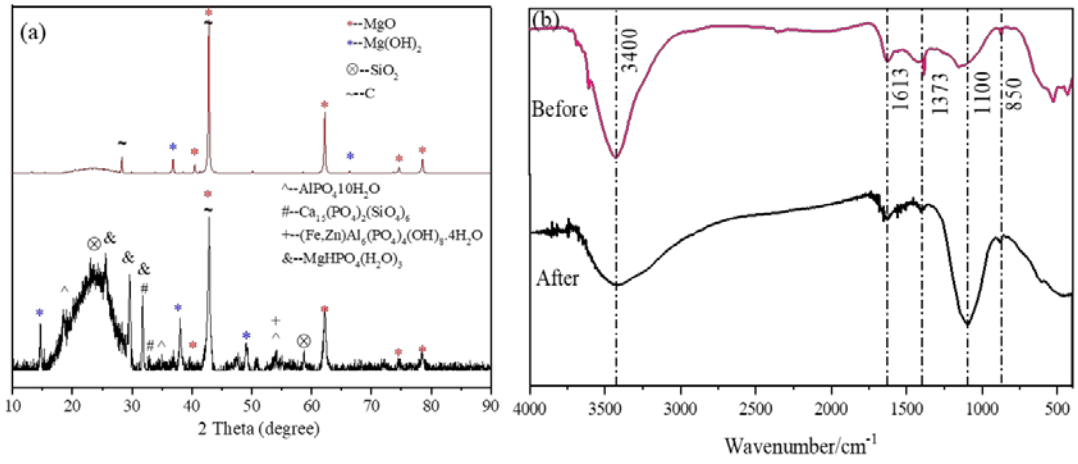

Figure 6-7 XRD and FTIR results of ScM700 before and after sorption (a: XRD; b: FTIR)

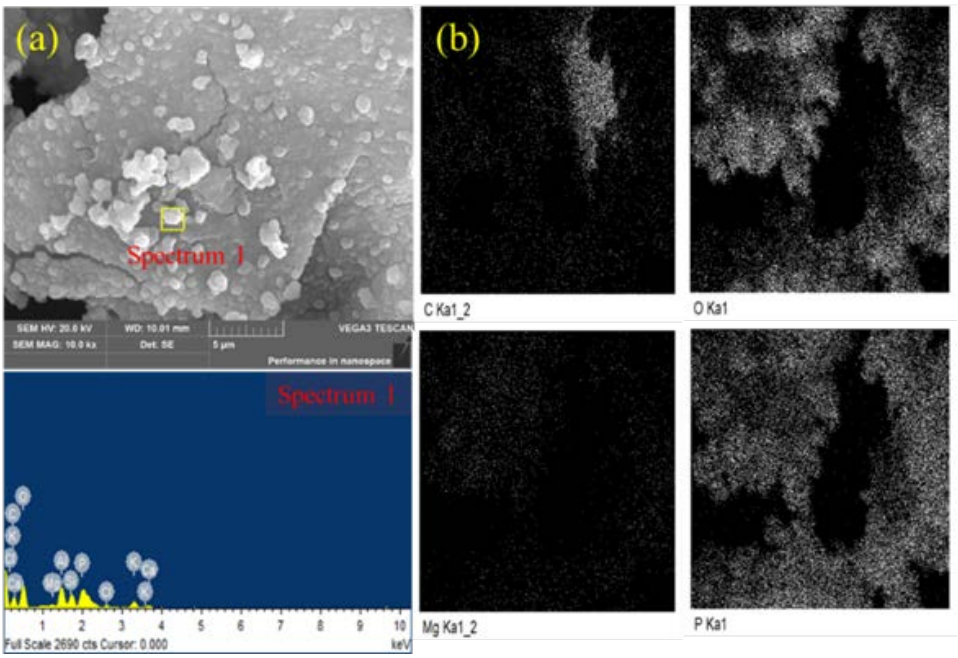

Figure 6-8 SEM-EDX analysis of ScM700 after sorption (a: SEM-EDX; b: elements mapping of carbon, oxygen, magnesium, and P using EDX on SEM)

The elemental composition of the post-sorption biochars was assessed by ICP analysis and the results are shown in Table 6-4. The acceptance

criterion for P-fertilizers in China only limits the contents of As, Cd, Pb, Cr and Hg, which were not detected in the post-sorption biochars. For Cu and Zn, their concentrations in the post-sorption biochar were far lower than the fertilizer limits reported in Germany [30] and Switzerland [26]. As such, the P-rich ScM700 could be considered as an efficient and environmentally friendly P-fertilizer.

Table 6-4 Total concentration of elements in post-sorption biochars（mg/g）

`	C	H	N	Al	Ca	Cu	Fe	K	Mg	Mn	Sr	Zn	Se	Na	Sn	P
ScM700-bef	390.13	25.77	3.70	1.92	4.19	-	53.62	53.62	602	-	-	-	-	1.29	-	-
PsM700-bef	450.14	21.50	8.45	19.05	21.54	-	4.96	31.01	551	-	-	-	-	1.29	-	-
ScM700-aft	-	-	-	17.82	16.49	0.12	0.58	3.58	47.42	0.15	0.13	0.31	0.06	9.72	0.23	34.92
PsM700-aft	-	-	-	27.54	3.08	0.09	2.46	4.01	32.85	0.11	0.07	0.21	0.07	5.83	0.06	31.4
Fertilizer limitation																
German	-	-	-	-	-	5	-	-	-	-	-	1.5	-	-	-	-
Swiss	-	-	-	-	-	0.4	-	-	-	-	-	1.3	-	-	-	-

Ps: ‘bef’ represents before absorption; ‘1s’ and ‘2s’ represents extraction methods of 1-step and 2-step processes, respectively.

6.3 Summary

The results showed that the Sc-based biochar modified by $MgCl_2$ and pyrolysis at 700 ^oC had the optimal effect for P sorption, due to its positive charged surface, relatively higher surface area (1440 m^2/g) and pore volume (1.6 cm^3/g). The Sips model could best fit the sorption isotherm data and the estimated sorption capacity of ScM700 to P in the acid-extract of ISSA was 130 mg/g biochar. Sorption kinetics generally followed a pseudo-second-order model, which suggested that the P sorption was dominantly controlled by chemical reaction (precipitation). To obtain a post-sorption biochar of high P purity, the initial pH of the acid-extract should be fixed at around 1.6. The sorption of P from the acid-extract by the Mg-modified biochar was mainly attributed to the chemical precipitation of P-Mg, P-Ca, P-Al and P-Fe. The P-enriched biochar produced has potential to be a highly effective P-fertilizer because it contained abundant plant nutrients and little metal(loid)s. However, a complete agronomic evaluation of the P fertilizer produced under different soil and climatic conditions on various crops still needs to be assessed in further work.

Chapter 7 Agronomic Effectiveness Evaluation of Three kinds of Recovered Phosphate Fertilizers (RPF) from ISSA

7.1 Introduction

P plays a fundamental role in agriculture and continual production of vegetation requires input of P fertilizers [238]. However, the manufacture of conventional P fertilizer would consume phosphate rock, which is a finite and non-renewable resource in the world [239]. It has been widely acknowledged that the reserves of phosphate rock is declining and the P fertilizer will not be as economically viable as ever before [240, 241].

To relieve the burden of the P ores scarcity, various secondary P sources were explored like animal manures, wastewater, sewage sludge and ISSA [242]. Of these, ISSA is a byproduct generated from sewage sludge incineration plants and is usually disposed of in landfill. In addition, ISSA is a potential P-source with significant amounts of P [22, 41]. But direct applications of ISSA as fertilizer is inadvisable due to its high heavy metal contents and poor bioavailability of P [30, 68]. Although various methods had been developed to recover P from ISSA, the produced phosphate fertilizers from ISSA still contains some heavy metals to different extents [243, 244].

Heavy metals, like Zn, Cu, Co and Ni, are essential microelements for plant growth, but excessive application of these metals is toxic for growing plants [245]. Their translocation from RPFs to soil eventually beneficiates in food chains which would pose a risk to the health of animals and human [130, 246, 247]. The metal uptake of plants is adsorbed by roots and transported in form of metal-complexes or free metals across the root cortex to stele [130, 248]. Hence, the metals in soils are accumulated in plants if excessive concentration occurred.

In addition, it is difficult to determine the quality of fertilizers only through the existing accepting criteria due to the complexity of RPFs. Hence, plant growth tests are essentially important in the study of new kinds of RPF to determine their applicability (which is agronomic effectiveness) for agriculture production.

The present study was therefore aimed at evaluating the agronomic effectiveness of three RPFs from ISSA as sources of P in two different systems for the cultivation of choy sum and ryegrass. Three kinds of RPF which produced in our previous studies: struvite (SP), calcium phosphate compounds (CaP), P-loaded biochar (BP) were used as P sources and two soluble inorganic P fertilizers (monopotassium phosphate (MP) and compound fertilizer (CoP)) were used as references [90, 127, 128]. The agronomic effectiveness of RPFs refers to the effects of RPFs in assisting

the growth of plants, which can be evaluated from the growth status. The growth status includes the leaf number, colour, and size, shoot length and weight of shoot. The main objectives of this study are: 1) to characterize the RPFs produced from ISSA; 2) to evaluate the agronomic effectiveness of the RPFs through pot trial tests for cultivation of choy sum via hydroponics and ryegrass via soil culture experiment; 3) to analyze the levels of nutrients and accumulation of heavy metals in the plants.

7.2 Results and discussion

7.2.1 Composition of RPFs

The P and heavy metal contents in SP, CP and BP were presented in Table 3-6. As shown, SP had the highest P contents with a value of 63.1 mg/g, closely followed by CaP with a P content at 61.9 mg/g. The P contents in these two recovered P products are well within the range of commercial P fertilizers (4% to 30 wt %) [249]. BP, in contrast, had the lowest P content at 30.8 mg/g. According to our previous studies, struvite was the main crystalline phase in SP [90] and $Ca_3(PO_4)_2$ was the dominant crystalline phase in CaP together with a small amount of $FePO_4$ [127]. As regards BP, four kinds P compounds including Al-P ($AlPO_4 \cdot 10H_2O$), Mg-P ($MgHPO_4$), Fe-P ($(Fe,Zn)Al_6(PO_4)_4(OH)_8 \cdot 4H_2O$) and Ca-P ($Ca_{15}(PO_4)_2(SiO_4)_6$) were identified [128]. As alluded, trace elements in nutrient are known to

pose the risk of potential accumulation in soils and can be transferred via the food chain [250]. Excessive concentrations of metals in soil or nutrient solution is essentially toxic for organism and growing plants. The regulation limits of trace elements for fertilizers in different countries are shown in Table 7-1. Comparing the values in Table 3-6 and Table 7-1, except CaP, the content of trace elements in BP and SP were within the limits of the fertilizer regulations in many countries. In CaP, content of Cd was slightly higher than the limit which might due to the precipitation of $Cd(OH)_2$ in the pH adjusting process.

Table 7-1 Legal limited values of different countries' Fertilizer Ordinances for relevant trace elements [72, 83, 227]

Trace element	Germany	Australia	China	Switzerland	Turkey	Japan
As (mg/kg)	40	-				50
Cd (mg/kg)	4	15	10	3		5
Cr (mg/kg)		667	500	299	270	500
Cu (mg/kg)	70	778	-	400		
Hg (mg/kg)	1	1	5	3		2
Ni (mg/kg)	80	100	-	50	120	300
Pb (mg/kg)	150	100	150	200		100
Zn (mg/kg)	1000	3333	-	1300	1100	
Co (mg/kg)				40		

Notes: Germany and Australia [29]; China, Switzerland and Turkey [65]; Japan [251]

7.2.2 Growth status of plants

The growth status of choy sum and ryegrass are presented in Fig 7-1. For choy sum, the worst growth status was in BC (control) group, since the leaf number (Fig 7-2), size (Fig7-3) and shoot length were the lowest among

the different treatment groups. The leaves in BC even turned yellow and became seriously withered at the end of the growth period. In comparison, choy sum fertilized with P grew well with larger and greener leaves, and SP performed best among all treatment. Similarly, ryegrass planted in BC was paler and thinner than other P fertilized groups, which were dark-green in colour. In addition, BP group had the highest germination rate mostly due to the soil amelioration effect caused by the biochar [252]. Meanwhile, other two kinds of RPF produced similar germination rates to the CoP group.

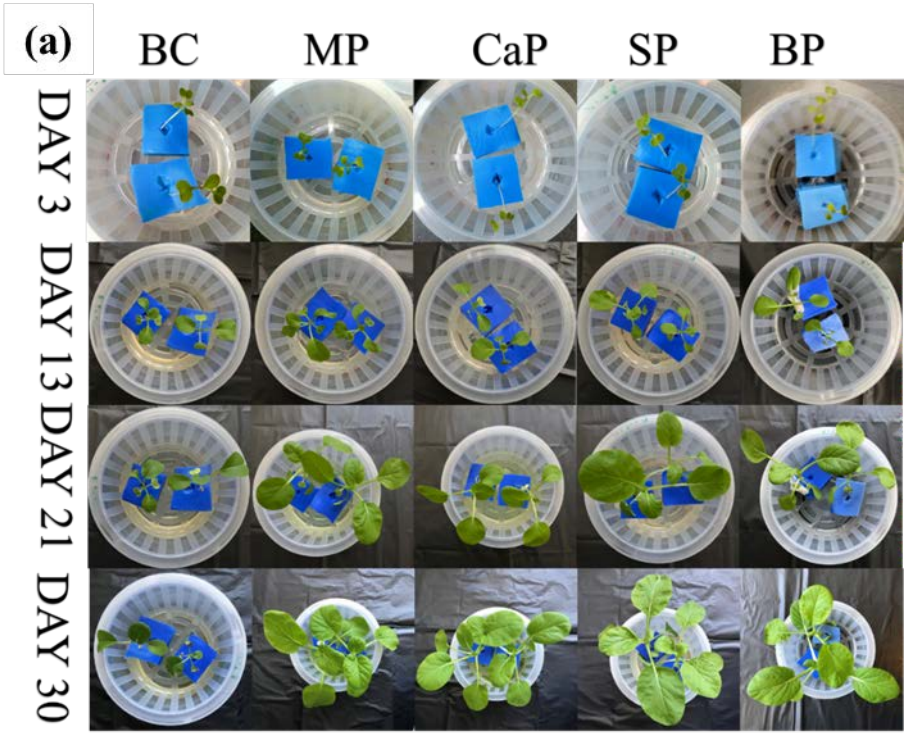

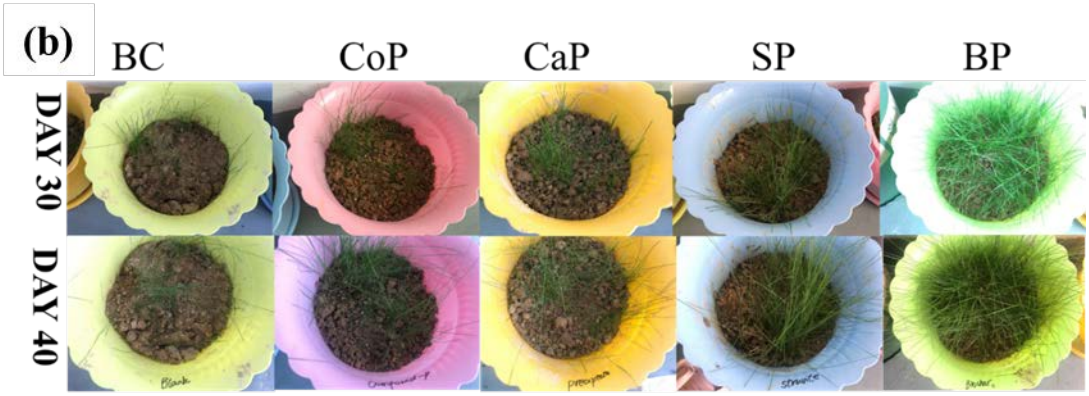

Figure 7-1 Growth status of (a) choy sum at day 7, 13, 21 and 30 and of (b) ryegrass at day 30 and 40

To order to further compare the agronomic effectiveness of RPFs, the indicators of plant growth including shoot height and weight of the plant shoot were determined after harvest. From Table 7-2 and Fig 7-4, the average shoot length of choy sum in BC group was 7.2 cm, which was significantly increased to 15.9, 15.5, 17.0 and 16.2 cm with the application of MP, CaP, BP and SP, respectively. Therefore, the addition of P fertilizers played a fundamental role in growth of choy sum and could significantly increases the shoot length. As shown, the effect of the RPFs was comparable or slightly superior than MP in terms of shoot length. However, no significant differences were observed in the shoot length among different RPFs used.

As for the plant weight, significant differences in biomass production of the choy sum were found among different treatments with that of the BC. To specific, the application of BP and SP resulted in the highest fresh and

dry weights of choy sum, closely followed by MP (Table 7-2 and Fig 7-5). In contrast, CaP was the least effective of the three RPFs. This might be due to its low solubility and the presence of a large amount of $CaSO_4$ in CaP which decreased the P accessibility. In particular, the dry weight of the choy sum fertilized with CaP was significant different from those with BP and SP. Even though the fresh weight and dry weight of the shoot for RPFs group were significantly higher than the BC group. Interestingly, SP produced a larger fresh weight despite it was applied at the same amount. This may be attributed to the Mg was involved and the high bioavailability of SP. Similar results were obtained when struvite was applied to cultivate lettuce, and it was attributed to the larger amount of Mg incorporated in struvite and the synergistic effect on P uptake [253]. Magnesium is an essential component of the chlorophyll molecule, thus it plays a critical role in photosynthesis [253]. This could be reflected from Fig 7-4(b), since SP produced the highest chlorophyll content that confirming Mg played a significant role in photosynthesis of the plant.

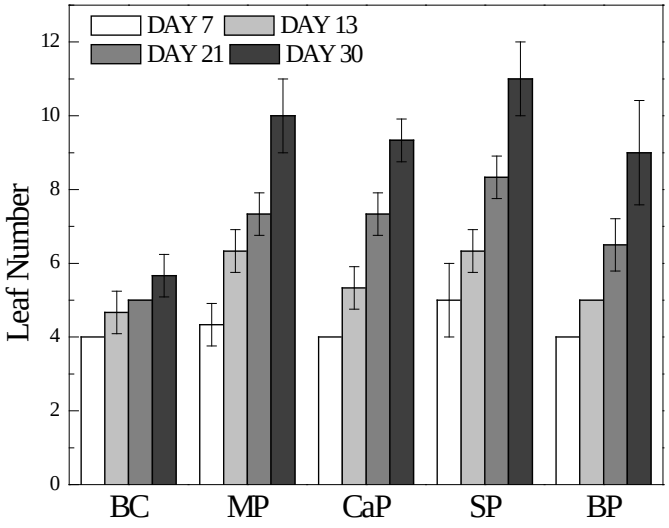

Figure 7-2 Leaf number of choy sum during the cultivation.

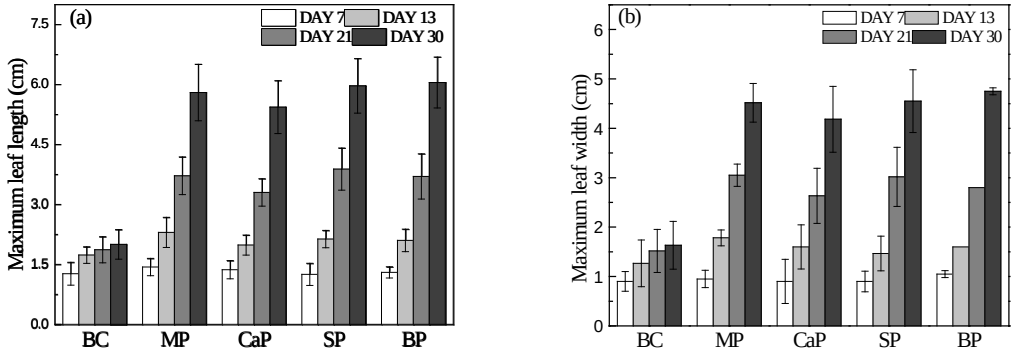

Figure 7-3 The maximum length (a) and width (b) of the largest leaf of choy sum during the cultivation

In the case of ryegrass, BP pots had the highest shoot length with a average value of 13.7 cm closely followed by CoP, SP and CaP pots with similar values (13.4 cm). As expected, the ryegrass in the control group had the shortest average shoot length (13.0 cm) for its lack of P. In addition, the

root system of BP group was obviously better developed and was longer than the other groups while BC group had the shortest and poorest root. The fresh weight of the plant followed the order of SP >CoP > BP > CaP > BC. Specifically, the fresh weight of SP group was 29.2 mg, which was 25% and 36% higher than those of BP and BC, respectively. Expectedly, ryegrass in SP group had the highest chlorophyll content. It should be noted that, due to the relatively small amount of the ryegrass after harvest, the dried masses of all pots were all low and similar.

Overall, SP containing a high content of Mg was beneficial for the photosynthesis of chlorophyll thus promoting the growth of plants. BP also stimulated the growing of plants (especially for the root systems) due to its high porous structure and the additional nutrient elements in the biochar. The agronomic effectiveness of BP and SP were comparable or even better than CoP as P sources for the cultivation of ryegrass. And the agronomic effectiveness of CaP was slightly lower than CoP but significantly better than BC group. Even though inferior to other P fertilizers, CaP could still be regarded as a potential P source due to its growth promoting effect on ryegrass.

Table 7-2 Indicators for the growth of choy sum after harvest

Items	BC	MP	CaP	SP	BP
Fresh weight (g/shoot)	0.23b	2.79a	2.49a	2.96a	2.93a
Dry weight (g/shoot)	0.029c	0.16a,b	0.13b	0.18a	0.23a
Shoot length (cm/shoot)	7.2b	15.9a	15.5a	17.0a	16.2a

Notes: Different lowercase letter means the result are statically different at $p < 0.05$.

Table 7-3 Indicators for the growth of ryegrass after harvest

Group	BC	CoP	CaP	SP	BP
Shoot length (cm)	13.0c	13.4b	13.4b	13.4b	13.7a
Root length (cm)	0.8c	1.2b	1.0b	1.1b	1.5a
Chlorophyll content (mg/g)	1.01d	2.09c	2.15b	2.05c	2.42a
Fresh weight (mg/shoot)	18.5c	26.6a,b	20.9b	29.2a	21.8b
Dry weight (mg/shoot)	2.6c	3.6a	2.9b,c	3.0b	3.0b

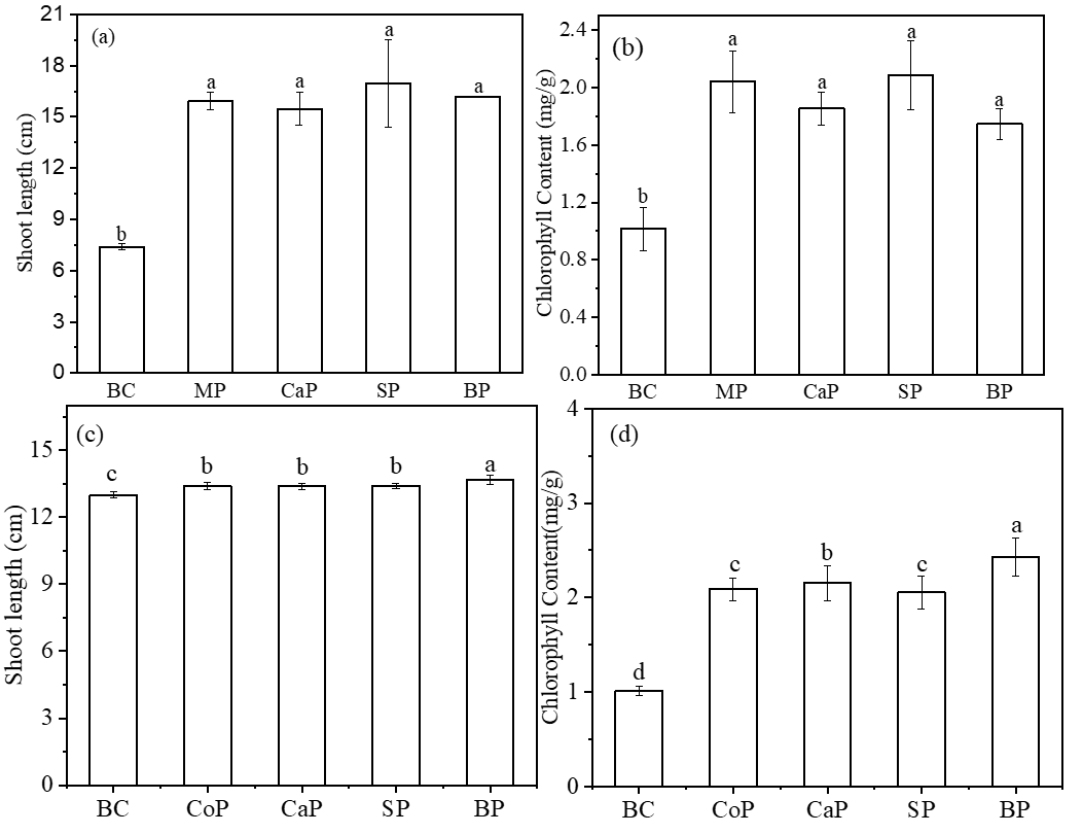

Figure 7-4 Shoot lengths and chlorophyll contents of choy sum (a and b) and ryegrass (c and d), respectively.

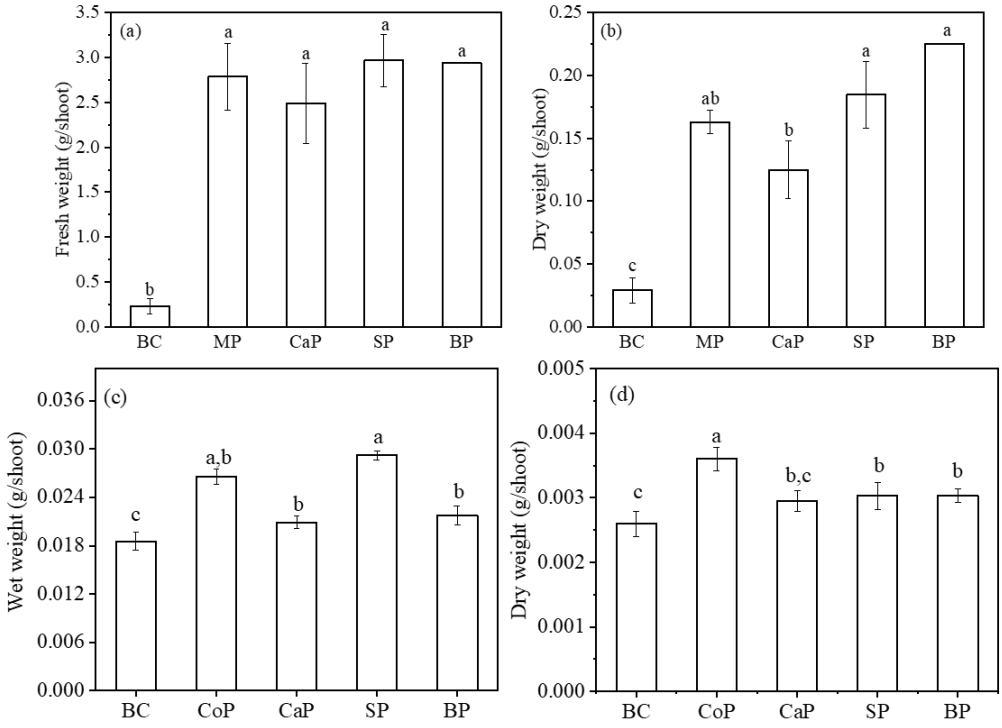

Figure 7-5 Fresh mass and dry mass of choy sum shoot (a and b) and ryegrass (c and d), respectively.

7.2.3 P uptake and accumulation of heavy metals in plants

(1) P uptake

Fig 7-6a shows P content in choy sum shoot after harvest using different P sources. The BC pots undoubtedly had the lowest P content which was far lower than the other groups. Enormous differences in shoot P content were observed despite the equal P application rate at the beginning of the cultivation was applied. MP pots had the highest P content with a value of 6.25 mg/kg mostly due to the high P-solubility of MP. SP and BP had similar P contents at 5.32 and 4.76 mg/kg, respectively. CaP pots only had

3.33 mg/kg. This was attributed to the lower solubility of CaP compared with SP, BP and MP.

Fig 7-6b shows the P contents in five groups of ryegrass. The highest uptake efficiency was attained by BP group. Besides the improvement of germination rates, BP can enhance soil and plant-availability due to it's highly-porous structure which provided more sites for contacting microorganism [104]. The P uptake of CaP was the lowest of the three recovered P products but was still higher than BC group, this might due to its slower P release rate. In contrast with groups of SP and BP, all these three kinds of RPFs had remarkable P uptake by ryegrass which identified their acceptable P availability.

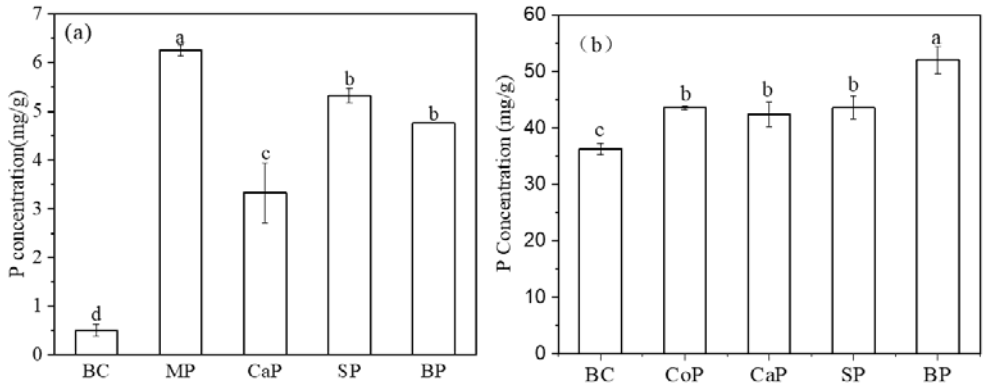

Figure 7-6 P contents in the dried choy sum shoot (a) and ryegrass (b)

(2) Accumulation of heavy metals

The heavy metal contents in choy sum shoot and ryegrass were determined and shown in Fig 7-7. The detected metals were different between these

two kinds of plants due to their different growth characteristics. The metal content in the dried choy sum shoot followed the order of Zn > Cu > Cd > Pb > Co ≈ As in different treatment groups. It is noticeable that the heavy metal contents except As of choy sum in BC pots were significantly higher than the other treatment groups, which could be originated from the P precipitation effect on the heavy metals. For As, its contents in all fertilized pots were similar and within the range of 0.19~0.23 mg/kg. Similarly, Co contents were comparable within the range of 0.25~0.45. Cd, Cu contents in the fertilized pots were also comparable with only minor differences. Specifically, both SP and BP pots had lower Cd contents than that of MP pots, and the CaP pots had the highest Cd content. As for Cu, CaP and BP pots had relatively lower contents than that of SP and MP pots. On the contrary, significant differences were observed with regards to Zn contents in different pots. MP pots had the highest Zn content with an average value of 75.05 mg/kg, followed by CaP, BP and SP. The Zn content in SP pots was 24.98 mg/kg which was significantly lower than the other pots.

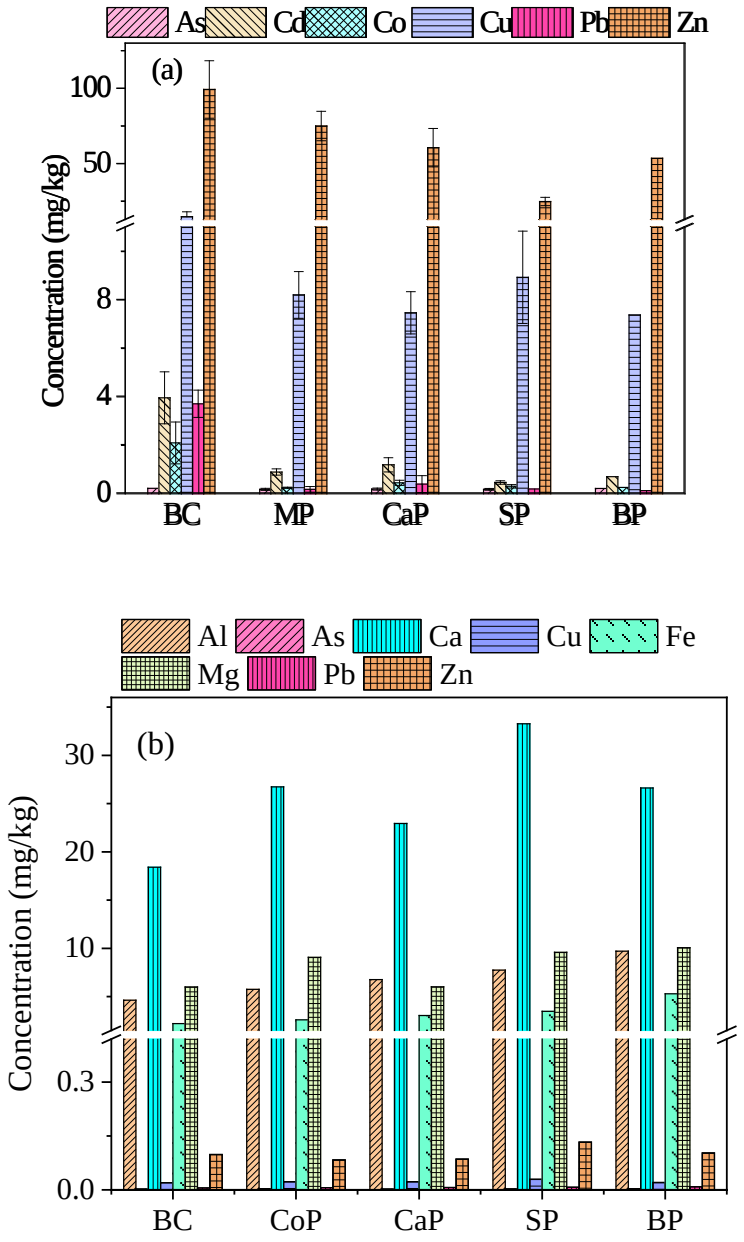

Figure 7-7 Uptake of heavy metals by choy sum shoot (a) and ryegrass (b)

The results indicated that contents of heavy metal in choy sum basically met the limits of heavy metals regulated by FAO/WHO and several other countries (Table 7-4). This reveals that the utilization of these RPFs to cultivate choy sum does not endanger human health in terms of accumulation in plants. In summary, the comparable or even lower heavy

metal contents in RPFs pots indicated that they could be safe for choy sum cultivation.

Table 7-4 Ranges and safe limits of heavy metals in Brassica vegetable family cultivated using recovered P fertilizers (mg/kg dry weight)

Items	(Ryu et al., 2012)	(Ryu and Lee, 2016)	This study	Safe limits		
				(SFDA, 2017)	(FAO/WHO, 2015)	(RC and A, 2015)
Zn	121.0	68.0	24.98~60.73			60
Cu	7.2	20.5	7.38~8.94			40
Co			0.27~0.45			0.05~0.1
As	n.d.	n.d.	0.19~0.22	0.5		0.2
Cd	n.d.	n.d.	0.47~1.20	0.05~0.2	0.02~0.2	0.3
Pb	n.d.	4.5	0.13~0.40	0.1~0.3	0.05~0.3	0.2/0.3

The various metals uptake by ryegrasses is shown in Fig 7-8. No obvious difference was found in heavy metals contents in the three kinds of RPFs along with CoP and BC. This might be because the trace amounts of heavy metals in natural soils and the low plant-availability of metals in the fertilizers used. The slightly lower heavy metal contents found in BP group might be attributed to its porous structure with a high adsorb capacity to heavy metals [104]. Though these three kinds of RPFs contained higher contents of metals, no obviously increase in these metal contents were found in their cultivated plants, like Zn, Al, Mg, etc.

For animal feed, only As (<4 ppm), Cd (<1 ppm) and Pb (<30 ppm) are regulated as the maximum allowable concentration in ryegrass with a moisture content of 12%. However, in this study, the maximum content of these element were As (2.8 ppm), Pb (7.8 ppm) and Cd (below detection

limits), respectively, which are much lower than the limit stipulated in the regulations [254, 255].

7.3 Summary

Recovering P as fertilizer from ISSA not only sustains the global P cycle but also is beneficial to ash management. The three RPFs produced from ISSA contained significant amounts of P within the commercial fertilizers range. This study evidenced that RPFs produced from ISSA exhibited comparable/better agronomic effectiveness for the growth of choy sum and ryegrass to commercial MP/CoP. BP enhanced the germination rate of ryegrasses significantly in the soil cultivation, while struvite facilitated the growth of choy sum effectively in the hydroponics environment. Negligible/no heavy metal contamination was found in the cultivated plants, indicating no risk of using the RPFs. In general, recovering P as struvite or adsorbing P from the acid-extract of ISSA using biochar are preferred options for producing fertilizers from ISSA.

Chapter 8 Conclusions and Recommendations

8.1 Conclusions

The overall aim of this research is to recover P from ISSA and transfer it into plant-available P fertilizer. For this purpose, research was developed for characterization of ISSA, optimization of P extraction agents, precipitation of P, absorption of P by modified biochar and eventually evaluation of the agronomic effectiveness of produced RPFs. The main conclusions are:

(1) High amount of P in ISSA can be extracted by both organic and inorganic acids while a marginal amount can be extracted by chelating agents. Regarding economic and efficiency, sulfuric acid was the optimal extraction agent. Its optimized P extraction conditions were 0.2 mol/L with pH ~ 0.9 at a liquid-to-solid ratio of 20:1 for 120-min. Meanwhile, the use of chelating agents of EDTA attained comparably metals/metalloids leachability but low extraction of P, which was optimal as a pre-treatment leaching agent. For metal(loid)s removal, the optimal ISSA pre-leaching conditions using EDTA were 0.02 mol/L at a liquid-to-solid ratio of 20:1 and 180 min of reaction time. The results of BET and SEM analysis showed the microstructure of the ISSA was not altered by the pre-leaching of EDTA.

(2) A novel two-step extraction method was developed to obtain a high purity P-extract from ISSA, which sequentially leached ISSA with EDTA and sulphuric acid. Specifically, ISSA was pre-extracted by EDTA (concentration of 0.02 M, L/S ratio of 20:1 and reaction time of 120 min), followed by P extraction with sulphuric acid (concentration of 0.2 M, L/S ratio at a 20:1 with a 120-min reaction time). Hence, metal(loid)s in the final extract was decreased, for example, Cr (by 92%), Zn (by 58%), Mn (by 50%), Mg (by 49%), Cu (by 49%), Al (by 37%) and Fe (by 23%).

Detectable levels of desirable minor elements for soil remediation (TiO_2, Y_2O_3 and SrO) were found only in the P-precipitate formed using the two-step method. Therefore, applying the two-step method for P recovery not only produces a P-extract with higher purity but also producing a P-precipitate which is advantageous for fertilizer applications.

(3) The optimal P adsorption biochar for the acid-extract of ISSA was the Sc-based based biochar modified by $MgCl_2$ and pyrolyzed at 700 ^oC. Its higher surface area and pore volume compared with other biochars ensured its good P adsorption capacity. Chemical precipitation of P-Mg, P-Ca, P-Al and P-Fe on the surface of the biochar was the major P adsorption mechanism of the Mg-modified biochar.

(4) Three kinds of recycled phosphate fertilizers (RPF): biochar-P, precipitate-P and struvite were produced for agronomic effectiveness

evaluation. These three RPFs from ISSA contained significant amounts of P which were comparable to P commercial fertilizers. This results showed that RPFs from ISSA exhibited comparable/better agronomic effectiveness for the growth of choy sum and ryegrass to the commercial MP/CoP. Negligible/no heavy metal contamination was found in the cultivated plants, indicating no risk of the RPFs.

(5) In general, recovering P as struvite or adsorbing P from the acid-extract of ISSA using biochar were feasible options for reutilizing P from ISSA.

8.2 Limitations of the present study and suggestions for further research

This thesis systematically studied the P recovery from ISSA by wet-extraction method for producing P-fertilizer in the laboratory scale. ISSA originated from HK is the only P sources. The following are some suggestions for further studies:

(1) For total recycling of ISSA, the acid-insoluble residues may be used in cement production. More studies can focus on the performance of acid-insoluble residues in cement.

(2) A plant-available media can be used to adsorb P from the acid-extract therefore producing a P enhanced material. Potential environmental absorption media like modified sepiolite and zeolite are suggested for

further studies.

(3) Further exploration can be focused on extraction media which can selectivity absorb heavy metals from ISSA. This extraction media should be stable in acidic solutions and can be regenerated.

References

1. Association, I.F.I., *Medium-Term Outlook for Global Fertilizer Demand, Supply and Trade*. June 2005: <http://www.fertilizer.org/ifa/archive.asp>.
2. FAO, *Plant Nutrition for Food Security: A Guide for Integrated Nutrient Management*. 2006, FAO Fertilizer And Plant Nutrition Bulletin 16: Food And Agriculture Organization Of The United Nations Rome.
3. Kauwenbergh, S.V., *World Phosphate Rock Reserves and Resources*, in *World Phosphate Rock Reserves and Resources*. November 16-18, 2010: Savannah, GA.
4. Smit, A.L., et al., *Phosphorus in agriculture: global resoources, trends and developments: report to the Steering Committee Technology Assessment of the Ministery of Agriculture, Nature and Food Quality, The Netherlands, and in collaboration with the Nutrient Flow Task Group (NFTG), supported by DPRN (Development Policy review Network)*. 2009, Plant Research International.
5. (USGS), U.S.G.S., *Mineral commodity summaries 2019: U.S. Geological Survey*. 2019. p. 200 p.
6. Donatello, S., *Characteristics of incinerated sewage sludge ashes:*

potential for phosphate extraction and re-use as a pozzolanic material in construction products,, in *Department of Civil and Environmental Engineering*. 2009, Imperial College London.

7. IFA, *International Fertilizer Industry Association*. 2015: www.fertilizer.org.
8. (UN), U.N., *Department of Economic and Social Affairs, Population Division*. 2019: World Population Prospects 2019.
9. Gorazda, K., et al., *Phosphorus cycle - possibilities for its rebuilding.* Acta Biochimica Polonica, 2013. **60**(4): p. 725.
10. Krüger, O. and C. Adam, *Recovery potential of German sewage sludge ash.* Waste Management, 2015. **45**: p. S0956053X15000641.
11. Zuloaga, O., et al., *Overview of extraction, clean-up and detection techniques for the determination of organic pollutants in sewage sludge: A review.* Analytica Chimica Acta, 2012. **736**(1): p. 7-29.
12. Cieślik, B. and P. Konieczka, *A review of phosphorus recovery methods at various steps of wastewater treatment and sewage sludge management. The concept of "no solid waste generation" and analytical methods.* Journal of Cleaner Production, 2017. **142**: p. 1728-1740.
13. Tarayre, C., et al., *New perspectives for the design of sustainable bioprocesses for phosphorus recovery from waste.* Bioresour Technol, 2016. **206**: p. 264-274.

14. K.Gorazda, B.T., Z.Worek, A.K.Nowak, K.Kulczycka, M.Smol, A.Henclik, *Sustainable use of sewage sludge ash in fertilisers production-PolFerAsh technology* in *Athens2017*. 2017: Athens.

15. Nättorp, A., K. Remmen, and C. Remy, *Cost assessment of different routes for phosphorus recovery from wastewater using data from pilot and production plants.* Water Science and Technology, 2017. **76**(2): p. 413-424.

16. Egle, L., et al., *Phosphorus recovery from municipal wastewater: An integrated comparative technological, environmental and economic assessment of P recovery technologies.* Science of The Total Environment, 2016. **571**: p. 522-542.

17. Destatis, *Amount and fate of sewage sludge in Germany 2012.*, G.F.S. Office, Editor. 2013.

18. Fytili, D. and A. Zabaniotou, *Utilization of sewage sludge in EU application of old and new methods—A review.* Renewable and Sustainable Energy Reviews, 2008. **12**(1): p. 116-140.

19. Kleemann, R., et al., *Comparison of phosphorus recovery from incinerated sewage sludge ash (ISSA) and pyrolysed sewage sludge char (PSSC).* Waste Management, 2017. **60**: p. 201-210.

20. Lundin, M., et al., *Environmental and economic assessment of sewage sludge handling options.* Resources, Conservation and Recycling, 2004. **41**(4): p. 255-278.

21. Milieu Ltd., W.a.R., *Study on the Environmental, Economic and Social Impacts of the use of Sewage Sludge on Land*. 2010: Contract DB ENV.G.4/ETU/2008/0076r, s.l.: s.n.

22. Donatello, S. and C.R. Cheeseman, *Recycling and recovery routes for incinerated sewage sludge ash (ISSA): a review.* Waste Management, 2013. **33**(11): p. 2328-40.

23. Raison, R., P. Khanna, and P. Woods, *Mechanisms of element transfer to the atmosphere during vegetation fires.* Canadian Journal of Forest Research, 1985. **15**(1): p. 132-140.

24. Tan, Z. and A. Lagerkvist, *Phosphorus recovery from the biomass ash: A review.* Renewable & Sustainable Energy Reviews, 2011. **15**(8): p. 3588-3602.

25. Biswas, B.K., et al., *Leaching of phosphorus from incinerated sewage sludge ash by means of acid extraction followed by adsorption on orange waste gel*. Journal of Environmental Sciences, 2009. **21**(12): p. 1753-1760.

26. Franz, M., *Phosphate fertilizer from sewage sludge ash (SSA).* Waste Management, 2008. **28**(10): p. 1809-1818.

27. Donatello, S., D. Tong, and C.R. Cheeseman, *Production of technical grade phosphoric acid from incinerator sewage sludge ash (ISSA).* Waste management, 2010. **30**(8-9): p. 1634-1642.

28. Mitrano, D.M., et al., *Mobility of metallic (nano) particles in*

leachates from landfills containing waste incineration residues. Environmental Science: Nano, 2017. **4**(2): p. 480-492.

29. Adam, C., et al., *Thermochemical treatment of sewage sludge ashes for phosphorus recovery.* Waste management, 2009. **29**(3): p. 1122-1128.

30. Herzel, H., et al., *Sewage sludge ash — A promising secondary phosphorus source for fertilizer production.* Science of The Total Environment, 2016. **542**: p. 1136-1143.

31. Nowak, et al., *Heavy metal removal from sewage sludge ash and municipal solid waste fly;ash - A comparison.* Fuel Processing Technology, 2013. **105**(105): p. 195-201.

32. Samolada, M.C. and A.A. Zabaniotou, *Comparative assessment of municipal sewage sludge incineration, gasification and pyrolysis for a sustainable sludge-to-energy management in Greece.* Waste Management, 2014. **34**(2): p. 411-420.

33. Mattenberger, H., et al., *Sewage sludge ash to phosphorus fertiliser (II): Influences of ash and granulate type on heavy metal removal.* Waste Management, 2010. **30**(8): p. 1622-1633.

34. Petzet, S. and P. Cornel, *Towards a complete recycling of phosphorus in wastewater treatment--options in Germany.* Water Science & Technology, 2011. **64**(1): p. 29-35.

35. Ottosen, L.M., P.E. Jensen, and G.M. Kirkelund, *Phosphorous*

recovery from sewage sludge ash suspended in water in a two-compartment electrodialytic cell. Waste Management, 2016. **51**: p. 142-148.

36. Pedersen, K.B., et al., *Comparison of 2-compartment, 3-compartment and stack designs for electrodialytic removal of heavy metals from harbour sediments.* Electrochimica Acta, 2015. **181**: p. 48-57.
37. Ebbers, B., L.M. Ottosen, and P.E. Jensen, *Comparison of two different electrodialytic cells for separation of phosphorus and heavy metals from sewage sludge ash.* Chemosphere, 2015. **125**: p. 122-129.
38. Gorazda, K., et al., *Characteristic of wet method of phosphorus recovery from polish sewage sludge ash with.* Open Chemistry, 2016. **14**(1): p. 37-45.
39. Petzet, S., B. Peplinski, and P. Cornel, *On wet chemical phosphorus recovery from sewage sludge ash by acidic or alkaline leaching and an optimized combination of both.* Water Research, 2012. **46**(12): p. 3769-3780.
40. Weigand, H., et al., *RecoPhos: full-scale fertilizer production from sewage sludge ash.* Waste Management, 2013. **33**(3): p. 540-4.
41. Petzet, S., et al., *Recovery of phosphorus and aluminium from sewage sludge ash by a new wet chemical elution process (SESAL-*

Phos-recovery process). Water Science and Technology, 2011. **64**(3): p. 693-699.

42. *20 critical raw materials - major challenge for EU industry. In.*, E. Commission, Editor. p. p. 2.

43. Van Kauwenbergh, S.J., *World phosphate rock reserves and resources*. 2010: IFDC Muscle Shoals.

44. Heffer, P. and M. Prud'homme. *Fertilizer outlook 2010–2014*. in *78th IFA annual conference, Paris*. 2010.

45. Gunther, F., *A solution to the heap problem: the doubly balanced agriculture: integration with population.* Online: http://www. holon. se/folke/kurs/Distans/Ekofys/Recirk/Eng/balanced. shtml (zuletzt aufgerufen: 2013-09-20), 2005.

46. Smil, V., *Feeding the world: A challenge for the 21st century*. 2000, MIT Press, Cambridge, MA.

47. Smil, V., *Phosphorus in the environment: natural flows and human interferences*. Annual Review of Energy and the Environment, 2000. **25**(1): p. 53-88.

48. Yang, G., G. Zhang, and H. Wang, *Current state of sludge production, management, treatment and disposal in China*. Water Res, 2015. **78**: p. 60-73.

49. Zhou, K., et al., *Phosphorus recovery from municipal and fertilizer wastewater: China's potential and perspective*. Journal of

Environmental Sciences, 2017. **52**: p. 151-159.

50. Wang, X., et al., *The present situation and research progress of treatment of sludge from city sewage treatment plant.* Tianjin Daxue Xuebao, 2015. **30**.

51. Jin, L., G. Zhang, and H. Tian, *Current state of sewage treatment in China.* Water Res, 2014. **66**: p. 85-98.

52. Ruban, V., et al., *Selection and evaluation of sequential extraction procedures for the determination of phosphorus forms in lake sediment.* Journal of Environmental Monitoring, 1999. **1**(1): p. 51-56.

53. Xie, C., et al., *The phosphorus fractions and alkaline phosphatase activities in sludge.* Bioresource Technology, 2011. **102**(3): p. 2455-2461.

54. Li, R., et al., *Transformation of apatite phosphorus and non-apatite inorganic phosphorus during incineration of sewage sludge.* Chemosphere, 2015. **141**(35): p. 57-61.

55. Pokhrel, S.P., et al., *Use of solid phosphorus fractionation data to evaluate phosphorus release from waste activated sludge.* Waste Management, 2018. **76**: p. 90-97.

56. Huang, R. and Y. Tang, *Evolution of phosphorus complexation and mineralogy during (hydro)thermal treatments of activated and anaerobically digested sludge: Insights from sequential extraction*

and P K-edge XANES. Water Research, 2016. **100**: p. 439-447.

57. Qian, T.-T. and H. Jiang, *Migration of Phosphorus in Sewage Sludge during Different Thermal Treatment Processes.* ACS Sustainable Chemistry & Engineering, 2014. **2**(6): p. 1411-1419.

58. Niu, X. and L. Shen, *Release and transformation of phosphorus in chemical looping combustion of sewage sludge.* Chemical Engineering Journal, 2018. **335**: p. 621-630.

59. Xu, Y., et al., *pH dependent phosphorus release from waste activated sludge: contributions of phosphorus speciation.* Chemical Engineering Journal, 2015. **267**: p. 260-265.

60. He, Z.-W., et al., *Clarification of phosphorus fractions and phosphorus release enhancement mechanism related to pH during waste activated sludge treatment.* Bioresource Technology, 2016. **222**: p. 217-225.

61. Cordell, D., et al., *Towards global phosphorus security: a systems framework for phosphorus recovery and reuse options.* Chemosphere, 2011. **84**(6): p. 747-58.

62. Huang, W., et al., *Species and distribution of inorganic and organic phosphorus in enhanced phosphorus removal aerobic granular sludge.* Bioresource Technology, 2015. **193**: p. 549-552.

63. Houben, D., et al., *Response of phosphorus dynamics to sewage sludge application in an agroecosystem in northern France.* Applied

Soil Ecology, 2019. **137**: p. 178-186.

64. Li, J.S., et al., *Characteristics and metal leachability of incinerated sewage sludge ash and air pollution control residues from Hong Kong evaluated by different methods.* Waste Management, 2017. **64**: p. 161.

65. Xu, H., et al., *Recovery of phosphorus as struvite from sewage sludge ash.* Journal of Environmental Sciences, 2012. **24**(8): p. 1533-1538.

66. Hernandez, A.B., et al., *Mineralogy and leachability of gasified sewage sludge solid residues.* Journal of Hazardous Materials, 2011. **191**(1): p. 219-227.

67. Frost, R.L., et al., *Dehydration of synthetic and natural vivianite.* Thermochimica Acta, 2003. **401**(2): p. 121-130.

68. Gorazda, K., et al., *Characteristic of wet method of phosphorus recovery from polish sewage sludge ash with nitric acid*, in *Open Chemistry*. 2016. p. 37.

69. Mattenberger, H., et al., *Sewage sludge ash to phosphorus fertiliser: Variables influencing heavy metal removal during thermochemical treatment.* Waste Management, 2008. **28**(12): p. 2709-2722.

70. Oliver, K., G. Angela, and A. Christian, *Complete survey of German sewage sludge ash.* Environmental Science & Technology, 2014. **48**(20): p. 11811-11818.

71. Kalmykova, Y. and K. Karlfeldt Fedje, *Phosphorus recovery from municipal solid waste incineration fly ash.* Waste Management, 2013. **33**(6): p. 1403-1410.

72. Fonts, I., et al., *Sewage sludge pyrolysis for liquid production: A review.* Renewable and Sustainable Energy Reviews, 2012. **16**(5): p. 2781-2805.

73. Cyr, M., M. Coutand, and P. Clastres, *Technological and environmental behavior of sewage sludge ash (SSA) in cement-based materials.* Cement & Concrete Research, 2007. **37**(8): p. 1278-1289.

74. Lin, K.L., K.Y. Chiang, and D.F. Lin, *Effect of heating temperature on the sintering characteristics of sewage sludge ash.* Journal of Hazardous Materials, 2006. **128**(2): p. 175-181.

75. Ottosen, L.M., G.M. Kirkelund, and P.E. Jensen, *Extracting phosphorous from incinerated sewage sludge ash rich in iron or aluminum.* Chemosphere, 2013. **91**(7): p. 963-969.

76. JA., R., *Dutch experience of sludge management and P-recovery pathways.* Environ 2018, 28 March, Cork, Ireland, 2018.

77. Lee, M. and D.J. Kim, *Identification of phosphorus forms in sewage sludge ash during acid pre-treatment for phosphorus recovery by chemical fractionation and spectroscopy.* Journal of Industrial & Engineering Chemistry, 2017. **51**: p. 64-70.

78. Liang, S., et al., *A comparison between sulfuric acid and oxalic acid*

leaching with subsequent purification and precipitation for phosphorus recovery from sewage sludge incineration ash. Water Research, 2019. **159**: p. 242-251.

79. Dissanayake, C. and R. Chandrajith, *Phosphate mineral fertilizers, trace metals and human health.* Journal of the National Science Foundation of Sri Lanka, 2009. **37**(3): p. 153-165.

80. Pantelica, A.I., et al., *INAA of some phosphates used in fertilizer industries.* Journal of Radioanalytical and Nuclear Chemistry, 1997. **216**(2): p. 261-264.

81. Sabiha, J., et al., *Heavy metal pollution from phosphate rock used for the production of fertilizer in Pakistan.* Microchemical Journal, 2009. **91**(1): p. 94-99.

82. Cheeseman, C. and G. Virdi, *Properties and microstructure of lightweight aggregate produced from sintered sewage sludge ash.* Resources, Conservation and Recycling, 2005. **45**(1): p. 18-30.

83. Lin, K., K. Chiang, and C. Lin, *Hydration characteristics of waste sludge ash that is reused in eco-cement clinkers.* Cement and Concrete Research, 2005. **35**(6): p. 1074-1081.

84. Park, Y.J., S.O. Moon, and J. Heo, *Crystalline phase control of glass ceramics obtained from sewage sludge fly ash.* Ceramics International, 2003. **29**(2): p. 223-227.

85. Tay, J.-H. and K.-Y. Show, *Resource recovery of sludge as a building*

and construction material—a future trend in sludge management. Water Science and Technology, 1997. **36**(11): p. 259-266.

86. Chen, Z., et al., *Compressive strength and microstructural properties of dry-mixed geopolymer pastes synthesized from GGBS and sewage sludge ash.* Construction and Building Materials, 2018. **182**: p. 597-607.

87. Budak, T.B., *Removal of heavy metals from wastewater using synthetic ion exchange resin.* Asian Journal of Chemistry, 2013. **25**(8): p. 4207-4210.

88. Fu, F. and Q. Wang, *Removal of heavy metal ions from wastewaters: A review.* Journal of Environmental Management, 2011. **92**(3): p. 407-418.

89. Donatello, S., D. Tong, and C.R. Cheeseman, *Production of technical grade phosphoric acid from incinerator sewage sludge ash (ISSA).* Waste Management, 2010. **30**(8): p. 1634-1642.

90. Wang, Q., et al., *Sustainable reclamation of phosphorus from incinerated sewage sludge ash as value-added struvite by chemical extraction, purification and crystallization.* Journal of Cleaner Production, 2018. **181**: p. 717-725.

91. Cohen, Y., *Phosphorus dissolution from ash of incinerated sewage sludge and animal carcasses using sulphuric acid.* Environmental Technology, 2009. **30**(11): p. 1215-1226.

92. Meng, X., et al., *Recovery of phosphate as struvite from low-temperature combustion sewage sludge ash (LTCA) by cation exchange.* Waste Management, 2019. **90**: p. 84-93.

93. Liu, Y. and H. Qu, *Design and optimization of a reactive crystallization process for high purity phosphorus recovery from sewage sludge ash.* Journal of Environmental Chemical Engineering, 2016. **4**(2): p. 2155-2162.

94. Greb, V.G., et al., *Understanding phosphorus phases in sewage sludge ashes: A wet-process investigation coupled with automated mineralogy analysis.* Minerals Engineering, 2016. **99**: p. 30-39.

95. Naoum, C., et al., *REMOVAL OF HEAVY METALS FROM SEWAGE SLUDGE BY ACID TREATMENT.* Journal of Environmental Science and Health, Part A, 2001. **36**(5): p. 873-881.

96. Schaum, C., *Verfahren fu¨ r eine zuku¨ nftige Kla¨ rschlammbehandlung-Kla¨rschlammkonditionierung und Ru¨ ckgewinnung von Phosphor aus Kla¨ rschlammasche (Processes for future sewage sludge treatment e sewage sludge conditioning and phosphorus recovery from sewage sludge ash).* 2007, Dissertation, Technische Universita¨t Darmstadt.

97. Huang, Y., C. Wang, and S. Yi, *The Application Situation of Fluid Fertilizer and Its Developmental Prospects.* China Academic Journal Electronic Publishing House, 2006(2): p. 198-200.

98. EC, *Regulation (EC) No 2003/2003 of the European Parliament and of the Council of 13 October 2003 relating to fertilizers*. 2003.

99. Ye, Z., et al., *A comparison of mobility and availability of granular and fluid phophate fertilizers in calcareous soils under laboratory conditions.* Plant Nutrition and Fertilizer Science, 2010. **16**(6): p. 1433-1438.

100. Lombi, E., et al., *Mobility, solubility and lability of fluid and granular forms of P fertiliser in calcareous and non-calcareous soils under laboratory conditions.* Plant & Soil, 2005. **269**(1-2): p. 25-34.

101. Paltrinieri, L., et al., *Improved phosphoric acid recovery from sewage sludge ash using layer-by-layer modified membranes.* Journal of Membrane Science, 2019. **587**: p. 117162.

102. Kataki, S., et al., *Phosphorus recovery as struvite from farm, municipal and industrial waste: feedstock suitability, methods and pre-treatments.* Waste Management, 2016. **49**: p. 437-454.

103. Xue, T. and X. Huang, *Releasing characteristics of phosphorus and other substances during thermal treatment of excess sludge.* Journal of Environmental Sciences, 2007. **19**(10): p. 1153-1158.

104. Ahmad, M., et al., *Biochar as a sorbent for contaminant management in soil and water: A review.* Chemosphere, 2014. **99**: p. 19-33.

105. Yang, Q., et al., *Effectiveness and mechanisms of phosphate*

adsorption on iron-modified biochars derived from waste activated sludge. Bioresource Technology, 2018. **247**: p. 537-544.

106. Glaser, B., J. Lehmann, and W. Zech, *Ameliorating physical and chemical properties of highly weathered soils in the tropics with charcoal-a review.* Biology and fertility of soils, 2002. **35**(4): p. 219-230.

107. Li, H., et al., *Mechanisms of metal sorption by biochars: Biochar characteristics and modifications.* Chemosphere, 2017. **178**: p. 466-478.

108. Fang, C., et al., *Application of Magnesium Modified Corn Biochar for Phosphorus Removal and Recovery from Swine Wastewater.* International Journal of Environmental Research and Public Health, 2014. **11**(9): p. 9217.

109. Antunes, E., et al., *Isotherms, kinetics and mechanism analysis of phosphorus recovery from aqueous solution by calcium-rich biochar produced from biosolids via microwave pyrolysis.* Journal of Environmental Chemical Engineering, 2017.

110. Takahashi, M., et al., *Technology for recovering phosphorus from incinerated wastewater treatment sludge.* Chemosphere, 2001. **44**(1): p. 23-29.

111. Lemming, C., et al., *Plant availability of phosphorus from dewatered sewage sludge, untreated incineration ashes, and other products*

recovered from a wastewater treatment system. Journal of Plant Nutrition and Soil Science, 2017. **180**(6): p. 779-787.

112. Cabeza, R., et al., *Effectiveness of recycled P products as P fertilizers, as evaluated in pot experiments.* Nutrient Cycling in Agroecosystems, 2011. **91**(2): p. 173.

113. (INE), I.N.-w.E., *Acid extraction of phosphorus from sewage sludge incineration ash: REMONDIS TetraPhos®.* 2018: https://www.nweurope.eu/media/5064/2_phos4you-tetraphos.pdf (accessed 15 23December 2019).

114. Nakagawa, H. and J. Ohta, *Phosphorus Recovery from Sewage Sludge Ash: A Case Study in Gifu, Japan*, in *Phosphorus Recovery and Recycling*, H. Ohtake and S. Tsuneda, Editors. 2019, Springer Singapore: Singapore. p. 149-155.

115. Mochiyama, T., *Industrial-Scale Manufacturing of Phosphoric Acid Using Sewage Sludge Ash*, in *Phosphorus Recovery and Recycling*, H. Ohtake and S. Tsuneda, Editors. 2019, Springer Singapore: Singapore. p. 133-142.

116. Morf, L., et al., *Urban Phosphorus Mining in the Canton of Zurich: Phosphoric Acid from Sewage Sludge Ash*, in *Phosphorus Recovery and Recycling*, H. Ohtake and S. Tsuneda, Editors. 2019, Springer Singapore: Singapore. p. 157-177.

117. Donatello, S., M. Tyrer, and C.R. Cheeseman, *EU landfill waste*

acceptance criteria and EU Hazardous Waste Directive compliance testing of incinerated sewage sludge ash. Waste Management, 2010. **30**(1): p. 63-71.

118. Konen, M.E., et al., *Equations for Predicting Soil Organic Carbon Using Loss-on-Ignition for North Central U.S. Soils.* Soil Science Society of America Journal, 2002. **66**(6): p. 1878-1881.
119. Li, C., et al., *Effect of calcium silicate hydrates (CSH) on phosphorus immobilization and speciation in shallow lake sediment.* Chemical Engineering Journal, 2017. **317**: p. 844-853.
120. Fang, L., et al., *Phosphorus recovery and leaching of trace elements from incinerated sewage sludge ash (ISSA).* Chemosphere, 2017.
121. Beiyuan, J., *Integrated remediation of metal-contaminated soils: biodegradable chelant-enhanced extraction and in-situ stabilization*. 2016, The Hong Kong Polytechnic University.
122. Li, J.-s., et al., *Fate of metals before and after chemical extraction of incinerated sewage sludge ash.* Chemosphere, 2017. **186**: p. 350-359.
123. Zhang, M., et al., *Synthesis of porous MgO-biochar nanocomposites for removal of phosphate and nitrate from aqueous solutions.* Chemical Engineering Journal, 2012. **210**: p. 26-32.
124. Johnson, P.R., N. Sun, and M. Elimelech, *Colloid transport in geochemically heterogeneous porous media: Modeling and*

measurements. Environmental science & technology, 1996. **30**(11): p. 3284-3293.

125. Fang, L., et al., *Phosphorus recovery and leaching of trace elements from incinerated sewage sludge ash (ISSA).* Chemosphere, 2018. **193**: p. 278-287.

126. Kołodyńska, D., et al., *Kinetic and adsorptive characterization of biochar in metal ions removal*. Chemical Engineering Journal, 2012. **197**: p. 295-305.

127. Fang, L., et al., *Recovery of phosphorus from incinerated sewage sludge ash by combined two-step extraction and selective precipitation.* Chemical Engineering Journal, 2018. **348**: p. 74-83.

128. Fang, L., et al., *Use of Mg/Ca modified biochars to take up phosphorus from acid-extract of incinerated sewage sludge ash (ISSA) for fertilizer application.* Journal of Cleaner Production, 2019. **118853**.

129. Chen, J., et al., *Development of EST-SSR markers in flowering Chinese cabbage (Brassica campestris L. ssp. chinensis var. utilis Tsen et Lee) based on de novo transcriptomic assemblies.* 2017. **12**(9): p. e0184736.

130. Zhao, Y.-p., et al., *Role of chelant on Cu distribution and speciation in Lolium multiflorum by synchrotron techniques.* Science of The Total Environment, 2018. **621**: p. 772-781.

131. Jia, J., et al., *Effects of biochar application on vegetable production and emissions of N2O and CH4.* 2012. **58**(4): p. 503-509.

132. Hao, Y., et al., *Carbon nanomaterials alter plant physiology and soil bacterial community composition in a rice-soil-bacterial ecosystem ☆.* 2017. **232**: p. S0269749117324843.

133. Cui, J.-l., et al., *Speciation, mobilization, and bioaccessibility of arsenic in geogenic soil profile from Hong Kong.* Environmental pollution, 2018. **232**: p. 375-384.

134. Li, J., et al., *Bioaccessibility of antimony and arsenic in highly polluted soils of the mine area and health risk assessment associated with oral ingestion exposure.* Ecotoxicology and environmental safety, 2014. **110**: p. 308-315.

135. Pettersson, A., L.E. Åmand, and B.M. Steenari, *Leaching of ashes from co-combustion of sewage sludge and wood - Part II: The mobility of metals during phosphorus extraction.* Biomass & Bioenergy, 2008. **32**(3): p. 236-244.

136. Adam, C., et al., *Thermochemical treatment of sewage sludge ashes for phosphorus recovery.* Waste Manag, 2009. **29**(3): p. 1122-1128.

137. Cordell, D., J.-O. Drangert, and S. White, *The story of phosphorus: Global food security and food for thought.* Global Environmental Change, 2009. **19**(2): p. 292-305.

138. Rolewicz, M., et al., *Obtaining of Suspension Fertilizers from Incinerated Sewage Sludge Ashes (ISSA) by a Method of Solubilization of Phosphorus Compounds by Bacillus megaterium Bacteria*. Waste & Biomass Valorization, 2016. **7**(4): p. 1-7.

139. Donatello, S. and C.R. Cheeseman, *Recycling and recovery routes for incinerated sewage sludge ash (ISSA): A review.* Waste Manag, 2013. **33**(11): p. 2328-2340.

140. Nowak, B., et al., *Limitations for heavy metal release during thermo-chemical treatment of sewage sludge ash.* Waste Management, 2011. **31**(6): p. 1285-1291.

141. Morf, L.S., P.H. Brunner, and S. Spaun, *Effect of operating conditions and input variations on the partitioning of metals in a municipal solid waste incinerator.* Waste Management & Research, 2000. **18**(1): p. 4-15.

142. Ferreira, C., et al., *Removal of selected heavy metals from MSW fly ash by the electrodialytic process.* Engineering Geology, 2005. **77**(3): p. 339-347.

143. Guedes, P., et al., *Phosphorus recovery from sewage sludge ash through an electrodialytic process*. Waste Management, 2014. **34**(5): p. 886-892.

144. Petzet, S., et al., *Recovery of phosphorus and aluminium from sewage sludge ash by a new wet chemical elution process (SESAL-*

Phos-recovery process). Water Science & Technology, 2011. **64**(3): p. 693-699.

145. Roncalherrero, T., et al., *Precipitation of Iron and Aluminum Phosphates Directly from Aqueous Solution as a Function of Temperature from 50 to 200 °C.* Crystal Growth & Design, 2009. **9**(12): p. 5197–5205.

146. Huang, K., et al., *Leaching of heavy metals by citric acid from fly ash generated in municipal waste incineration plants.* Journal of Material Cycles & Waste Management, 2011. **13**(2): p. 118-126.

147. Beiyuan, J., et al., *Selective dissolution followed by EDDS washing of an e-waste contaminated soil: Extraction efficiency, fate of residual metals, and impact on soil environment.* Chemosphere, 2017. **166**: p. 489-496.

148. Kinoshita, T., et al., *Hydrometallurgical recovery of zinc from ashes of automobile tire wastes.* Chemosphere, 2005. **59**(8): p. 1105-1111.

149. Qiao, J., et al., *EDTA-assisted leaching of Pb and Cd from contaminated soil.* Chemosphere, 2017. **167**: p. 422-428.

150. Tsang, D.C.W., W. Zhang, and I.M.C. Lo, *Copper extraction effectiveness and soil dissolution issues of EDTA-flushing of artificially contaminated soils.* Chemosphere, 2007. **68**(2): p. 234-243.

151. Hu, P., et al., *Assessment of EDTA heap leaching of an agricultural*

soil highly contaminated with heavy metals. Chemosphere, 2014. **117**(1): p. 532-537.

152. Janos, P., M. Wildnerová, and T. Loucka, *Leaching of metals from fly ashes in the presence of complexing agents.* Waste Management, 2002. **22**(7): p. 783-789.

153. Ma, T.Y. and Z.Y. Yuan, *Metal phosphonate hybrid mesostructures: environmentally friendly multifunctional materials for clean energy and other applications.* Chemsuschem, 2011. **4**(10): p. 1407-1419.

154. Möller, S., S. Prikler, and J.W. Einax, *Pulse polarographic determination of the complexation capacity of various organic phosphonates of heavy metals with the aid of design of experiments.* Microchemical Journal, 2010. **96**(2): p. 296-300.

155. Kim, E.J., E.K. Jeon, and K. Baek, *Role of reducing agent in extraction of arsenic and heavy metals from soils by use of EDTA.* Chemosphere, 2016. **152**: p. 274-283.

156. Stoltz, E. and M. Greger, *Accumulation properties of As, Cd, Cu, Pb and Zn by four wetland plant species growing on submerged mine tailings.* Environmental & Experimental Botany, 2002. **47**(3): p. 271-280.

157. Mapanda, F. and E. Mangwayana, *The Effects of Long-Term Irrigation Using Water on Heavy Metal Contents of Soils under Vegetables.* Agriculture, Ecosystems and Environment, 2005. **107**(2):

p. 151-165.

158. Rout, G.R. and P. Das, *Effect of Metal Toxicity on Plant Growth and Metabolism: I. Zinc*. 2009: Springer Netherlands. 3-11.

159. Li, J.-s., et al., *Characteristics and metal leachability of incinerated sewage sludge ash and air pollution control residues from Hong Kong evaluated by different methods.* Waste Management, 2017.

160. Zhang, F.-S., S.-i. Yamasaki, and M. Nanzyo, *Application of waste ashes to agricultural land—effect of incineration temperature on chemical characteristics.* Science of the total environment, 2001. **264**(3): p. 205-214.

161. Kleemann, R., et al., *Comparison of phosphorus recovery from incinerated sewage sludge ash (ISSA) and pyrolysed sewage sludge char (PSSC).* Waste Management, 2016.

162. Onireti, O.O. and C. Lin, *Mobilization of soil-borne arsenic by three common organic acids: Dosage and time effects.* Chemosphere, 2016. **147**: p. 352-360.

163. Nowack, B. and A.T. Stone, *Competitive adsorption of phosphate and phosphonates onto goethite.* Water Research, 2006. **40**(11): p. 2201-2209.

164. Kim, A.G. and G. Kazonich, *The Silicate/non-silicate distribution of metals in fly ash and its effect on solubility.* Fuel, 2004. **83**(17): p. 2285-2292.

165. Jankowski, J., et al., *Mobility of trace elements from selected Australian fly ashes and its potential impact on aquatic ecosystems.* Fuel, 2006. **85**(2): p. 243-256.

166. Kleemann, R., et al., *Comparison of phosphorus recovery from incinerated sewage sludge ash (ISSA) and pyrolysed sewage sludge char (PSSC).* Waste Management, 2016. **60**: p. 201-210.

167. Nowack, B., F.G. Kari, and H.G. Krüger, *The Remobilization of Metals from Iron Oxides and Sediments by Metal-EDTA Complexes.* Water Air & Soil Pollution, 2001. **125**(1): p. 243-257.

168. Polettini, A., R. Pomi, and E. Rolle, *The effect of operating variables on chelant-assisted remediation of contaminated dredged sediment.* Chemosphere, 2007. **66**(5): p. 866-877.

169. Wei, M., J. Chen, and X. Wang, *Removal of arsenic and cadmium with sequential soil washing techniques using Na 2 EDTA, oxalic and phosphoric acid: Optimization conditions, removal effectiveness and ecological risks.* Chemosphere, 2016. **156**: p. 252-261.

170. Singh, J. and B.-K. Lee, *Kinetics and extraction of heavy metals resources from automobile shredder residue.* Process Safety and Environmental Protection, 2016. **99**: p. 69-79.

171. Matsunaga, T., et al., *Crystallinity and selected properties of fly ash particles.* Materials Science & Engineering A, 2002. **325**(1-2): p. 333-343.

172. U, K., et al., *Composition and element solubility of magnetic and non-magnetic fly ash fractions.* Environmental Pollution, 2003. **123**(2): p. 255-266.

173. Grčman, H., et al., *EDTA enhanced heavy metal phytoextraction: metal accumulation, leaching and toxicity.* Plant & Soil, 2001. **235**(1): p. 105-114.

174. Steen, I., *Management of a non-renewable resource*. Phosphorus and potassium, 1998(217): p. 25-31.

175. Johansson, S., M. Ruscalleda, and J. Colprim, *Phosphorus recovery through biologically induced precipitation by partial nitritation-anammox granular biomass.* Chemical Engineering Journal, 2017. **327**: p. 881-888.

176. Peccia, J. and P. Westerhoff, *We Should Expect More out of Our Sewage Sludge*. Environmental Science & Technology, 2015. **49**(14): p. 8271-8276.

177. Meier, C., et al., *Transformation of Silver Nanoparticles in Sewage Sludge during Incineration.* Environmental Science & Technology, 2016. **50**(7): p. 3503-3510.

178. Hong, K.-J., et al., *Study on the recovery of phosphorus from waste-activated sludge incinerator ash.* Journal of Environmental Science and Health, 2005. **40**(3): p. 617-631.

179. Pettersson, A., L.-E. Åmand, and B.-M. Steenari, *Leaching of ashes*

from co-combustion of sewage sludge and wood—Part II: The mobility of metals during phosphorus extraction. Biomass and bioenergy, 2008. **32**(3): p. 236-244.

180. Krüger, O., A. Grabner, and C. Adam, *Complete Survey of German Sewage Sludge Ash.* Environmental Science & Technology, 2014. **48**(20): p. 11811-11818.
181. Gunn, A., *Use of sewage sludge in construction*. Vol. 608. 2004: Ciria.
182. Gorazda, K., et al., *Characteristic of wet method of phosphorus recovery from polish sewage sludge ash with nitric acid.* Open Chemistry, 2016. **14**(1): p. 37-45.
183. Donatello, S. and C.R. Cheeseman, *Recycling and recovery routes for incinerated sewage sludge ash (ISSA): A review.* Waste Management, 2013. **33**(11): p. 2328-2340.
184. Nowak, B., et al., *Heavy metal removal from municipal solid waste fly ash by chlorination and thermal treatment.* Journal of Hazardous Materials, 2010. **179**(1-3): p. 323-331.
185. Nakić, D., et al., *Environmental impact of sewage sludge ash assessed through leaching.* Engineering Review: Međunarodni časopis namijenjen publiciranju originalnih istraživanja s aspekta analize konstrukcija, materijala i novih tehnologija u području strojarstva, brodogradnje, temeljnih tehničkih znanosti,

elektrotehnike, računarstva i građevinarstva, 2017. **37**(2): p. 222-234.

186. Vogel, C. and C. Adam, *Heavy metal removal from sewage sludge ash by thermochemical treatment with gaseous hydrochloric acid.* Environmental science & technology, 2011. **45**(17): p. 7445-7450.

187. Nziguheba, G. and E. Smolders, *Inputs of trace elements in agricultural soils via phosphate fertilizers in European countries.* Science of the Total Environment, 2008. **390**(1): p. 53-57.

188. Hermassi, M., et al., *Fly ash as reactive sorbent for phosphate removal from treated waste water as a potential slow release fertilizer.* Journal of Environmental Chemical Engineering, 2017. **5**(1): p. 160-169.

189. Yang, S., et al., *Investigation of phosphate adsorption from aqueous solution using Kanuma mud: behaviors and mechanisms.* Journal of Environmental Chemical Engineering, 2013. **1**(3): p. 355-362.

190. Uddin, M.K., *A review on the adsorption of heavy metals by clay minerals, with special focus on the past decade.* Chemical Engineering Journal, 2017. **308**: p. 438-462.

191. Sturm, G., et al., *Electrokinetic phosphorus recovery from packed beds of sewage sludge ash: yield and energy demand.* Journal of Applied Electrochemistry, 2010. **40**(6): p. 1069-1078.

192. Finžgar, N. and D. Leštan, *Multi-step leaching of Pb and Zn contaminated soils with EDTA.* Chemosphere, 2007. **66**(5): p. 824-

832.

193. Yang, B., et al., *Promoting effect of EDTA on catalytic activity of highly stable Al–Ni bimetal alloy for dechlorination of 2-chlorophenol.* Chemical Engineering Journal, 2014. **250**: p. 222-229.

194. Zhang, Z.-Z., et al., *A novel strategy for accelerating the recovery of an anammox reactor inhibited by copper (II): EDTA washing combined with biostimulation via low-intensity ultrasound.* Chemical Engineering Journal, 2015. **279**: p. 912-920.

195. Zhang, T., et al., *Releasing phosphorus from calcium for struvite fertilizer production from anaerobically digested dairy effluent.* Water Environment Research, 2010. **82**(1): p. 34-42.

196. Kozinski, J.A., K.K. Rink, and J.S. Lighty. *Combustion of sludge waste in FBC. Distribution of metals and particle sizes.* in *Proceedings of the 13th International Conference on Fluidized Bed Combustion. Part 2 (of 2)*. 1995. ASME.

197. Vintiloiu, A., et al., *Effect of ethylenediaminetetraacetic acid (EDTA) on the bioavailability of trace elements during anaerobic digestion.* Chemical engineering journal, 2013. **223**: p. 436-441.

198. Kim, C. and S.-K. Ong, *Recycling of lead-contaminated EDTA wastewater.* Journal of hazardous materials, 1999. **69**(3): p. 273-286.

199. Yoo, J.-C., et al., *Extraction characteristics of heavy metals from marine sediments.* Chemical engineering journal, 2013. **228**: p. 688-

699.

200. Ito, A., et al., *Separation of metals and phosphorus from incinerated sewage sludge ash.* Water Science and Technology, 2013. **67**(11): p. 2488-2493.

201. Nzihou, A. and P. Sharrock, *Calcium phosphate stabilization of fly ash with chloride extraction.* Waste Management, 2002. **22**(2): p. 235-239.

202. Wu, X., et al., *BaCO3 modification of TiO2 electrodes in quasi-solid-state dye-sensitized solar cells: performance improvement and possible mechanism.* The Journal of Physical Chemistry C, 2007. **111**(22): p. 8075-8079.

203. Tang, Q., et al., *Removal of Cd (II) and Pb (II) from soil through desorption using citric acid: Kinetic and equilibrium studies.* Journal of Central South University, 2017. **24**(9): p. 1941-1952.

204. T-Park. 2018 [cited accessed 2018. 09.17.

205. Xu, C., W. Chen, and J. Hong, *Life-cycle environmental and economic assessment of sewage sludge treatment in China.* Journal of Cleaner Production, 2014. **67**: p. 79-87.

206. Wang, J., et al., *Existing state and development of sludgy researches in domestic and foreign.* Mun. Eng. Technol., 2006. **24**: p. 140-143.

207. Cui, X., et al., *Removal of phosphate from aqueous solution using magnesium-alginate/chitosan modified biochar microspheres*

derived from Thalia dealbata. Bioresource Technology, 2016. **218**: p. 1123-1132.

208. Fang, L., et al., *Recovery of phosphorus from incinerated sewage sludge ash by combined two-step extraction and selective precipitation.* Chemical Engineering Journal, 2018. **348**: p. 74-83.
209. Li, R., et al., *An overview of carbothermal synthesis of metal–biochar composites for the removal of oxyanion contaminants from aqueous solution.* Carbon, 2018. **129**: p. 674-687.
210. Yao, Y., et al., *Biochar derived from anaerobically digested sugar beet tailings: characterization and phosphate removal potential.* Bioresource technology, 2011. **102**(10): p. 6273-6278.
211. Xu, R.-k., et al., *Adsorption of methyl violet from aqueous solutions by the biochars derived from crop residues.* Bioresource technology, 2011. **102**(22): p. 10293-10298.
212. Fang, C., et al., *Phosphorus recovery from biogas fermentation liquid by Ca–Mg loaded biochar.* Journal of Environmental Sciences, 2015. **29**: p. 106-114.
213. Zhang, M. and B. Gao, *Removal of arsenic, methylene blue, and phosphate by biochar/AlOOH nanocomposite.* Chemical engineering journal, 2013. **226**: p. 286-292.
214. Chen, B., Z. Chen, and S. Lv, *A novel magnetic biochar efficiently sorbs organic pollutants and phosphate.* Bioresource technology,

2011. **102**(2): p. 716-723.

215. Le Leuch, L. and T. Bandosz, *The role of water and surface acidity on the reactive adsorption of ammonia on modified activated carbons.* Carbon, 2007. **45**(3): p. 568-578.

216. Yao, Y., et al., *Engineered carbon (biochar) prepared by direct pyrolysis of Mg-accumulated tomato tissues: characterization and phosphate removal potential*. Bioresource technology, 2013. **138**: p. 8-13.

217. Tang, J., et al., *Characteristics of biochar and its application in remediation of contaminated soil.* Journal of bioscience and bioengineering, 2013. **116**(6): p. 653-659.

218. Uchimiya, M., et al., *Sorption of deisopropylatrazine on broiler litter biochars.* Journal of agricultural and food chemistry, 2010. **58**(23): p. 12350-12356.

219. Ahmad, M., et al., *Effects of pyrolysis temperature on soybean stover-and peanut shell-derived biochar properties and TCE adsorption in water.* Bioresource technology, 2012. **118**: p. 536-544.

220. Xue, Y., et al., *Hydrogen peroxide modification enhances the ability of biochar (hydrochar) produced from hydrothermal carbonization of peanut hull to remove aqueous heavy metals: Batch and column tests.* Chemical Engineering Journal, 2012. **200-202**: p. 673-680.

221. Zhang, M., et al., *Synthesis of porous MgO-biochar nanocomposites*

for removal of phosphate and nitrate from aqueous solutions. Chemical Engineering Journal, 2012. **210**(4): p. 26-32.

222. Marshall, J.A., et al., *Recovery of phosphate from calcium-containing aqueous solution resulting from biochar-induced calcium phosphate precipitation.* Journal of Cleaner Production, 2017. **165**: p. 27-35.

223. Rathod, M.K. and J. Banerjee, *Thermal stability of phase change materials used in latent heat energy storage systems: A review.* Renewable and Sustainable Energy Reviews, 2013. **18**: p. 246-258.

224. Tyagi, V.V. and D. Buddhi, *Thermal cycle testing of calcium chloride hexahydrate as a possible PCM for latent heat storage.* Solar Energy Materials and Solar Cells, 2008. **92**(8): p. 891-899.

225. Lonappan, L., et al., *An insight into the adsorption of diclofenac on different biochars: Mechanisms, surface chemistry, and thermodynamics.* Bioresource technology, 2018. **249**: p. 386-394.

226. Wang, S.-L. and P.-C. Wang, *In situ XRD and ATR-FTIR study on the molecular orientation of interlayer nitrate in Mg/Al-layered double hydroxides in water.* Colloids and Surfaces A: Physicochemical and Engineering Aspects, 2007. **292**(2): p. 131-138.

227. Jung, K.-W., et al., *Characteristics of biochar derived from marine macroalgae and fabrication of granular biochar by entrapment in calcium-alginate beads for phosphate removal from aqueous*

solution. Bioresource technology, 2016. **211**: p. 108-116.

228. Zhang, Y., et al., *Study on the rheological properties of fresh cement asphalt paste.* Construction & Building Materials, 2012. **27**(1): p. 534-544.

229. Loganathan, P., et al., *Removal and Recovery of Phosphate From Water Using Sorption.* Critical Reviews in Environmental Science and Technology, 2014. **44**(8): p. 847-907.

230. Sarkar, S., et al., *Hybrid ion exchanger supported nanocomposites: Sorption and sensing for environmental applications.* Chemical Engineering Journal, 2011. **166**(3): p. 923-931.

231. Uchimiya, M., et al., *Immobilization of Heavy Metal Ions (CuII, CdII, NiII, and PbII) by Broiler Litter-Derived Biochars in Water and Soil.* Journal of Agricultural and Food Chemistry, 2010. **58**(9): p. 5538-5544.

232. Karaca, S., et al., *Kinetic modeling of liquid-phase adsorption of phosphate on dolomite.* Journal of Colloid and Interface Science, 2004. **277**(2): p. 257-263.

233. Jung, K.-W., et al., *Phosphate adsorption ability of biochar/Mg–Al assembled nanocomposites prepared by aluminum-electrode based electro-assisted modification method with MgCl2 as electrolyte.* Bioresource Technology, 2015. **198**: p. 603-610.

234. Smith, Y.R., et al., *Adsorption of aqueous rare earth elements using*

carbon black derived from recycled tires. Chemical Engineering Journal, 2016. **296**: p. 102-111.

235. Liu, Y., *New insights into pseudo-second-order kinetic equation for adsorption.* Colloids and Surfaces A: Physicochemical and Engineering Aspects, 2008. **320**(1): p. 275-278.

236. Jung, K.W., et al., *Preparation of modified-biochar from Laminaria japonica : Simultaneous optimization of aluminum electrode-based electro-modification and pyrolysis processes and its application for phosphate removal.* Bioresource Technology, 2016. **214**: p. 548-557.

237. Dai, L., et al., *Engineered hydrochar composites for phosphorus removal/recovery: Lanthanum doped hydrochar prepared by hydrothermal carbonization of lanthanum pretreated rice straw.* Bioresource Technology, 2014. **161**: p. 327-332.

238. Hilt, K., et al., *Agronomic Response of Crops Fertilized with Struvite Derived from Dairy Manure.* 2016. **227**(10): p. 388.

239. Talboys, P.J., et al., *Struvite: a slow-release fertiliser for sustainable phosphorus management?* 2016. **401**(1-2): p. 109-123.

240. Cordell, D., J.O. Drangert, and S. White, *The story of phosphorus: Global food security and food for thought.* Global Environmental Change, 2009. **19**(2): p. 292-305.

241. Matsubae-Yokoyama, K., et al., *A Material Flow Analysis of Phosphorus in Japan: The Iron and Steel Industry as a Major*

Phosphorus Source. 2009. **volume 13**(5): p. 687-705(19).

242. Cordell, D., ., et al., *Towards global phosphorus security: a systems framework for phosphorus recovery and reuse options.* 2011. **84**(6): p. 747-758.

243. De-Bashan, L.E. and B.J.W.R. Yoav, *Recent advances in removing phosphorus from wastewater and its future use as fertilizer (1997-2003).* 2004. **38**(19): p. 4222-4246.

244. Shiba, N.C. and F.J.W.M. Ntuli, *Extraction and precipitation of phosphorus from sewage sludge.* 2016. **60**: p. S0956053X16304081.

245. DeForest, D.K. and J.S. Meyer, *Critical review: toxicity of dietborne metals to aquatic organisms.* Critical Reviews in Environmental Science and Technology, 2015. **45**(11): p. 1176-1241.

246. Yu, S., Y.-g. Zhu, and X.-d. Li, *Trace metal contamination in urban soils of China.* Science of the total environment, 2012. **421**: p. 17-30.

247. Li, Z., et al., *A review of soil heavy metal pollution from mines in China: pollution and health risk assessment.* Science of the total environment, 2014. **468**: p. 843-853.

248. Niu, L., Z. Shen, and C. Wang, *Sites, pathways, and mechanism of absorption of Cu-EDDS complex in primary roots of maize (Zea mays L.): anatomical, chemical and histochemical analysis.* Plant and soil, 2011. **343**(1-2): p. 303-312.

249. Raptopoulou, C., et al., *Phosphate Removal from Effluent of Secondary Wastewater Treatment: Characterization of Recovered Precipitates and Potential Re-use as Fertilizer.* 2016. **7**(4): p. 851-860.

250. Jiao, W., et al., *Environmental risks of trace elements associated with long-term phosphate fertilizers applications: A review.* 2012. **168**(1): p. 44-53.

251. Imai, T., *Calcination Technology for Manufacturing Mineral Fertilizer Using CaO-Enriched Sewage Sludge Ash*, in *Phosphorus Recovery and Recycling*, H. Ohtake and S. Tsuneda, Editors. 2019, Springer Singapore: Singapore. p. 179-187.

252. Yuan, J.H. and R.K. Xu, *The amelioration effects of low temperature biochar generated from nine crop residues on an acidic Ultisol.* Soil Use & Management, 2015. **27**(1): p. 110-115.

253. Gonzálezponce, R., E.G. Lópezdesá, and C.J.H.A.P.o.t.A.S.f.H.S. Plaza, *Lettuce response to phosphorus fertilization with struvite recovered from municipal wastewater.* 2009. **44**(2): p. 426-430.

254. Healy, M.G., et al., *Bioaccumulation of metals in ryegrass (Lolium perenne L.) following the application of lime stabilised, thermally dried and anaerobically digested sewage sludge.* Ecotoxicology and Environmental Safety, 2016. **130**: p. 303-309.

255. EC, *Directive 2002/32/EC of the European Parliament and the*

Council of 7 May 2002 on Undesirable Substances in Animal Feed (OJ L 140). 2002.